

CONTRACT NAS 9-6470

DEVELOPMENT AND FABRICATION OF ADVANCED BATTERY  
ENERGY STORAGE SYSTEM

Prepared by

THE BOEING COMPANY  
SPACE DIVISION  
SEATTLE, WASHINGTON

Sidney Gross - Technical Leader

November 27, 1967

FINAL REPORT

September 27, 1966 through  
October 26, 1967

Prepared for

National Aeronautics and Space Administration  
Manned Spacecraft Center  
Houston, Texas

## NOTICE

This report was prepared as an account of Government-sponsored work. Neither the United States, nor the National Aeronautics and Space Administration (NASA), nor any person acting on behalf of NASA:

- a. Makes warranty or representation, expressed or implied, with respect to the accuracy, completeness, or usefulness of the information contained in this report, or that the use of any information, apparatus, method, or process disclosed in this report may not infringe privately-owned rights; or
- b. Assumes any liabilities with respect to the use of, or for damages resulting from the use of any information, apparatus, method, or process disclosed in this report.

As used above, "person acting on behalf of NASA" includes any employee or contractor of NASA, or employee of such contractor, to the extent that such employees or contractor of NASA, or employee of such contractor prepares, disseminates, or provides access to, any information pursuant to his employment with such contractor.

Requests for copies of this report should be referred to:

National Aeronautics and Space Administration  
Office of Scientific and Technical Information  
Washington, D.C., 20025

## CONTENTS

1. INTRODUCTION
2. PROGRAM ACCOMPLISHMENTS
3. CELL DESIGN AND PERFORMANCE
4. VENTING
5. BATTERY PACKAGING
6. THERMAL ANALYSIS
7. CALORIMETER DESIGN
8. BATTERY CHARGE-DISCHARGE CONTROLLER
9. CONCLUSIONS
10. REFERENCES
11. APPENDIX

## LIST OF FIGURES

- 1 Program Schedule
- 2 Vented Silver Cadmium Cell
- 3 Weight and Thickness Variation of Negative Plates
- 4 Weight and Thickness Variation of Positive Plates
- 5 Silver-Cadmium Cell Voltage During High Current Pulses
- 6 Half-Cell Voltage Characteristics at End of Charge on Reject Cell
- 7 Gas Evolution Rate Measurement Test
- 8 Gassing Rates at Constant Potential Overcharge
- 9 Transient Gassing Rates at End of Charge
- 10 Cell Venting System
- 11 Pressure Relief Valve Leakage Test
- 12 Maximum Detected Leakage Rate of Pressure Relief Valve
- 13 Flow Characteristics of Pressure Relief Valve
- 14 Temperature Profiles for Ag-Cd Cell With Isothermal Boundaries
- 15 Ag-Cd Cell Plate Temperatures with Fins on Two Faces and Bottom
- 16 Battery Case Assembly
- 17 Battery Case (Sheet 1)
- 18 Battery Case (Sheet 2)
- 19 Silver-Cadmium Battery
- 20 Battery Installation
- 21 Thermocouple Locations
- 22 Watt-Hour Efficiency of Silver Cadmium Cell
- 23 Silver-Cadmium Test Cell
- 24 Specific Heat Test of 70 AH Silver Cadmium Cell
- 25 Typical Heat Generation Test Results
- 26 Correlation of Heat Generation Enthalpy Voltage During Charge
- 27 Correlation of Heat Generation Enthalpy Voltage During Discharge
- 28 Cell Thermal Conductivity Test
- 29 Comparison of Analytical and Experimental Battery Temperatures, Case 1



## LIST OF FIGURES (Continued)

- 30 Comparison of Analytical and Experimental Battery Temperatures, Case 2
- 31 Calorimeter Concept
- 32 Calorimeter Heat Exchanger
- 33 Heat Exchanger, Calorimeter
- 34 Schematic of Calorimeter Temperature Difference Sensor
- 35 Test Set-Up for Calibration of Calorimeter Temperature Difference Sensors
- 36 Typical Calibration Data for Temperature Difference Sensor No. 2
- 37 Sensitivity Curve - Calorimeter Temperature Difference Sensor
- 38 Calorimeter Insulated Box
- 39 Calorimeter Insulated Box Assembly
- 40 Thermal Conductance of Battery Calorimeter Insulation Box
- 41 Simplified Charge-Discharge Controller
- 42 Charge-Discharge Controller Front View
- 43 Charge-Discharge Controller Rear View
- 44 Front Cabinet Layout
- 45 Battery Charge-Discharge Controller Block Diagram
- 46 Battery Charge-Discharge Controller Schematic
- 47 Manually Adjustable Load
- 48 Programmed Load
- 49 Punched Tape Programmer
- 50 Pressure Measurement Schematic
- 51 Ampere-Hour Meter Schematic
- 52 Calibration of Ampere-Hour Meter
- 53 Watt-Hour Meter Schematic
- 54 Calibration of Watt-Hour Meter

## LIST OF TABLES

1	Equipment Delivered to NASA
2	Reports and Computer Programs Delivered to NASA
3	Typical Discharge Voltage Characteristics at 35 Amperes (C/2)
4	Identification of Cells Within Batteries
5	Spectroscopic Analysis of Evolved Gas During Overcharge
6	Guidelines for Battery Cell Thermal Control
7	Thermal Comparison of Magnesium and Aluminum Alloys
8	Summary of Battery Packaging Concepts
9	Evaluation of Battery Packaging Concepts
10	Battery Weight Breakdown
11	Heat Generation Runs
12	Calculated Partition of Calorimeter Thermal Conductance
13	Typical Charge-Discharge Controller Settings
14	Switch Combinations for Manually Adjustable Load
15	Punched Tape Combinations for Programmable Loads
16	Voltage Regulation of Charge-Discharge Controller Power Supply

## 1. INTRODUCTION

The Manned Spacecraft Center (MSC) of NASA has contracted with The Boeing Company for the development and fabrication of an advanced battery energy storage system using silver-cadmium cells. The contract number is NAS 9-6470. The work was started on September 27, 1966, and was completed October 27, 1967. Henry Oman was the program manager, Sidney Gross was the principle investigator, and Bob J. Bragg was the NASA technical monitor. This document is a final report, which summarizes the accomplishments.

The objective of this program is to develop a silver-cadmium secondary battery energy storage system to meet the power requirements of manned orbital missions of up to one year in duration. Boeing's major tasks are:

- 1) Develop and provide eight 28-volt silver-cadmium batteries of more than 70 ampere-hours capacity each.
- 2) Develop and provide four charge-discharge controllers for cycling the batteries, plus instruction manuals.
- 3) Perform a detailed thermal analysis of the battery to accurately predict heat generation and temperatures over a wide range of operating modes. A computer program for performing the thermal analysis is to be delivered.
- 4) Provide calorimeters for measurement of internal heat generation in two specially instrumented batteries.

All requirements of the contract have been met or exceeded. Important work has been completed in the areas of cell design, cell venting, battery packaging, calorimeter design, thermal analysis, and controlling the battery charge-discharge test cycle. Each of these areas is the subject of a chapter in this final report. Each chapter starts with a summary of the pertinent contract requirements, and continues with a discussion of the results obtained during the contract period.

## 2. PROGRAM ACCOMPLISHMENTS

Figure 1 shows the schedule and major milestones for the accomplishment of the program tasks. All tasks have been successfully completed, and deliverable items have been shipped and received at NASA. Table 1 lists the equipment which has been delivered and Table 2 lists the reports and computer programs which have been delivered.

All delivered items were tested at Boeing to assure satisfactory performance. Batteries functioned satisfactorily at each of the orbital design conditions, leaving only the life requirements yet to be demonstrated. The charge-discharge controller components and instruments were tested separately, and the assembled controllers were operated over a wide range of conditions to assure trouble-free operation. The calorimeters were tested using two of the batteries, and the calorimeter computer program was checked out with test data. Both thermal analysis computer programs were checked out, and their accuracy was verified by comparison with data from laboratory tests on the batteries. No problems or deficiencies are known to exist with any delivered item.

The technical items considered to be unique are:

- 1) Ampere-hour and watt-hour meters.
- 2) Liquid-vapor separation for the cells.
- 3) Battery packaging, which permits cells to be removed, yet provides effective heat removal.
- 4) The heat generation correlation.
- 5) Calorimeter design and associated computer program for analyzing data.
- 6) The use of a programmer and delay timers to give charge-discharge control flexibility.

# BATTERY DEVELOPMENT, CONTRACT NAS 9-6470

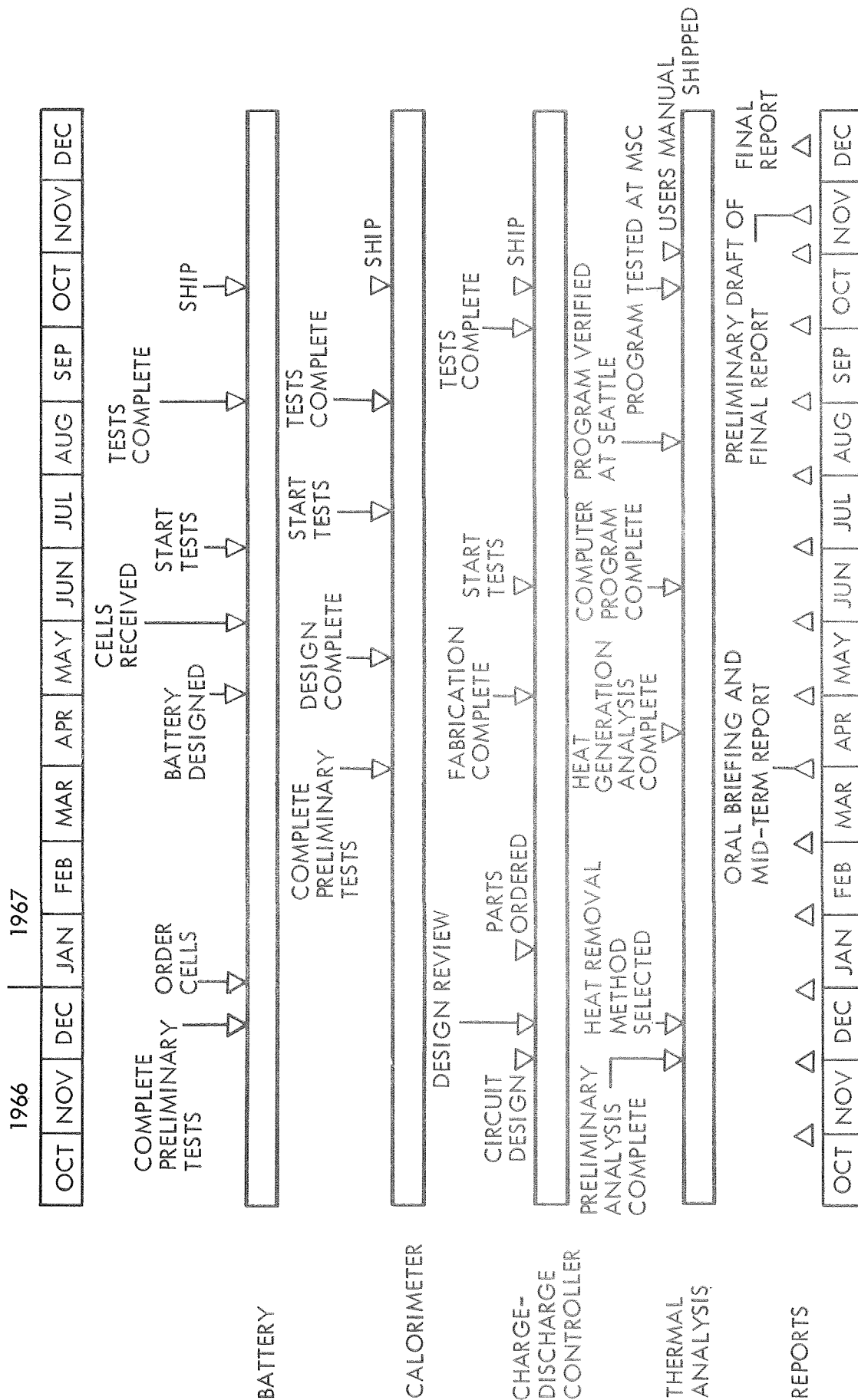


FIGURE 1

## PROGRAM SCHEDULE

TABLE 1  
EQUIPMENT DELIVERED TO NASA

<u>ITEM</u>	<u>NUMBER</u>	<u>DESCRIPTION</u>	<u>PART NO.</u>
1	8	Batteries	25-60600-1
2	2	Charge-Discharge Controller Cabinets	25-60600-2
3	2	Calorimeter Heat Exchangers	25-60600-3
4	2 Sets	Calorimeter Insulated Boxes	25-60600-4
5	4	Battery Cables	25-60600-5
6	2	Power Cables	25-60600-6
7	2	Temperature Difference Sensor Cables	25-60600-7
8	3	Temperature Readout Cable	25-60600-8
9	1	Shorting Plug for Connectors P5 and P8	25-60600-9
10	1	Programmer Hole Puncher	25-60600-10
11	1 Roll	Programmer Punched Tape	
12	1 Roll	Splicing Tape for Punched Tape	
13	1	Spare Timer	
14	2 Sets	Matching Connectors	
15	1 Jar	Silicon Grease for Battery-to- Calorimeter Surfaces	
16	2 Sets	Screws and Washers for Calorimeter	
17	1 Lot	Hose and Fittings for Calorimeter	

TABLE 2  
REPORTS AND COMPUTER PROGRAMS DELIVERED TO NASA

<u>ITEM</u>	<u>DESCRIPTION</u>
1	Monthly Progress Reports (11)
2	Mid-Term Report
3	Final Report
4	Computer Program for Analyzing Experimental Calorimeter Data, with User's Manual and Test Cases
5	Battery Thermal Analysis Computer Program, with User's Manual and Test Cases
6	Cell Thermal Analysis Computer Program, with User's Manual and Test Cases
7	Instruction Manual, Battery Charge-Discharge Controller Cabinet
8	Components Information Manual, Battery Charge-Discharge Controller Cabinet
9	Quality Assurance Requirements and Inspection Plan for Silver-Cadmium Cell

### 3. CELL DESIGN AND PERFORMANCE

#### REQUIREMENTS

Each battery has 28 vented silver cadmium cells. The electrical performance requirements of the cells are as follows:

1. Nominal Cell Rating. Cell rating at a C/2 rate of discharge to an end voltage of 0.6 volts shall be greater than 70 ampere-hours with cells operating between 60°F to 90°F. At the end of a 75-percent depth of discharge on this test, battery voltage shall be greater than 28.0 volts.
2. Cycling Capability. When packaged as a battery of 28 series-connected cells, the cells shall be capable of operation under the following range of test conditions with programmed and fixed loads:
  - a) At least 5500 charge/discharge cycles at 25-percent depth of discharge with a 58-minute charge, 36-minute discharge cycle.
  - b) At least 200 charge/discharge cycles at 75-percent depth of discharge with a ten-hour charge, two-hour discharge.
  - c) At least 100 charge/discharge cycles at up to 75-percent depth of discharge on a 24-hour cycle (22-hour charge, two-hour discharge) with a widely varying load which includes maximum-duration peaks of ten seconds at a 3C rate.
3. Cell Voltage. The battery steady-state voltage shall not fall below 25 volts during the above testing.

The battery is required to operate in the pressure range of  $10^{-6}$  mm Hg to 760 mm Hg, and in an ambient temperature range of 0 to 160°F when mounted on coldplating having a temperature range of 60 to 90°F.

The objective of this program was to build batteries for laboratory testing; the batteries are not required to be flight prototypes. Battery design was based on vented cells.



In order to insure meeting the above requirements, The Boeing Company specified careful quality control during cell manufacture. A specification was written, "Quality Assurance Requirements and Inspection Plan for Silver-Cadmium Cell" (Reference 1). The manufacture of the battery cells was controlled by this specification.

The weight and density of all plates was controlled. Allowable deviations from average values were as follows.

	Negative Plate (Cadmium)	Positive Plate (Silver)
Maximum deviation from average plate thickness	0.002 inches	0.001 inches
Maximum deviation from average plate weight	4 percent	2 percent

#### WORK ACCOMPLISHED

Cell Design. The cells were designed with 12 positive plates (silver oxide) and 13 negative plates (cadmium). These plates are 2.313 inches by 6.188 inches in size. The total area of the positive electrode of one cell is 345 square inches, which provides a maximum charge-current density of 0.05 amperes per square inch for the 94 minute orbit. The maximum discharge current density is 0.61 amperes per square inch at 210 amperes. The separators are pellaon and a modified cellululose known as C-19.

Yardney Electric Corporation was selected to build the cells. Eight prototype cells were built and tested to verify performance. One problem encountered was maintenance of voltage during high current pulses, especially when the high-current pulses were applied to a cell having a high state of charge. Low voltage at this condition is characteristic of the silver cadmium system, and is due primarily to a highly resistive layer of argentous oxide ( $\text{Ag}_2\text{O}$ ).

Design modifications that would overcome this problem were explored. These included a 90 degree reorientation of the exmet, use of a thicker exmet, use of wider tabs from the plates to the terminals, and the use of greater plate area. The design choice was to reorient the exmet 90 degrees and to use wider tabs from the plates to the terminals. Since design for large current pulses was not a primary objective, additional changes were not made because they would have compromised the design in other respects.

The cell case is made from a styrene acrylonitrile copolymer. Although this material is not so good thermally as some other plastics, it was selected because its transparency is important in quality-control inspection. Each cell has a Swagelock fitting for attachment of vent lines.

Figure 2 is a photograph of the cell. Cell case outside dimensions are 1.72 inches by 2.81 inches by 7.73 inches. Fifteen cell cases were measured at twelve locations to obtain data on dimensional variations for battery packaging design. The maximum variation was  $\pm 3$  mils, which was acceptable for the adopted battery packaging design.

Cell Performance. Complete records were kept during cell manufacture to aid in quality control. Figures 3 and 4 show typical weight and thickness of individual plates. The variations are within the allowed tolerances. These records can be used by NASA to correlate manufacturing quality with subsequent performance during life testing.

Cell tests have verified that the cell charge and discharge characteristics are suitable for all three simulated orbits. The critical requirement for charge is the 94 minute orbit; under a charge current of 18.1 amperes, the cells will cycle properly with a limiting voltage of 1.55 volts. The critical requirement for discharge is the 24 hour orbit, where the end-of-discharge voltage will be around 1.06 to 1.07 volts. Figure 5 shows typical voltage characteristics during high current pulses in the 24 hour cycle. Typical voltage-time data at the C/2 discharge rate is given in Table 3.

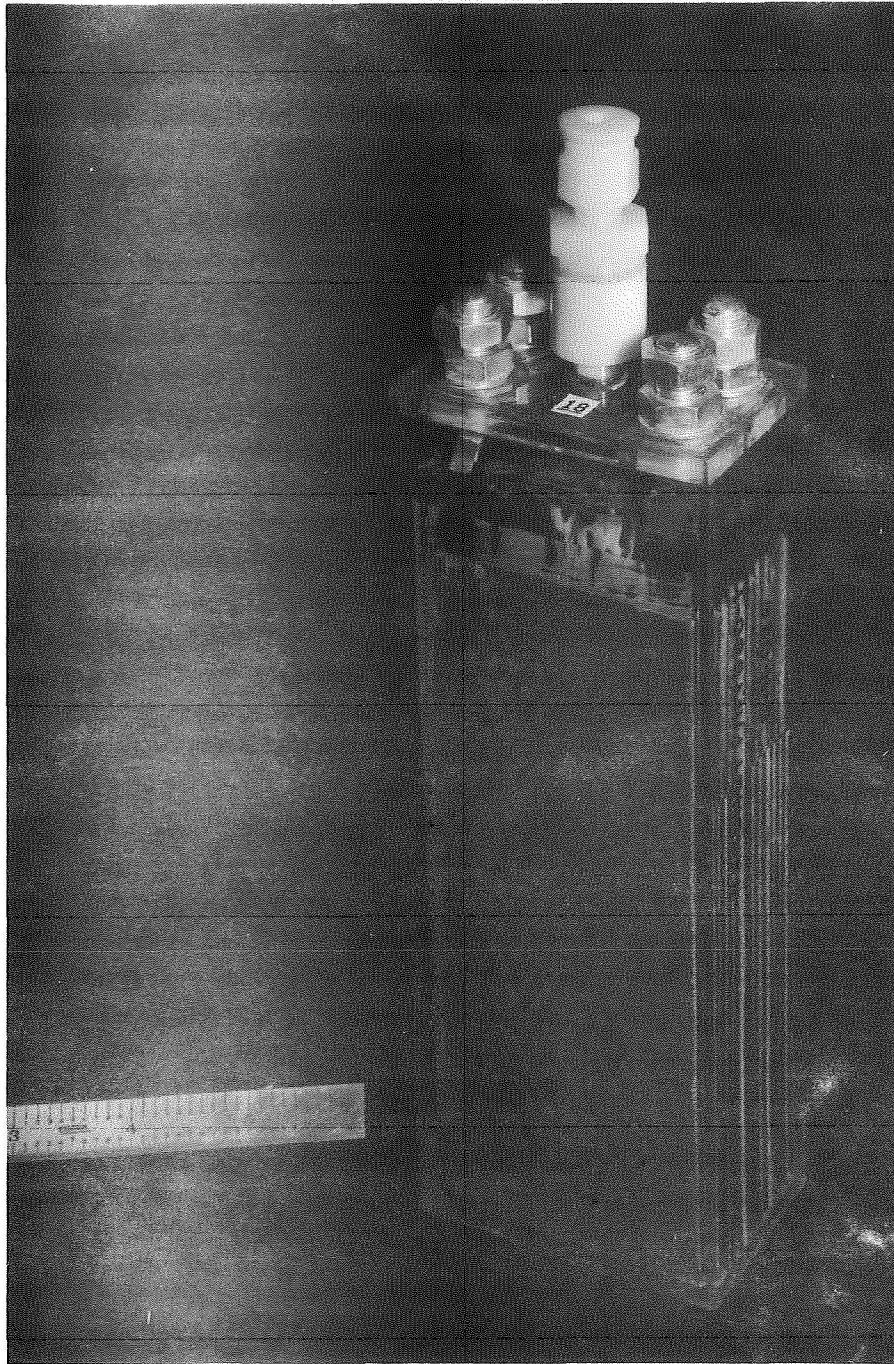


FIGURE 2  
VENTED SILVER CADMIUM CELL

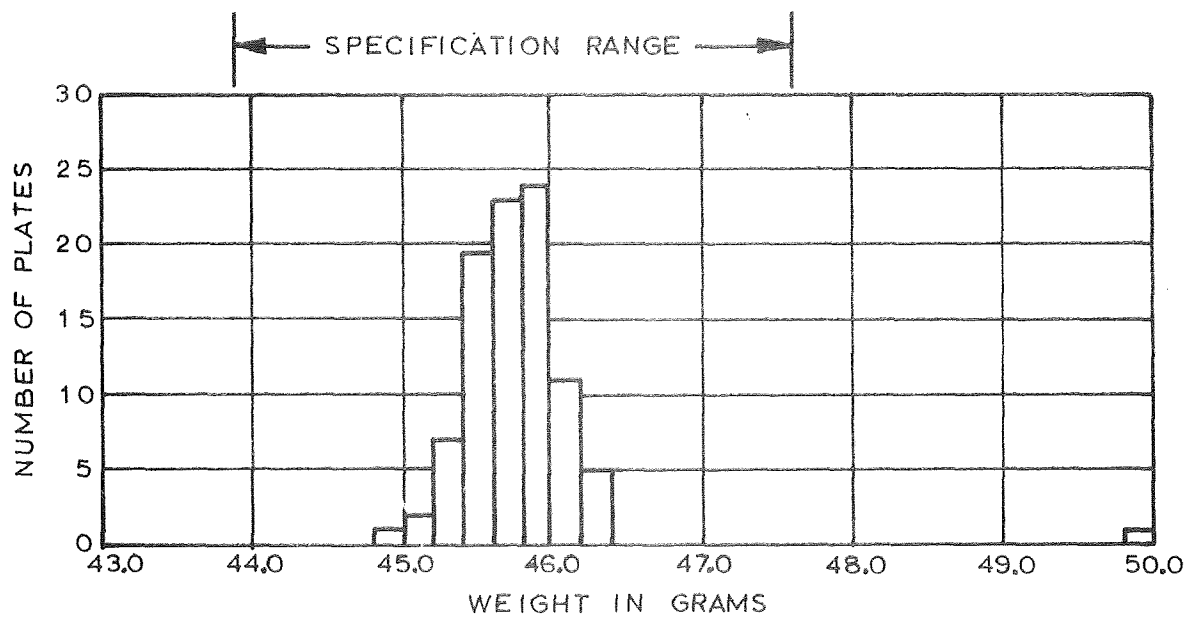
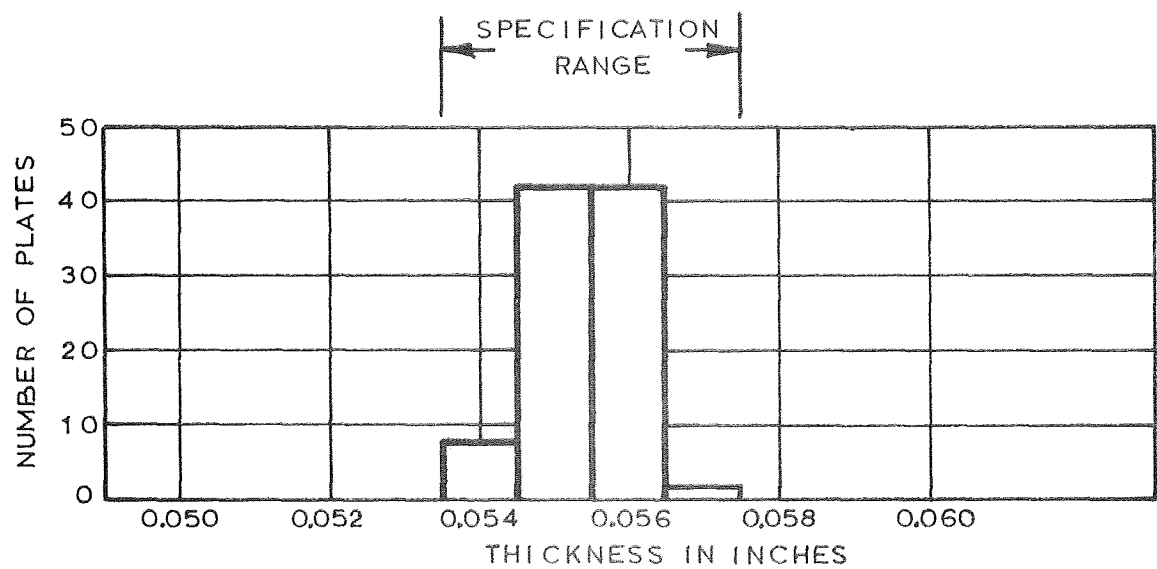


FIGURE 3  
WEIGHT AND THICKNESS VARIATION OF NEGATIVE PLATES

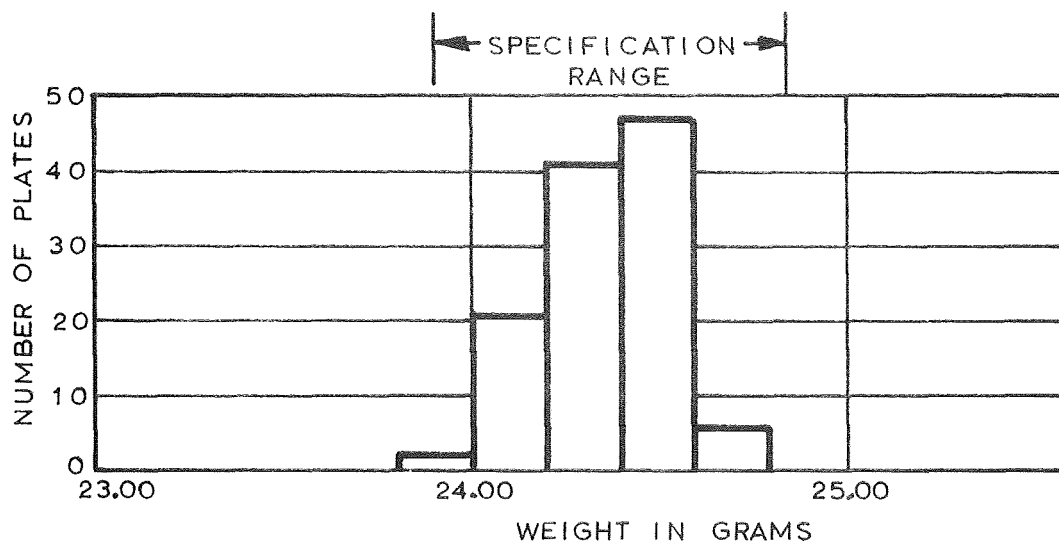
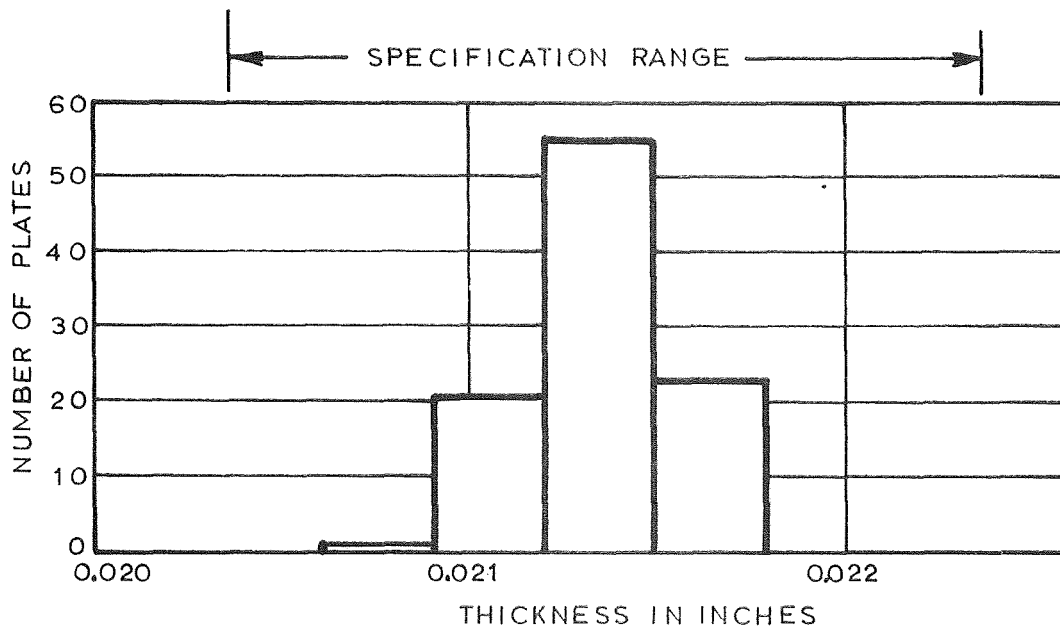


FIGURE 4

WEIGHT AND THICKNESS VARIATION OF POSITIVE PLATES

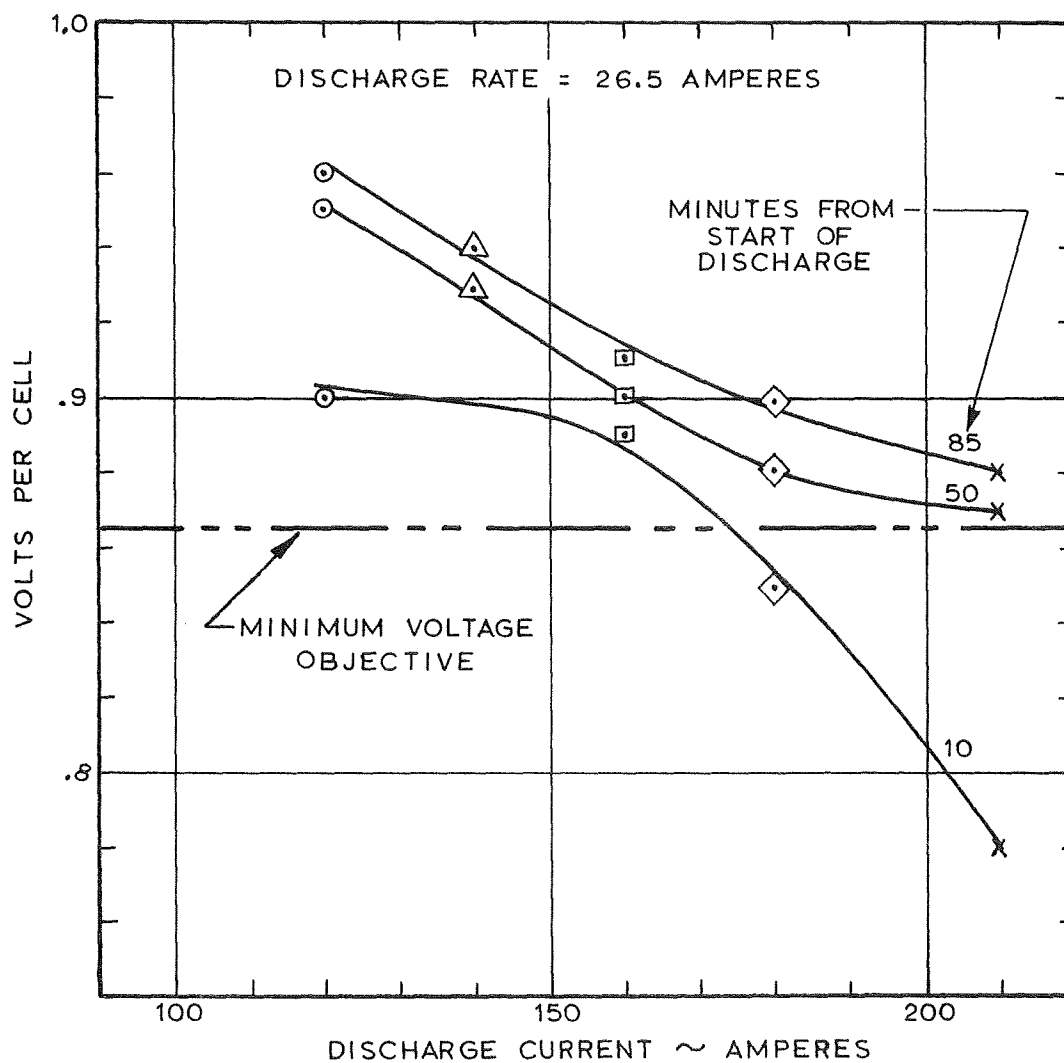


FIGURE 5

SILVER-CADMIUM CELL VOLTAGE DURING HIGH CURRENT PULSES

TABLE 3  
TYPICAL DISCHARGE VOLTAGE CHARACTERISTICS AT 35 AMPERES (C/2)

TIME FROM START OF DISCHARGE MINUTES	CELL POTENTIAL ~ VOLTS																			
	CELL NUMBER																			
	244	245	246	247	248	249	250	251	252	253	254	255	256	257	258	259	260	261	262	263
0 (O.C.V.)	1.40	1.40	1.40	1.40	1.40	1.40	1.40	1.40	1.40	1.40	1.40	1.40	1.40	1.40	1.40	1.40	1.40	1.40	1.40	1.40
15	1.23	1.23	1.22	1.24	1.22	1.24	1.23	1.20	1.23	1.22	1.22	1.22	1.24	1.22	1.23	1.17	1.17	1.04	1.22	1.23
30	1.09	1.08	1.04	1.04	1.04	1.02	1.04	1.03	1.04	1.04	1.03	1.04	1.16	1.04	1.18	1.10	1.04	1.03	1.09	1.09
45	1.04	1.03	1.03	1.03	1.03	1.03	1.03	1.03	1.03	1.03	1.03	1.03	1.03	1.03	1.03	1.03	1.03	1.03	1.03	1.03
60	1.04	1.04	1.04	1.04	1.04	1.04	1.04	1.04	1.04	1.04	1.04	1.04	1.04	1.04	1.04	1.04	1.04	1.04	1.03	1.04
75	1.04	1.04	1.04	1.04	1.04	1.04	1.04	1.04	1.04	1.04	1.05	1.04	1.05	1.04	1.05	1.04	1.04	1.04	1.04	1.04
90	1.04	1.04	1.04	1.04	1.04	1.04	1.04	1.04	1.04	1.04	1.04	1.04	1.04	1.04	1.04	1.04	1.04	1.04	1.04	1.04
105	1.03	1.03	1.03	1.03	1.03	1.04	1.04	1.04	1.03	1.04	1.04	1.04	1.04	1.04	1.04	1.04	1.04	1.04	1.04	1.04
120*	1.04	1.03	1.04	1.04	1.04	1.04	1.04	1.04	1.04	1.04	1.04	1.04	1.04	1.04	1.04	1.04	1.04	1.04	1.04	1.04
135	1.04	1.04	1.03	1.04	1.03	1.04	1.04	1.04	1.04	1.04	1.04	1.03	1.03	1.04	1.03	1.03	1.03	1.04	1.03	1.03
156	1.02	1.02	1.02	1.02	1.02	1.02	1.02	1.02	1.03	1.02	1.02	1.02	1.02	1.02	1.02	1.02	1.02	1.02	1.02	1.01
165	1.00	1.01	1.02	1.00	0.99	1.01	1.01	1.01	1.01	1.00	0.98	1.00	0.97	0.99	0.98	0.93	0.99	0.96	0.98	0.93

\* Contract requirement is at least 120 minutes discharge at 35 amperes.

Some of the cells received at Boeing were found to have low capacity (below 70 ampere-hours), and hence were not acceptable for use in the batteries. A test was conducted on one of the rejected cells to determine the cause of the low capacity. In this test the voltage during charge of the silver and cadmium electrodes was measured against a reference electrode ionically connected to the electrolyte through a salt bridge in the vent port. The test results (Figure 6) showed that the cell was negative-electrode limited. It is clear that the cadmium negative electrode is at fault, since it is the cadmium and not the silver electrode potential which rises at the end of charge. NASA should be alert to this failure mode should any of the cells in the batteries being supplied show low capacity during life tests.

Cell Selection and Matching. Closely matched cells in a battery minimize out-of-balance cell-voltages at the end of charge. The objective of cell-matching tests was to cull out defective cells and to divide the good cells into eight closely matched sets.

Two switch boards were constructed to permit testing 60 cells at one time. The cells were charged and discharged in series, and individual cells were disconnected as they reached full charge or discharge. Each cell was subjected to the following charges and discharges during forming and matching tests. The data from the last charge and discharge were used for the matching.

- 1) Formation charge at 5 amperes for 32 hours
- 2) Discharge at 35 amperes to 0.6 volts
- 3) Charge at 5 amperes to 1.6 volts
- 4) Discharge at 35 amperes to 0.6 volts
- 5) Charge at 5 amperes to 1.6 volts
- 6) Four 94-minute cycles, 16-ampere discharge and 9-ampere charge
- 7) Discharge at 30 amperes to 0.9 volts
- 8) Charge at 6 amperes to 1.6 volts
- 9) Discharge at 30 amperes to 0.9 volts
- 10) Charge at 6 amperes to 1.6 volts
- 11) Discharge at 30 amperes to 0.9 volts



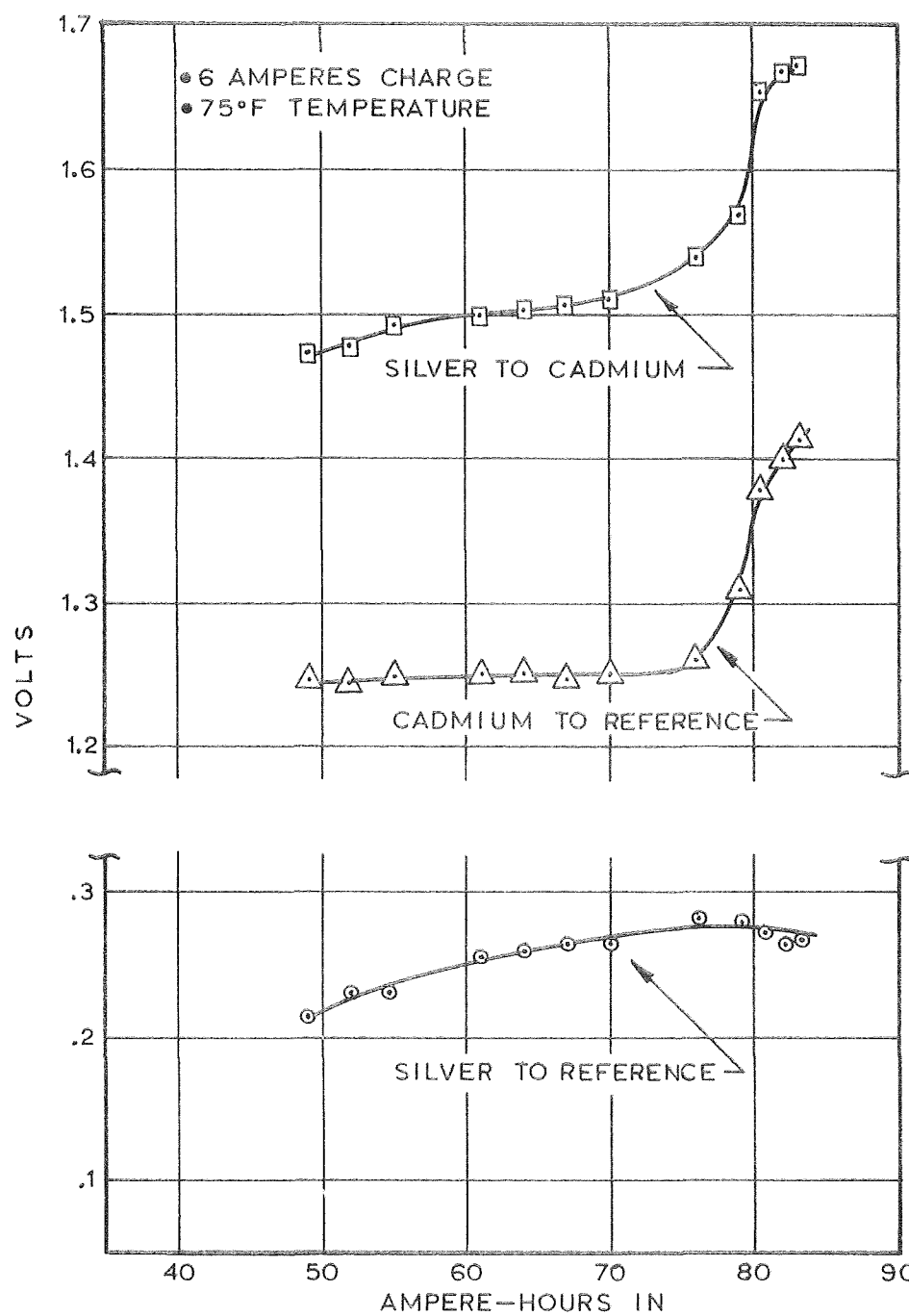


FIGURE 6  
HALF-CELL VOLTAGE CHARACTERISTICS AT END OF CHARGE ON  
REJECT CELL

Capacity was believed to be the most useful basis for matching silver cadmium cells. We found, however, that although cells of a group have the same capacity, they will often differ in other respects. Therefore, some weight can be given in cell matching to these other factors:

- 1) Charge ampere hours at constant current to a limiting voltage.
- 2) Capacity at constant current discharge to a limiting voltage.
- 3) Remaining capacity at discharge from limiting voltage to 0.1 volts.
- 4) Charge ampere hours at transition from lower plateau to upper plateau.
- 5) Upper plateau voltage (mid-range) during charge.
- 6) Lower plateau voltage (mid-range) during discharge.

Cells can be matched with multiple criteria by assigning a weighting factor, based on judgment, to each criterion. A short computer program was written for this purpose, the essentials of which can be described as follows.

Let the cells be designated  $i, i + 1, \dots, N$ , in groups  $j, j + 1, \dots, M$ . Let matching characteristics of individual cells be designated  $A, B$ , etc., with maximum and minimum values of all the cells designated  $A_{\min}, A_{\max}, B_{\min}, B_{\max}$ , etc. Assign weighting factors  $A_F, B_F$ , etc. such that the spread from  $A_{\min}$  to  $A_{\max}$  is equal in weight to the spread from  $B_{\min}$  to  $B_{\max}$ , etc. The average values of the characteristics in each group are

$$\bar{A} = \frac{\sum A_j}{N}, \bar{B} = \dots, \text{etc.} \quad (1)$$

Thus, for a particular cell the mismatch of each characteristic can be represented by

$$\frac{A}{\bar{A}} - 1, \quad \frac{B}{\bar{B}} - 1, \text{etc.} \quad (2)$$

Applying the weighting factors, the mismatch E for any cell can be represented by

$$E = \frac{A_F \left( \frac{A_{\min}}{A_{\max}} \right) \left| \frac{A}{\bar{A}} - 1 \right| + B_F \left( \frac{B_{\min}}{B_{\max}} \right) \left| \frac{B}{\bar{B}} - 1 \right| + \dots}{A_F \left( \frac{A_{\min}}{A_{\max}} \right) + B_F \left( \frac{B_{\min}}{B_{\max}} \right) + \dots} \quad (3)$$

Cells are then relocated from group to group to achieve minimum values of E.

Matching tests were conducted with commercial silver-cadmium cells, and it was found that if the largest weighting is given to capacity factors (items 1 and 2) then the grouping of cells changed very little if the other factors were ignored. Since large weighting to factors other than capacity could not be justified, matching was done with 45 percent weighting applied to item 1, and 55 percent to item 2.

As part of the matching procedure, spare cells were provided for each group for the event that one or more cells became damaged prior to final assembly of the batteries. Cells which had apparent or suspected defects were excluded from consideration. This included several cells with damaged cases and others with corrosion at the terminals.

Table 4 gives the results of the matching tests, showing the cells selected for each battery, their positions in the batteries, and their capacities.

TABLE 4

## IDENTIFICATION OF CELLS WITHIN BATTERIES

CELL POSITION	BATTERY No. 1			BATTERY No. 2			BATTERY No. 3			BATTERY No. 4			BATTERY No. 5			BATTERY No. 6			BATTERY No. 7			BATTERY No. 8		
	CELL NO.	CELL AMPERE HOURS	CELL NO.	CELL AMPERE HOURS	CELL NO.	CELL AMPERE HOURS	CELL NO.	CELL AMPERE HOURS	CELL NO.	CELL AMPERE HOURS	CELL NO.	CELL AMPERE HOURS	CELL NO.	CELL AMPERE HOURS	CELL NO.	CELL AMPERE HOURS	CELL NO.	CELL AMPERE HOURS	CELL NO.	CELL AMPERE HOURS	CELL NO.	CELL AMPERE HOURS	CELL NO.	CELL AMPERE HOURS
1	168	75.50	173	78.79	160	81.80	163	82.12	158	83.88	143	86.37	103	87.67	62	93.17								
2	204	76.50	115	76.63	181	80.54	236	82.33	154	84.71	32	85.86	117	87.63	59	89.00								
3	208	73.88	189	80.08	171	80.50	211	82.54	183	84.04	148	86.21	146	87.92	33	91.38								
4	174	73.79	212	77.25	232	80.33	246	83.28	234	84.58	38	85.63	138	87.42	65	92.50								
5	233	72.67	215	77.69	109	81.96	220	82.50	151	84.75	152	86.00	123	88.09	36	90.13								
6	243	76.21	179	80.04	167	81.80	166	83.17	142	84.67	135	86.62	125	88.29	61	90.92								
7	203	72.96	128	80.21	155	81.04	162	84.80	159	83.79	99	85.92	104	86.84	63	89.79								
8	198	76.50	170	77.38	105	81.33	60	83.50	186	83.54	113	85.89	101	87.54	71	92.63								
9	194	75.58	110	77.38	147	82.08	77	82.92	175	84.60	91	85.88	97	87.42	64	89.87								
10	200	76.50	114	79.88	93	81.67	118	83.42	108	84.58	153	86.33	92	86.80	51	89.16								
11	229	75.84	169	77.00	231	81.75	112	82.50	80	84.83	72	85.47	56	88.25	46	92.84								
12	214	76.00	195	80.17	185	81.38	107	82.50	75	83.09	102	86.25	79	88.75	81	91.58								
13	176	76.34	144	76.67	197	80.96	120	83.75	39	84.13	89	86.46	87	88.09	45	91.50								
14	235	73.92	119	79.71	137	81.96	149	82.95	180	85.21	78	86.00	52	86.34	42	92.67								
15	219	74.00	193	79.79	126	80.92	145	82.32	29	84.63	90	85.50	55	88.05	88	91.71								
16	250	74.08	165	78.00	17	80.71	134	83.62	11	84.21	13	85.71	86	86.46	40	90.67								
17	238	76.08	205	78.67	15	80.70	20	82.88	27	84.33	21	86.17	48	87.21	49	93.09								
18	216	75.00	26	80.08	18	81.17	16	82.71	12	84.71	08	85.88	07	86.88	66	91.67								
19	172	74.67	124	77.84	30	80.96	28	83.63	10	84.21	02	85.50	04	88.29	95	89.54								
20	161	76.38	199	78.04	19	80.88	22	83.80	24	84.96	09	85.88	14	88.21	34	91.79								
21	249	74.63	221	77.92	213	82.08	5	83.75	23	84.38	01	86.88	69	86.87	53	95.58								
22	247	74.50	192	79.29	164	81.08	25	83.67	03	85.04	47	85.59	73	87.13	76	89.30								
23	178	73.29	177	77.99	35	80.59	150	83.34	06	84.08	133	85.71	50	87.96	85	91.08								
24	227	74.83	228	77.92	127	80.46	106	82.42	140	85.21	141	85.56	63	87.83	67	92.33								
25	223	76.38	209	77.67	157	81.42	37	83.25	74	84.34	41	86.17	70	88.38	68	91.34								
26	207	75.79	196	78.88	222	81.13	156	82.63	43	85.09	54	86.34	57	88.34	84	90.25								
27	187	75.46	244	79.25	248	80.38	184	83.21	98	84.29	96	86.13	94	88.13	44	91.09								
28	210	76.17	116	77.59	131	81.08	188	82.08	139	84.38	132	85.84	100	87.75	58	91.84								
AVERAGE		75.12		78.49		81.16		83.05		84.50		85.99		87.66		91.37								

#### 4. VENTING

##### REQUIREMENTS

Venting of the cells is required to limit gas pressure within cells during charge and during inadvertant cell reversal. The vent must maintain a minimum internal cell pressure during operation at ambient pressures as low as  $10^{-6}$  mm Hg. Pressure-measuring instrumentation is also required.

##### WORK ACCOMPLISHED

Gassing Considerations. As a silver cadmium cell approaches full charge, some of the current goes into the charge reactions, and some goes into the production of gaseous oxygen. It was necessary to measure gassing rates to provide criteria for the venting components and to establish the best charge control settings.

The setup used in gassing tests is shown in Figure 7. Cells were placed in a controlled-temperature water bath, and the rate of gas evolution was measured by displacement of oxygen-saturated water in glass tubes. The tubes were adjusted in height to eliminate pressure differentials. A micro-rotometer was used to measure high gas flow rates.

Steady state gassing rates at constant voltage appear in Figure 8. These data show that operation at elevated temperature results in higher gassing rates, and also causes the onset of gassing to occur at lower voltages. Thus high temperatures and high charging voltages should be avoided to minimize gas evolution.

Figure 9 shows transient gassing rates as a cell approaches full charge. These data show that to minimize gassing the charge should be terminated before the current stabilizes at its lower level.

Operation of a battery at low pressure is expected to cause gassing to start at lower voltage. The magnitude of this effect was calculated. Assuming 3.5 psia in the cell, the calculation showed that gassing will start at 0.01 volts less than at atmospheric pressure.

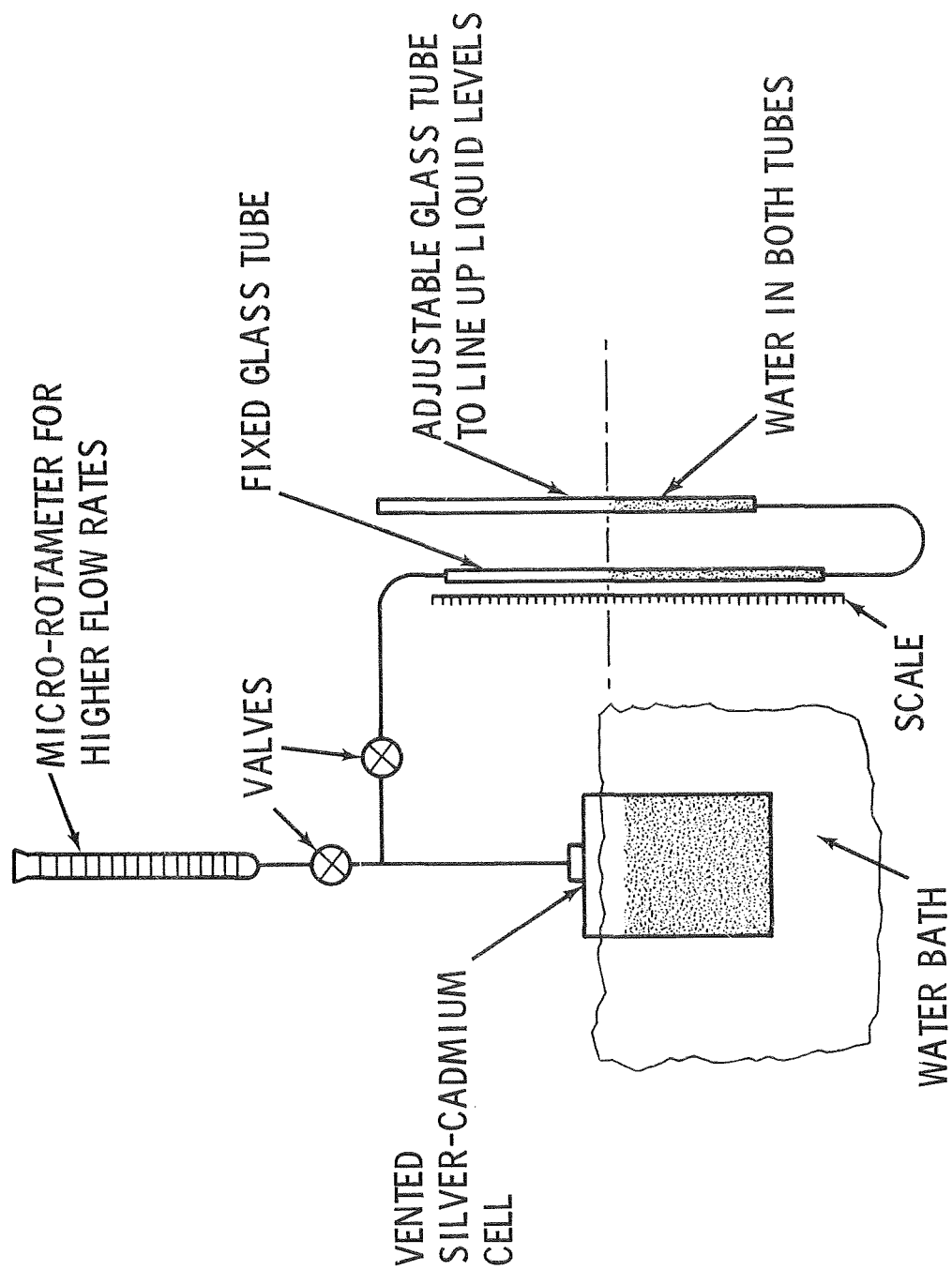
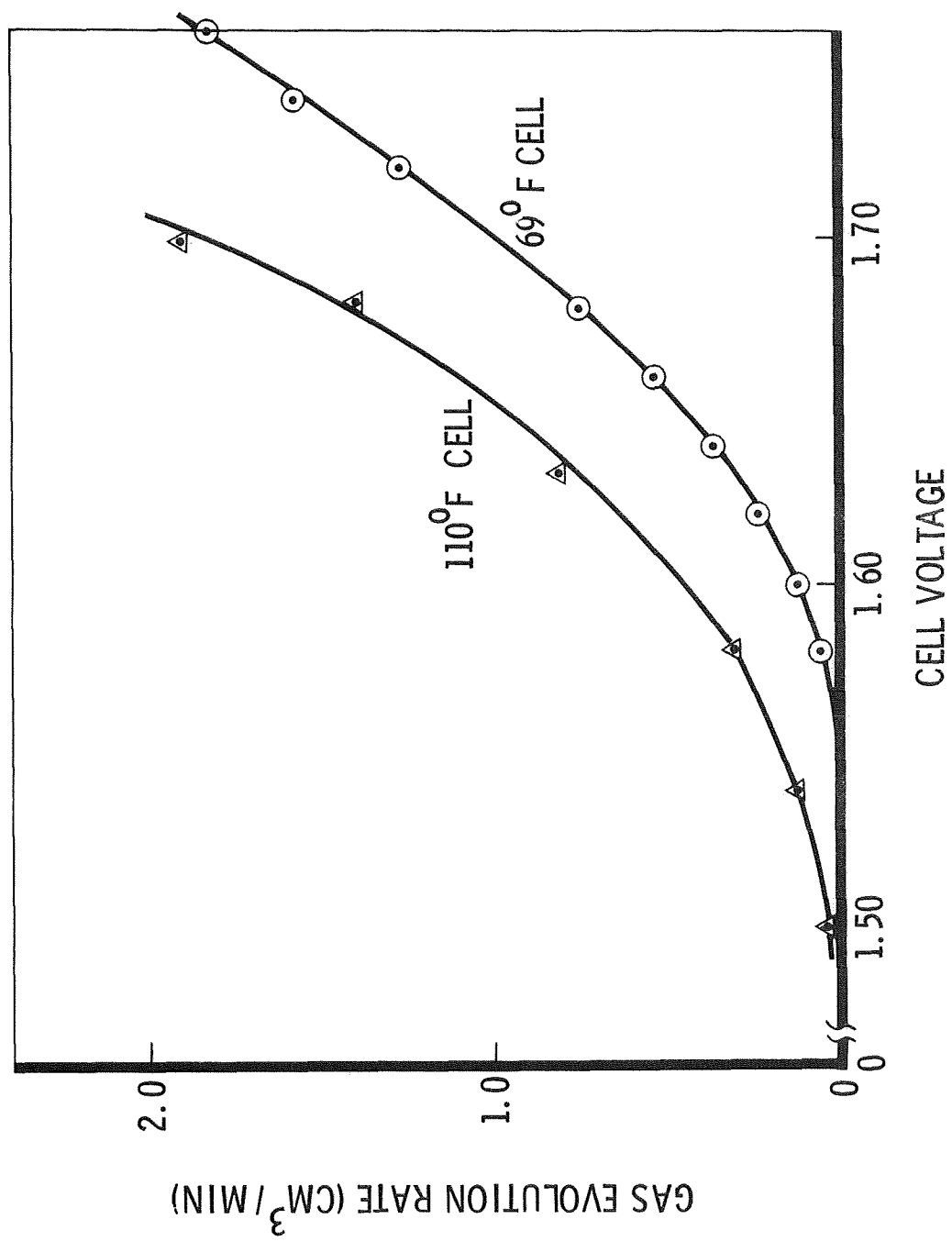


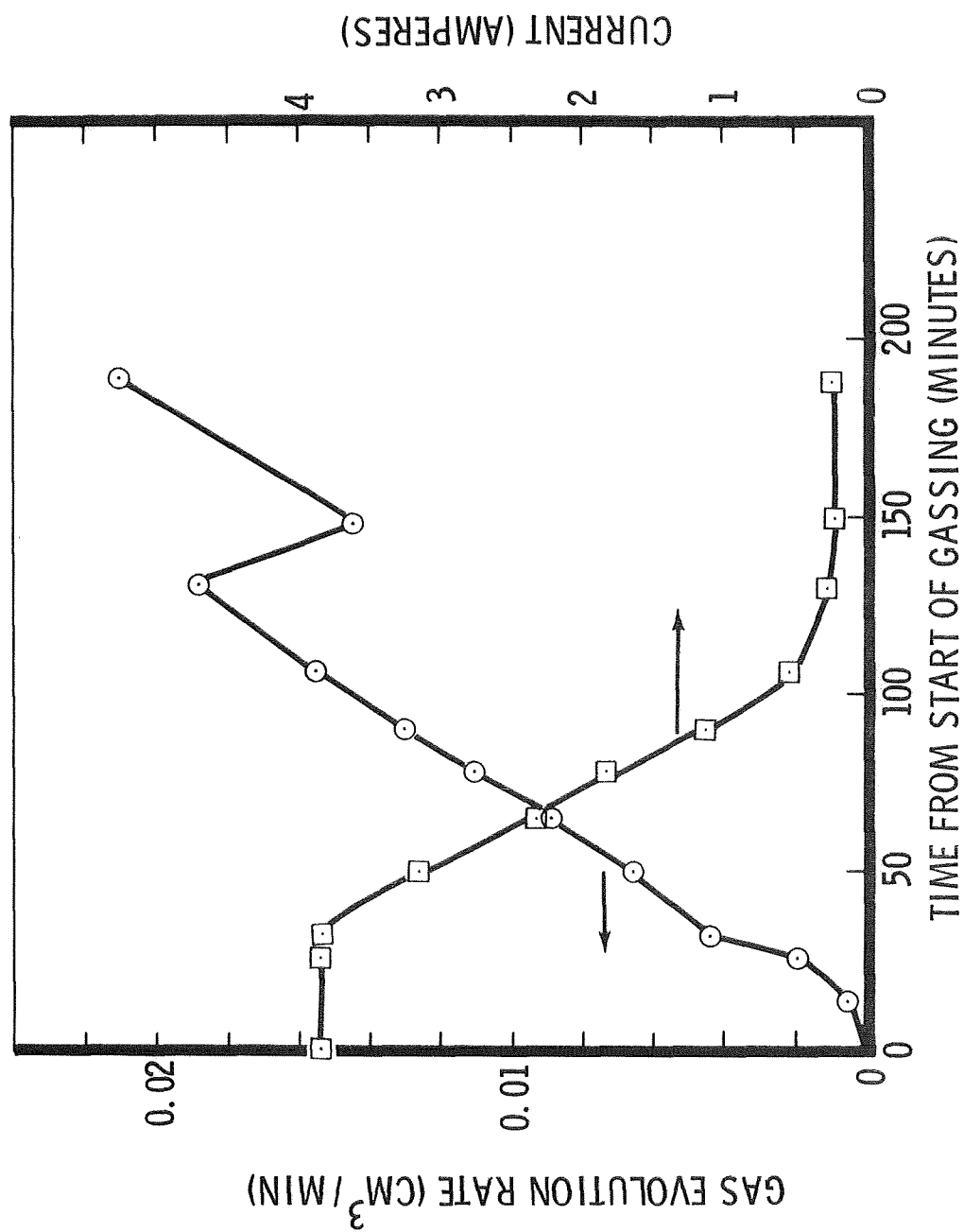
FIGURE 7  
GAS EVOLUTION RATE MEASUREMENT TEST



BASIS  
CURRENT DECAYED TO NEAR ASYMPTOTE LEVEL

FIGURE 8

GASSING RATES AT CONSTANT POTENTIAL OVERCHARGE



BASIS  
 • CHARGE AT 3.9 AMPERES TO 1.55 VOLTS  
 • CELL TEMPERATURE = 70°F

FIGURE 9  
 TRANSIENT GASSING RATES AT END OF CHARGE



The gas evolved at the maximum voltage used in the gassing tests (2.12 volts) was analyzed in a high resolution mass spectrometer, and the results are shown in Table 5. As expected, the evolved gas was mostly oxygen, with only traces of other gases. No hydrogen was present. It is concluded, therefore, that venting of normal silver cadmium cells to the interior of a spacecraft does not create a health hazard. Further investigation may be warranted to ascertain hydrogen evolution from degraded cells.

Design Concept. The adopted cell venting system is shown in Figure 10. All 28 cells are connected to a common manifold having a single pressure relief valve. A removable CO<sub>2</sub> scrubber protects the relief valve from carbonate formation during storage, and a filter protects the relief valve and the pressure transducer from inadvertent contamination.

Two items in venting are critical. One is the separation of gas from liquid in the cell, to prevent liquid carry-over into the manifold. The other is the reliability and performance of the pressure relief valve. These two items have been resolved during investigations summarized below.

Liquid Vapor Separation. Flight-qualified vented batteries will require a means to separate liquid and gas during venting. Though beyond the scope of this program, an attempt was made to see if a simple device could be incorporated into the vent port to achieve this separation at very low gravity. Theoretical studies showed the possibility of using the low wettability of teflon to achieve phase-separation. Various types of teflon and other materials were therefore acquired and tested for ability to separate gas from liquid. These studies and tests showed that:

1. Liquid carryover by gas during venting under gravity conditions is not expected to be a problem, since carryover occurs at vent rates approximately six times higher than the maximum vent rate expected.

TABLE 5  
SPECTROSCOPIC ANALYSIS OF EVOLVED GAS DURING OVERCHARGE

Molecular Weight	Gas	Approximate Quantity	Comment
15	CH <sub>4</sub>	Slight Trace	*
18	H <sub>2</sub> O	Nearly Saturated	Expected
20	Ne	Very Slight Trace	Atmospheric Tract
28	N <sub>2</sub>	Less than 1%	Diluent Gas
29	C <sub>2</sub> H <sub>4</sub>	Slight Trace	*
32	O <sub>2</sub>	Almost 100%	Expected
33	O <sup>16</sup> =O <sup>17</sup>	Very Slight Trace	Natural Isotope
34	O <sup>16</sup> =O <sup>18</sup>	Trace	Natural Isotope
40	A	Slight Trace	Atmospheric Trace
41	Hydrocarbon	Very Slight Trace	*
43	Hydrocarbon	Very Slight Trace	*
44	CO <sub>2</sub>	Trace	

\* Possibly from Apezone grease or Tygon tubing

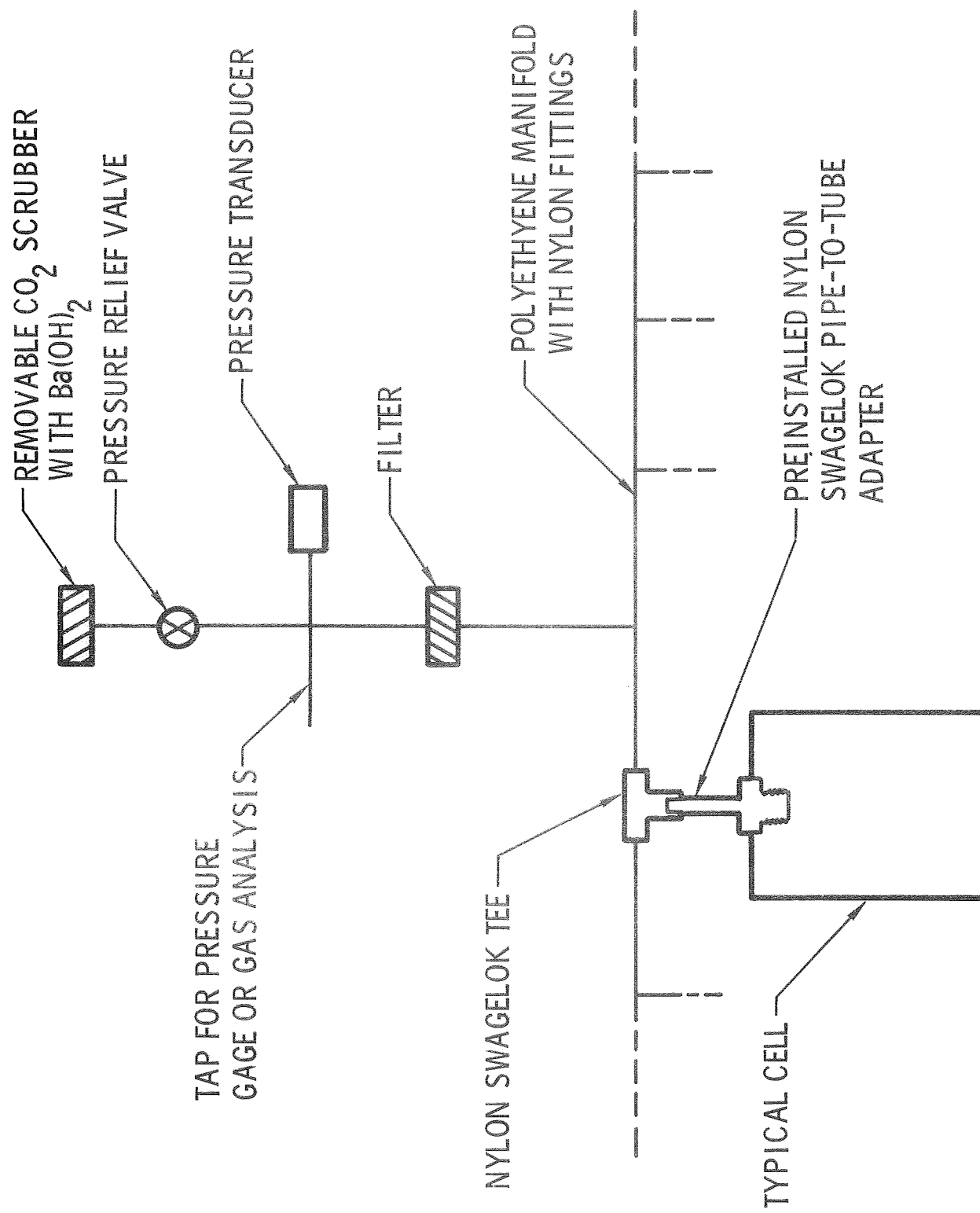


FIGURE 10

CELL VENTING SYSTEM

2. Some type of separation device should be used to trap fine mist, and to confine the electrolyte during occasional sloshing or splashing.
3. Phase separation under gravity conditions is enhanced by increased spacing of the vent above the liquid level.
4. Teflon repels KOH solution well enough to show promise as a liquid-gas separation mechanism in very low gravity.

Based on these tests, a cell-vent was designed to pass gas readily yet restrict the flow of potassium hydroxide solution (KOH). The vent consists of a porous teflon-felt disc with a compression seal near its outside edge. Liquid cannot pass around the edge of the disc, and the non-wetting characteristic of the teflon inhibits liquid escape. In tests with cells inverted for one "g" liquid pressure, no liquid KOH would pass through the vent. It appears that this vent design can be adapted for venting cells in space.

Phase separation for the cells for this program was achieved by appropriate spacing of the vent above the liquid level, and by the use of teflon felt in the vent to trap fine mist.

Pressure Relief Valve. A search for a good pressure relief valve resulted in the choice of a James Pond and Clark "Circle-Seal" pressure relief valve. This valve had been used on several prior space programs. This valve was tested for leakage under several conditions. Figure 11 shows the test set-up used. Air was scrubbed of  $\text{CO}_2$ , and then bubbled through a KOH solution to simulate mist picked up during gassing.

In the first test, the sensitivity of the valve to carbonate formation was determined. The valve was subjected to repeated opening and closing, and no  $\text{CO}_2$  scrubber was used. Reaction of atmospheric carbon dioxide with potassium hydroxide caused potassium carbonate to form within the valve.

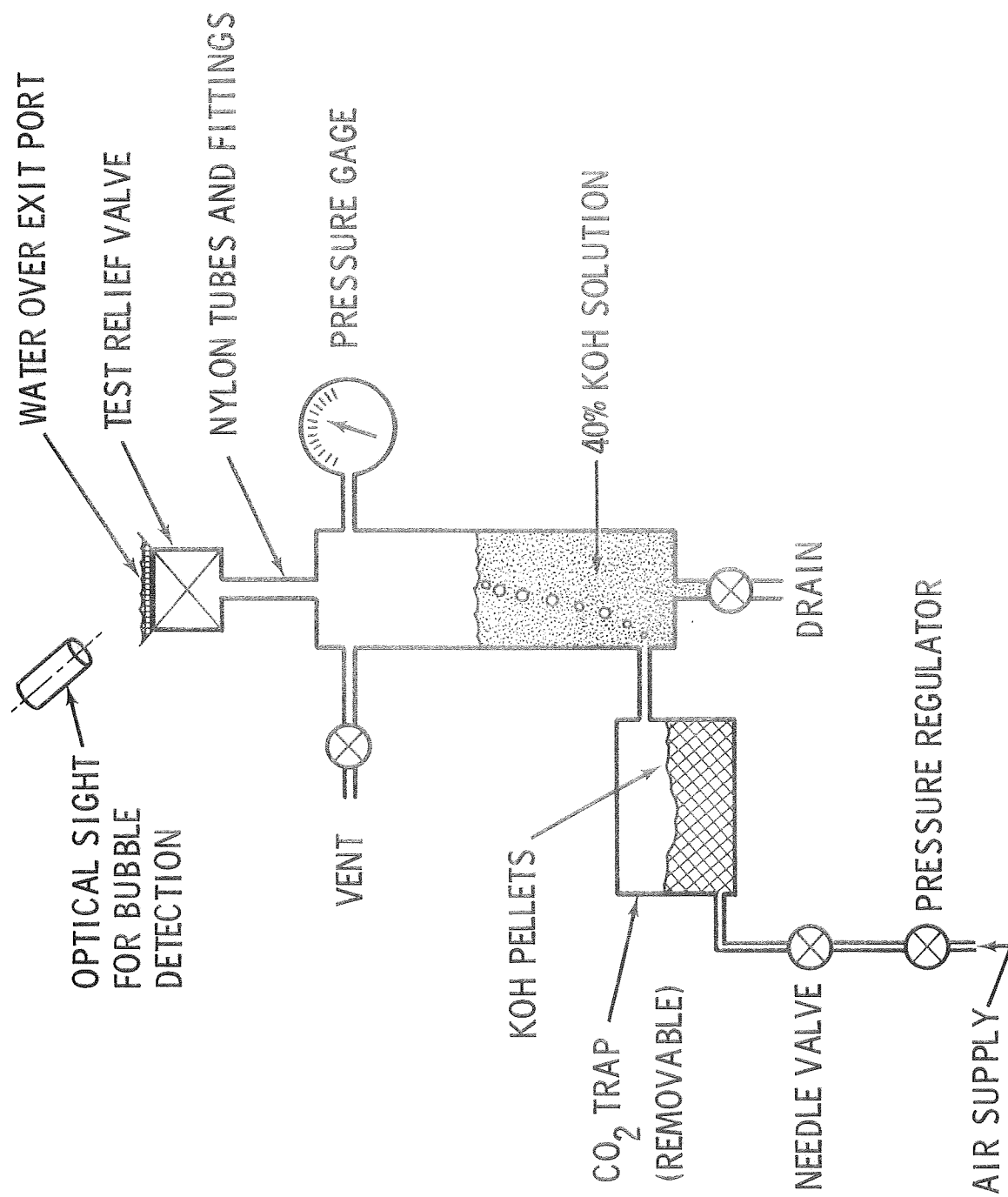


FIGURE 11  
PRESSURE RELIEF VALVE LEAKAGE TEST

The initial effect was increased leakage. As potassium carbonate built up, however, the valve would occasionally stick shut. Once the opening pressure increased from 4.2 psig to 8.1 psig. From this test it was concluded that the valve should be protected from carbonate formation; therefore a removable cannister containing  $\text{Ba}(\text{OH})_2$  is used for  $\text{CO}_2$  removal.

In a second test we measured the leakage of a new valve in a simulated life test. KOH corrosion was accelerated by prior immersion of the valve in a KOH solution at 130°F. After ten days, the valve housing was mildly etched, and the grease in the "O" ring seat had disappeared. The "O" ring itself did not appear to be affected. This valve was then tested for leakage in the test setup shown in Figure 11, with the  $\text{CO}_2$  scrubber installed. Consistent leakage did not appear until approximately three psig was reached, although occasional leakage was observed at lower pressures. Figure 12 shows the highest leakage rates measured.

A reasonable annual oxygen loss in one cell is 1860 cc of gas per year, which corresponds to the electrolysis of 3 cc of water. If one valve per cell is used, the maximum expected leakage is significantly less than 1860 cc per year, as shown in Figure 12. Since one valve will be used to vent 28 cells, the design margin is so large that leakage should not be a problem.

A concern with the pressure relief valve was whether it would pass gas easily enough to prevent significant pressure rise in the cell. Flow characteristics were therefore tested, and the results are shown in Figure 13. Using gas evolution test data as a basis, an estimate was made of the maximum gassing rate that could occur, which is also shown in Figure 13. It was concluded that the maximum pressure in the cell would not exceed 4.4 psig.

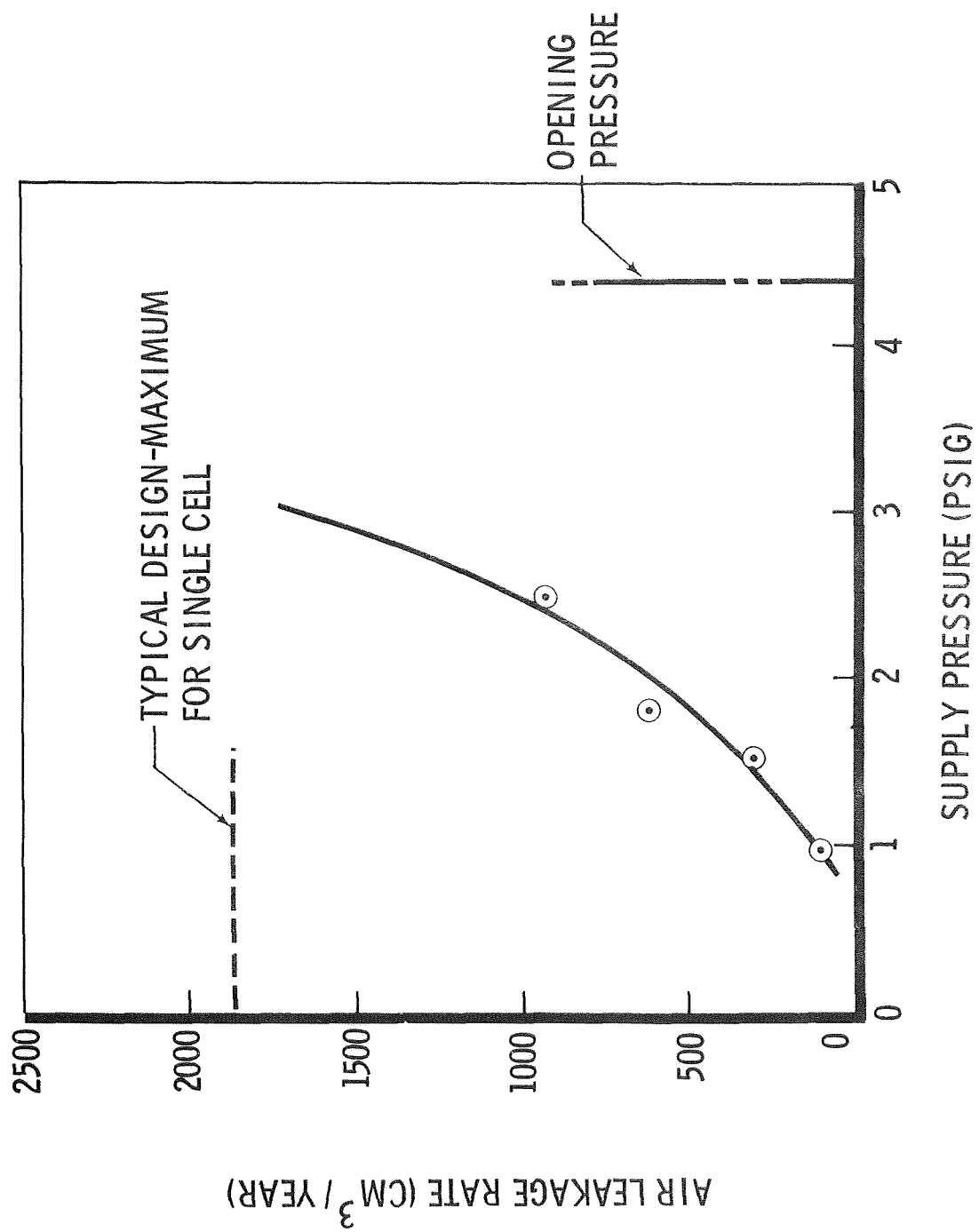


FIGURE 12  
MAXIMUM DETECTED LEAKAGE RATE OF PRESSURE RELIEF VALVE

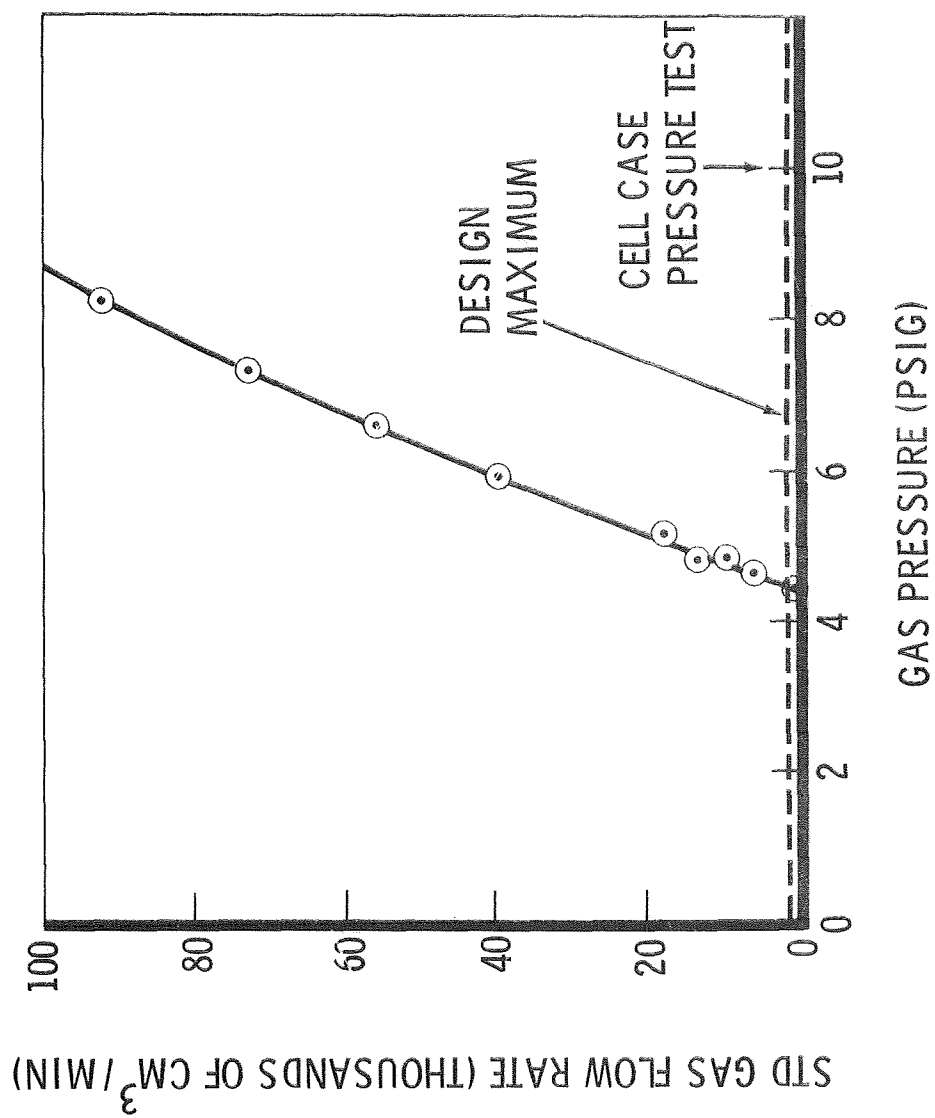


FIGURE 13  
FLOW CHARACTERISTICS OF PRESSURE RELIEF VALVE



## 5.0 BATTERY PACKAGING

### REQUIREMENTS

The batteries built on this contract are for laboratory use, and are not to be flight prototypes. To meet the requirement of 28 volts minimum, we chose to use 28 cells, each of which generates slightly over one volt under critical load. The temperature of the battery is controlled by a NASA-furnished supporting plate which will be maintained between 60°F and 90°F. The battery package must provide for venting of the cells, and must also include instrumentation to measure temperature, pressure and voltage of the cells.

Thermal considerations were important in designing the battery package. The thermal design objectives were:

1. Limit battery internal temperature. Since the cold plate can be as hot as 90°F, it would be possible for a poorly designed battery to have excessive internal temperatures which shorten life.
2. Obtain uniform cell-to-cell temperatures. Some of the battery package designs considered would have permitted centrally located cells to become hotter than peripheral cells. The objective of balanced cells can be met only if all the cells are at nearly the same temperature.
3. Obtain uniform temperature within cells. All the plates in a cell should come to full charge at the same time, the current density should be uniform, and material should not migrate. These objectives are approached only if temperature gradients within cells are limited.

### WORK ACCOMPLISHED

#### Thermal Design

A detailed thermal analysis of a single cell was made to determine the best method of removing internally generated heat. This analysis was based on a 3-dimensional heat transfer model of a rectangular cell with

exterior dimensions of 1.75 in by 2.81 in by 7.25 in, excluding the terminals, which are on the smallest surface and on the top. A cell is composed of 25 plates in a styrene case. Each plate was represented thermally by 20 nodes, resulting in a 530-node model for the cell. Thermal conductances were then calculated.

Six heat-transfer conditions were analyzed to determine the basic limitations on temperature control imposed by characteristics of the cell itself:

1. One face isothermal (2.81 in x 7.25 in surface)
2. One edge isothermal (1.75 in x 7.25 in surface)
3. Bottom isothermal
4. Terminals isothermal
5. One face and bottom isothermal
6. One face, one edge, and bottom isothermal

The isothermal surfaces were heat sinks, held at 70°F. Figure 14 gives the resulting temperature profiles between the centers of the two faces. Results show that the best single surface for heat removal is the face, followed by the edge, bottom, and terminals, in that order. Therefore, further heat removal studies and packaging concepts were based on the use of exterior surfaces, rather than on the use of the terminals.

One possible heat-removal concept used the cell bottom surface and fins on the two faces. Results of an analysis of this approach are given in Figure 15 for 0.040 in. and 0.080 in. fins. The temperature gradients are small for both fin thicknesses. Further calculations have shown that diminishing returns are obtained from fins thicker than 0.040 in. For example, going from 0.040 in. to 0.080 in. fin thickness reduces the average temperature rise by only 5°F from 22°F.

Using the single-cell thermal analyses as a basis, thermal performance guidelines were established to aid in selecting the final packaging design. These guidelines are shown in Table 6.

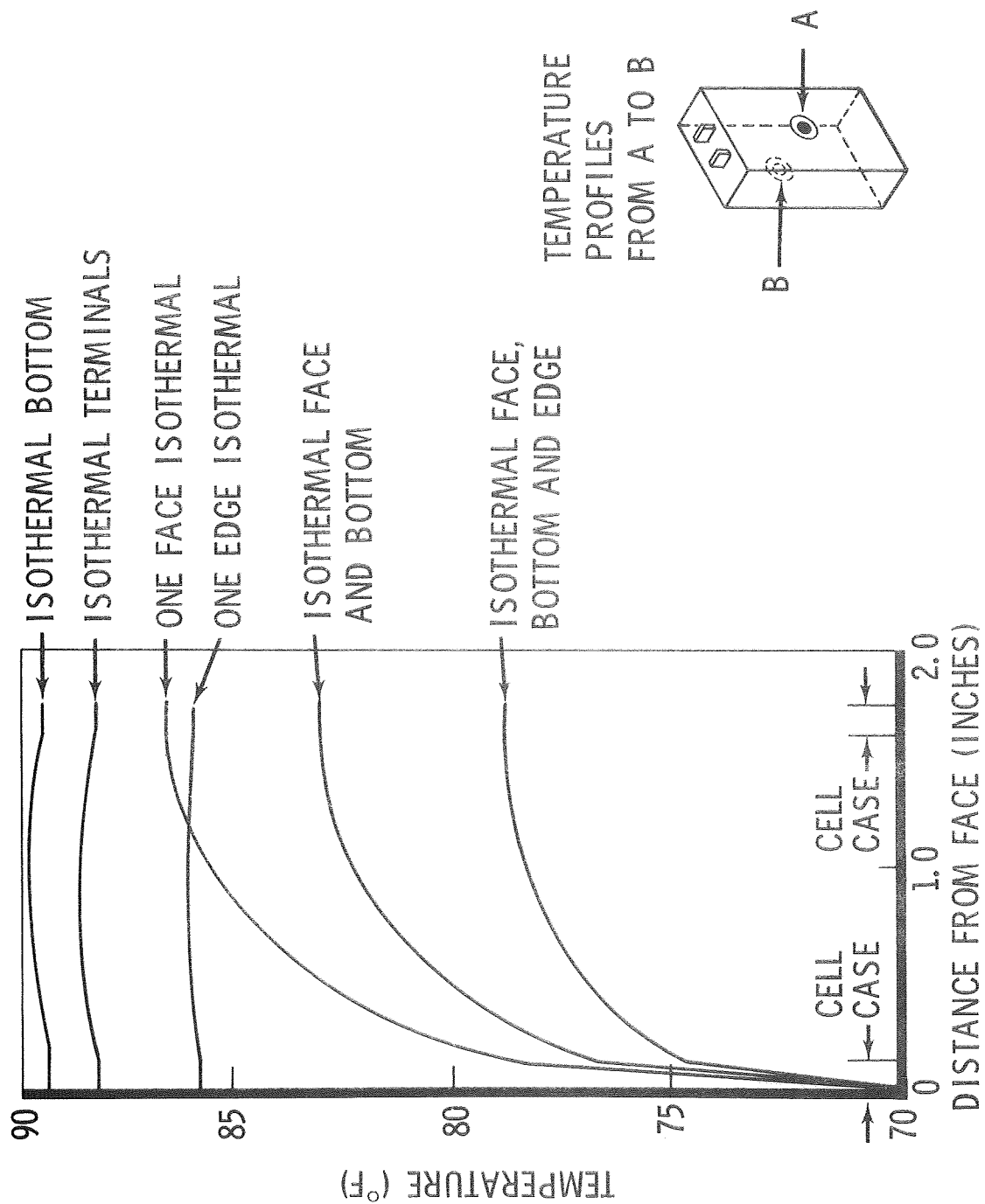


FIGURE 14

TEMPERATURE PROFILES FOR AG-CD CELL WITH ISOTHERMAL BOUNDARIES

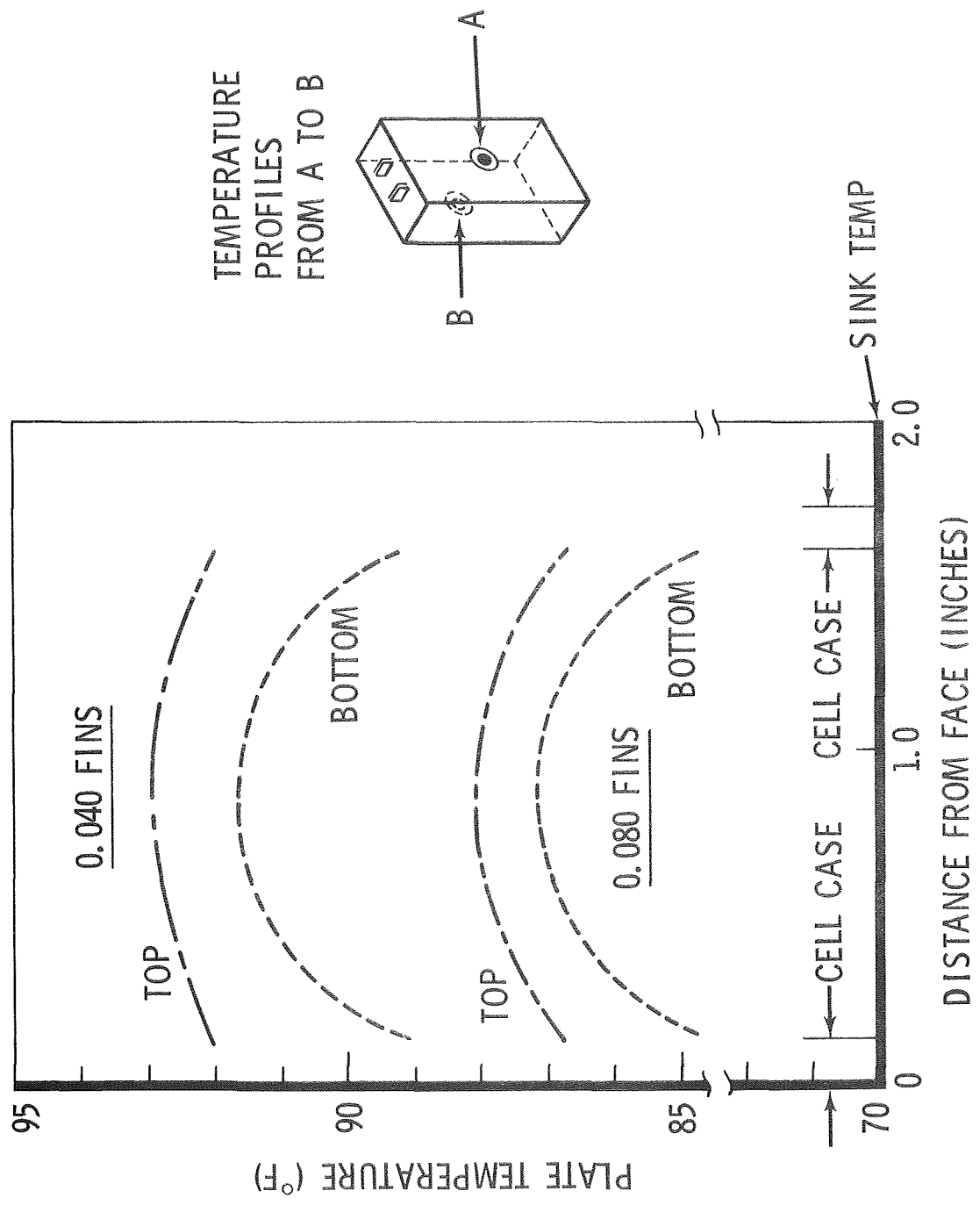


FIGURE 15

AG-CD CELL PLATE TEMPERATURES WITH FINS ON TWO FACES AND BOTTOM

TABLE 6  
GUIDELINES FOR BATTERY CELL THERMAL CONTROL

CELL COOLING APPROACH		THERMAL PERFORMANCE
One Surface	Terminals	Poor, unacceptable
	Bottom	
Two Surfaces	Edge	Fair, acceptable
	Face	
	Edge and bottom	
	Face and bottom	
Three Surfaces	Face and edge	Good, acceptable
	Two edges	
	Two faces	
	Two edges and bottom	
Four Surfaces	One face, one edge and bottom	
	Two edges, one face	
	Two faces and bottom	
	Two faces, one edge	
Five Surfaces	Two edges, one face and bottom	
	Two faces, one edge and bottom	
	Two edges, two faces	
Five Surfaces	Two edges, two faces and bottom	

### Material Selection

The major functions of the package material are to conduct heat and provide mechanical support with low weight. The spectrum of possible materials was narrowed to the magnesium and aluminum alloys in Table 7 which also shows their thermal characteristics. Constant weight is believed to be more applicable of the two comparison criteria, and on this basis the magnesium alloys are generally best, although there is a wide spread between the best and the worst magnesium alloys.

Magnesium was selected for packaging. Advantages of magnesium over aluminum for the battery case and heat transport fins are:

1. Higher strength-to-weight ratio.
2. Higher thermal conduction per unit weight.
3. Greater resistance to potassium hydroxide (KOH) attack.
4. Closer match in thermal expansion with cell case.

The disadvantages of magnesium are:

1. Corrodes easily, and the required corrosion protection may increase the thermal resistance between cells and the cold plate.
2. Fabrication is sometimes difficult and costly.
3. Long delivery time is involved in acquiring some sizes and alloys.

Initial inquiries on the delivery time of magnesium alloys showed that excessively long delivery would be encountered for anything other than thin sheets. Therefore, methods of protecting aluminum from KOH were evaluated to determine if aluminum could be a suitable backup. Tests with a two-step protective coating (BAC 10-16B) showed that good resistance to KOH is achieved if scratches and nicks are absent. This suggests that aluminum could be used if necessary, since KOH would reach the aluminum only in the event of simultaneous cell-case failure, adhesive parting, and damage of the protective coating.

TABLE 7  
THERMAL COMPARISON OF MAGNESIUM AND ALUMINUM ALLOYS

Material		Density ( $\rho$ )  lb/in <sup>3</sup>	Constant Thickness Comparison		Constant Weight Comparison	
			Thermal Conduc- tivity (K) BTU/sec, in, °F	Relative Standing	K/ $\rho$	Relative Standing
Magnesium Alloys	AZ 31B	0.064	$1039 \times 10^{-6}$	10	$1.62 \times 10^{-2}$	12
	HM 21A-T5	0.064	$1828 \times 10^{-6}$	2	$2.86 \times 10^{-2}$	1
	HK 31A-H24	0.065	$1520 \times 10^{-6}$	8	$2.34 \times 10^{-2}$	5
	M1A	0.065	$1740 \times 10^{-6}$	3	$2.68 \times 10^{-2}$	2.
	ZK60-T6	0.066	$1630 \times 10^{-6}$	5	$2.47 \times 10^{-2}$	3
	ZK60A-T5	0.066	$1575 \times 10^{-6}$	7	$2.39 \times 10^{-2}$	4
	ZE10A	0.066	$1470 \times 10^{-6}$	9	$2.23 \times 10^{-2}$	7
Aluminum Alloys	2014-T6	0.101	$1620 \times 10^{-6}$	6	$2.05 \times 10^{-2}$	8
	2024-T3	0.101	$1620 \times 10^{-6}$	6	$1.60 \times 10^{-2}$	13
	2024-T4	0.101	$1620 \times 10^{-6}$	6	$1.60 \times 10^{-2}$	13
	2219-T6	0.102	$1740 \times 10^{-6}$	3	$1.71 \times 10^{-2}$	9
	6061-T6	0.098	$2240 \times 10^{-6}$	1	$2.28 \times 10^{-2}$	6
	7075-T6	0.101	$1680 \times 10^{-6}$	4	$1.66 \times 10^{-2}$	11
	7079-T6	0.099	$1680 \times 10^{-6}$	4	$1.70 \times 10^{-2}$	10

Magnesium of adequate thickness did become available in time, however, though not in the preferred alloys. AZ 31B is the alloy used for the battery package. The preferred alloy was HM 21A-T5, but this alloy could not be obtained in time.

An adhesive is used to thermally and mechanically bond the cells into the battery box. Properties required of this adhesive are:

1. Inert to KOH
2. Inert to magnesium alloys
3. High thermal conductivity
4. Low outgassing
5. Low viscosity for assembly with thin bonding joints
6. High shear and tensile strength, but low peel strength to permit disassembly
7. Good flexibility

Many adhesives were tested. The adhesive finally selected was Boeing formula BMS 8-68, which is a catalytically cured silicon rubber.

#### Battery Package Design

Twenty-three packaging designs were conceived, studied and evaluated. These concepts differed in geometrical layout, structural arrangement, manufacturing technique, and thermal effectiveness as shown in Table 8

In evaluating these designs, substantial weight was given to heat-transfer considerations. Table 9 summarizes the evaluation of battery packaging designs. This evaluation showed the best choice to be concept 6b which was then developed in detail, using a mockup as an aid.

Figure 16 is a photograph of the empty battery case, a drawing of which appears in Figure 17 and 18. Figure 19 is a photograph of the assembled battery package, for which a drawing is given in Figure 20.



TABLE 8  
SUMMARY OF BATTERY PACKAGING CONCEPTS

PACKAGING FEATURE		DESIGN CONCEPT																							
		1a	1b	2a	2b	3a	3b	3c	3d	4a	4b	4c	4d	4e	5a	5b	5c	5d	6a	6b	6c	7a	7b	7c	
Layout	2 x 14 Cells	x	x																	x	x	x			
	4 x 7 Cells			x	x																				
	4-Cell Modules																								
Manufacture	Formed Sheets																								
	Milling	x	x																						
	Welding																								
	Screw Joints																								
	Bolt Joints																								
Heat Transfer	1 Edge	x	x																						
	2 Edges																								
	1 Face																								
	2 Faces	x	x																						
Surfaces of Cells	Bottom	x	x																						
Stacking of Cells	Compact	x	x																						
	Gaps Between Rows																								

## TABLE 9

KEY:  
Poor = 1  
Fair = 2  
Good = 3

[illegible]

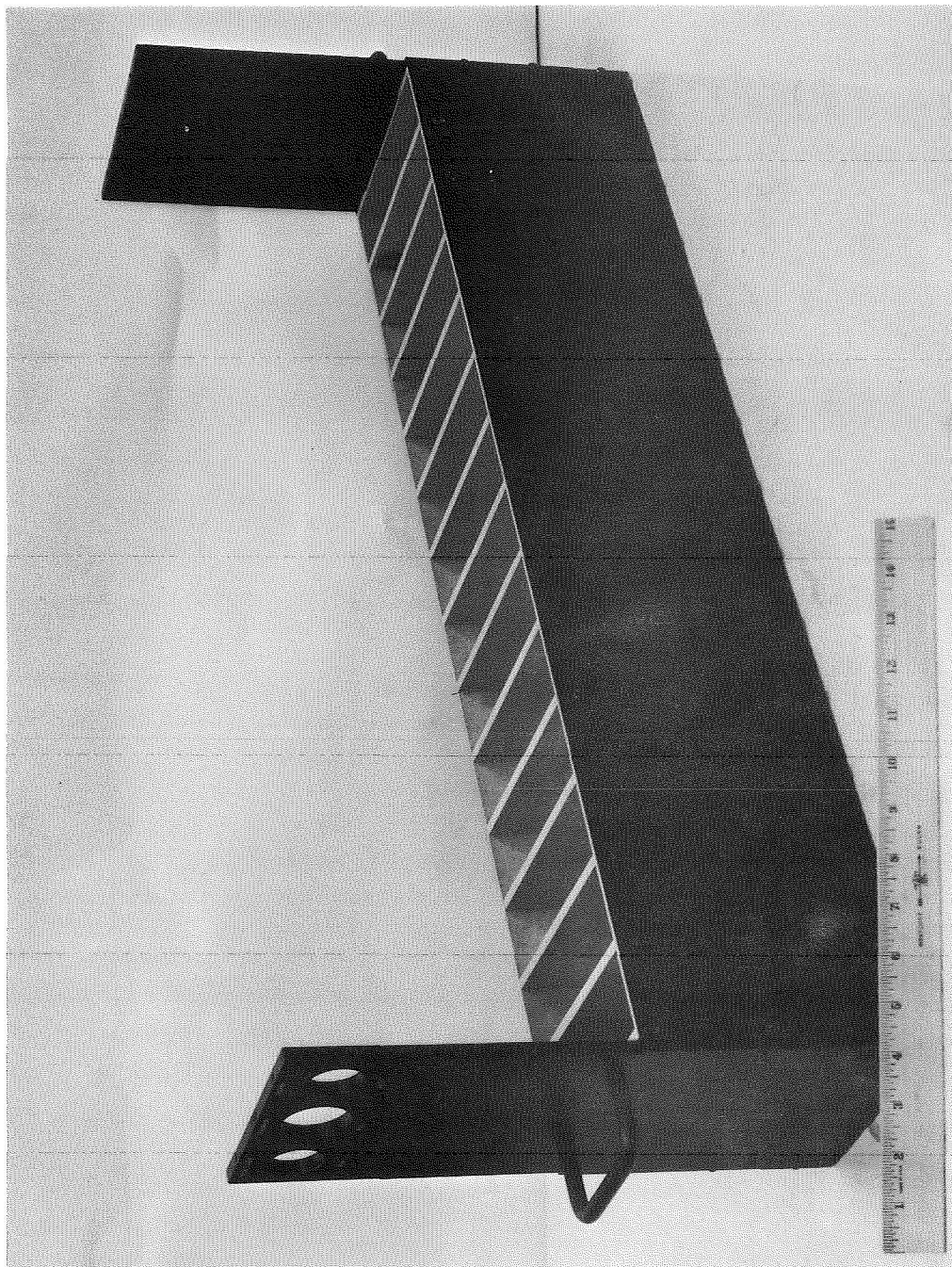


**FIGURE 16**  
**BATTERY CASE ASSEMBLY**







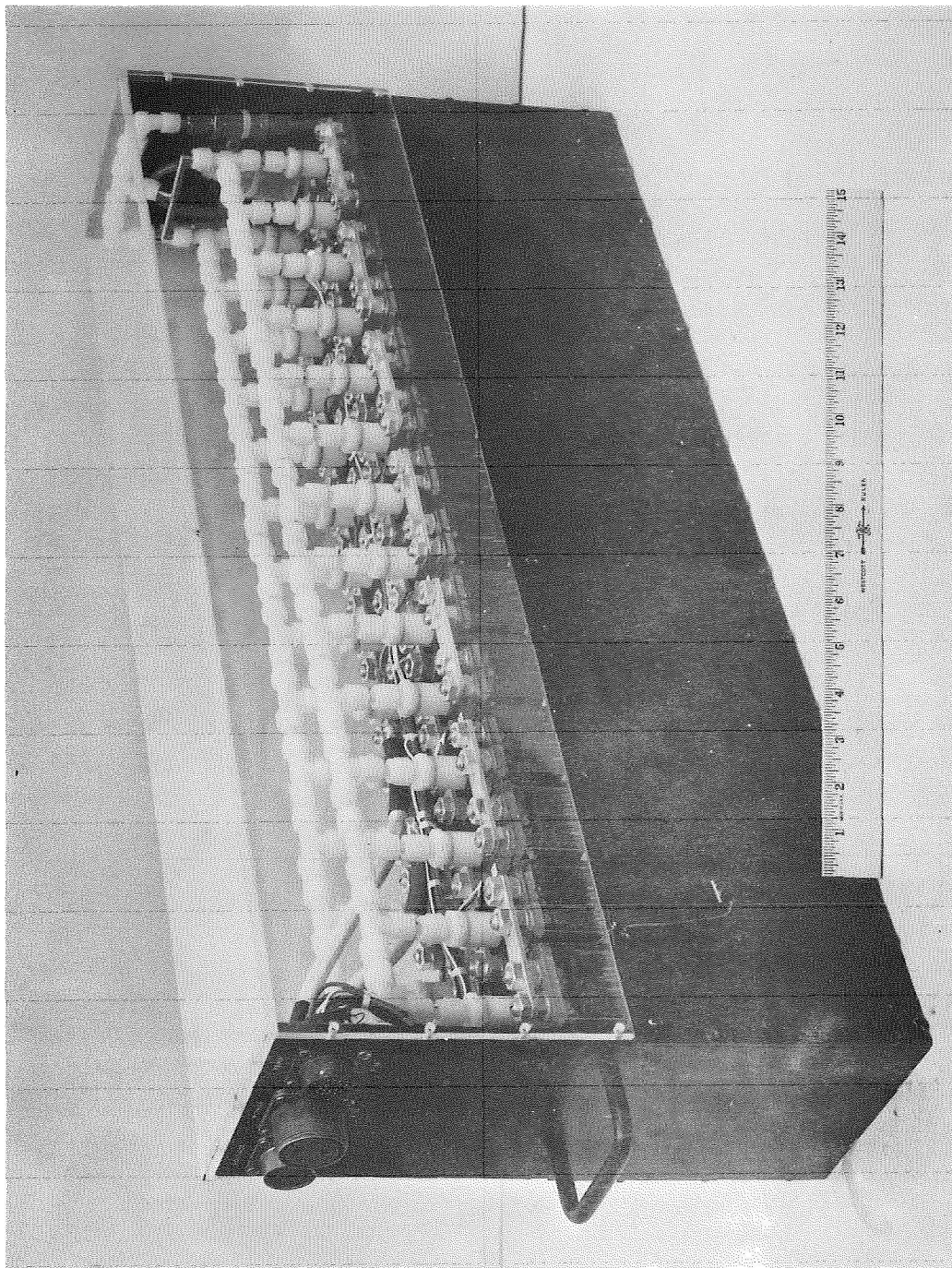
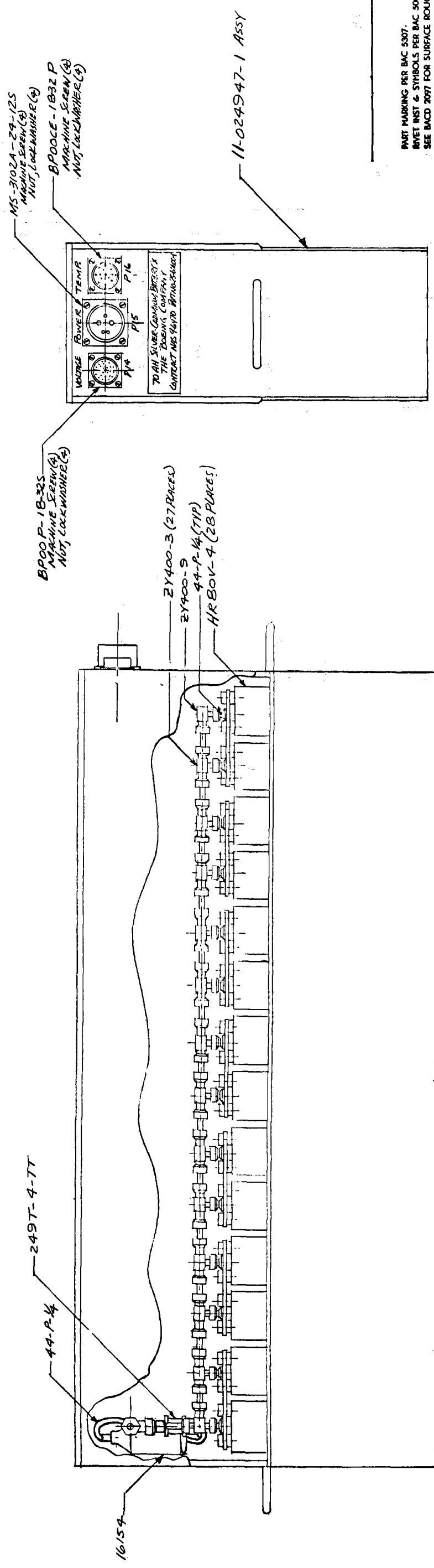
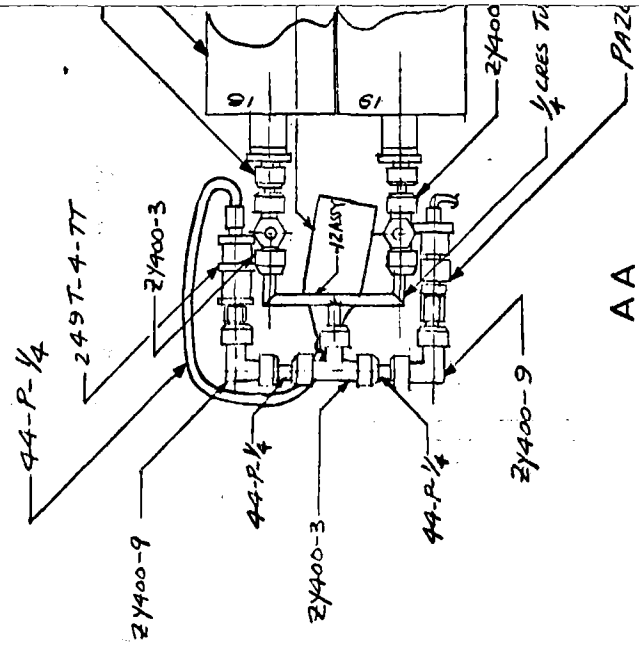


**FIGURE 19**  
**SILVER-CADIUM BATTERY**

PLAIN VIEW  
(PRESSURE TRANSDUCER CHECK VALVE, PLASTIC BOTTLE  
AND 1/2" 4947-4 COVER NOT SHOWN FOR CLARITY)



SIDE VIEW  
(REQUIRE TRANSPARENCY NOT SHOWN FOR CLARITY)

PART MARKING PER BAC 5307.  
 RIVET INCT & SYMBOLS PER BAC 550A.  
 SEE BAC 2097 FOR SURFACE ROUGH-  
 NISS, PUNCH, STRAIGHTEN & FIT  
 METAL PARTS PER BAC 5300.  
 BOLT & NUT INSTALLATION PER BAC 50  
 MATERIAL SUBSTITUTION &  
 EQUIVALENTS PER BAC 5005.  
 FOR FINISH, CODE SEE DC 5000.  
 DWG ORG BY (GROUP) :

2

HRBOV-4 (28 PLATES)

16154

1-3

BNG ASSY

BTC-25-350

16154

PAGE 51

FIGURE 20

1	11-0299474	BATTERY CASE		
15	44-R 1/4	TUBING-PLASTIC	IMPERIAL PL/IRON	EASTMAN
4	21400-9	ELBOW-NYLON		SWAGelok
27	21400-3	TEE-NYLON		SWAGelok
1	16154	PLASTIC BOTTLE		SSCO
2	3676	BUS BAR		YARDNEY ELECT. CORP NEW YORK, N.Y.
25	3677	BUS BAR		YARDNEY ELECT. CORP NEW YORK, N.Y.
1	2474-TT	CHECK VALVE		CIRCLE SEAL ANAHEIM, CALIF.
1	PA2876-25350	PRESSURE TRANSDUCER		STATHAM
1	M3302A-2415	CONNECTOR P15		CANNON
1	EP0000-1833P	CONNECTOR P16		BENDIX CORP.
1	EP0000-1832S	CONNECTOR P14		BENDIX CORP.
28	HRBOV-4	CELL ASSY	DWG 115 3318-1 REV A	YARDNEY ELECT. CORP NEW YORK, N.Y.
-1		CELL INSTALLATION		
1	PART 1A	NOMENCLATURE	MATERIAL	FILE SIZE PART MARK FINISH

DIMENSIONING & TOLERANCING PER MIL-STD-8 UNLESS OTHERWISE SPECIFIED: DIMENSIONS ARE IN INCHES. TOLERANCES: ANGLES ±     DECIMALS ± RIVET & BOLT EDGE MARGINS ± .05 BEND RADIUS: ± .01 ON .03 & .06 ± .03 ON .09 & GREATER SHEET METAL CORNER RADIUS: INT .16 .19 .25 EXT .22 .30 .40	CONTR DR H CLEAVER CHK STRUCT ENGR		THE <b>BOEING</b> COMPANY AERO-SPACE DIVISION SEATTLE, WASHINGTON	
	GR     PROJ NAS-9-6470		BATTERY INSTALLATION	
	SIZE D     CODE IDENT NO 81205		25-60600	
	SCALE 1/2 SIZE		SH 1 OF 2	

ESS.

39.



VENDOR ITEM-SEE  
SOURCE CONTROL  
OR SPECIFICATION  
CONTROL DRAWING.

CHANGE NO.





Weight of each battery less instrumentation is approximately 114.5 pounds with a weight breakdown shown in Table 10. This exceeds the design objective of 85 pounds, primarily because the cells were designed to provide more than the minimum of 70 ampere-hours capacity. A flight-weight version of this battery is expected to be approximately 101.4 pounds, with most of the weight saving in the battery case. Power density of the laboratory and flight versions is at least 17.1 and 19.3 watt-hours/pound, respectively.

Some of the design features are:

1. Cells are laid out in a row two cells wide and 14 cells long.
2. Metal fins are located between each pair of cells.
3. Each cell is cooled by conduction from two faces, one edge, and the bottom. Surfaces not cooled are the top and the second edge.
4. Magnesium is used throughout except for the two high end-pieces, which are non-metallic.

#### Instrumentation

Twelve copper constant thermocouples, terminating at a connector are installed on each battery for temperature measurement. Additional thermocouples are installed on three batteries for calorimetry tests. Thermocouple locations are shown in Figure 21.

Gas pressure in the vent line of each battery is monitored by one absolute-reading pressure transducer. The pressure transducer is resistant to KOH, but a filter is also used to isolate the transducer from KOH mist in the vent line. The transducer circuit is brought to terminals at a connector on the battery case. An amplifier in the charge-discharge controller cabinet converts the pressure transducer output signal to a reading on a panel instrument.

The pressure transducers and their associated circuits were calibrated with a secondary pressure standard having an accuracy of  $\pm 0.05$  percent. Regulated dry nitrogen gas was used as a constant-pressure source, and a Wiancko pressure standard was used for pressure measurements. The electronic circuit description and calibration results are given in Reference 6.

TABLE 10  
BATTERY WEIGHT BREAKDOWN

	NAS 9-6470 Battery <sup>a</sup>	Postulated Flight Design of NAS 9-6470 Battery <sup>a</sup>
	<hr/>	<hr/>
28 Cells	92.07	88.00 <sup>b</sup>
Battery case	17.52	9.50
Vent plumbing	0.57	0.30
Cell connections	3.01	2.00
Power leads and fitting	0.46	0.26
Adhesive	0.90	1.00
Plastic cover	- - <sup>c</sup>	0.30
	<hr/>	<hr/>
TOTAL	114.53 <sup>d</sup>	101.36 <sup>e</sup>

<sup>a</sup>Weight of instrumentation not included

<sup>b</sup>Modifications to cell cases only

<sup>c</sup>Weight of 6.28 lb cover not included

<sup>d</sup>Minimum power density is 17.13 watt-hours/lb based on minimums of 28 volts and 70 ampere-hours.

<sup>e</sup>Minimum power density is 19.3 watt-hours/lb based on minimums of 28 volts and 70 ampere-hours.

Thermocouple No.	Cell No.	Mounting Surface					Location
		Plastic Cell Case	Magnesium Base Plate	Magnesium Edge Plate	Magnesium Cell Spacer	Copper Heat Exchanger	
All Batteries	1	11	X				Near face, centerline, 0.75" from top of cell case
	2	11	X				Bottom surface, centered
	3	7	X				Far face, centerline, 0.75" from top of cell case
	4	7	X				Bottom surface, centered
	5	7		X			Topside slot, centerline, 0.44" from cell inside edge
	6	11		X			Topside slot, centerline, 0.44" from cell inside edge
	7	5	X				Inside edge, centerline, 0.75" from top of cell case
	8	19	X				Inside edge, centerline, 0.75" from top of cell case
	9	6			X		Centerline, 3.62" from bottom of edge plate
	10	26			X		Centerline, 3.62" from bottom of edge plate
	11	--				X	Top edge center of spacer separating cells 4 and 5 from cells 3 and 6
	12	--				X	Top edge center of spacer separating cells 11 and 26 from cells 12 and 25
Extras on batteries 1, 2 & 4	13	11	X				Near face, centerline, 4.88" from bottom of cell
	14	11	X				Near face, centerline, 1.75" from bottom of cell
	15	11	X				Outside edge, centerline, 3.5" from bottom of cell
	16	11	X				Inside edge, centerline, 3.5" from bottom of cell
	17	24		X			Topside slot, centerline, 0.44" from cell inside edge
	18	19		X			Topside slot, centerline, 0.44" from cell inside edge
	19	20			X		Centerline, 3.62" from bottom of edge plate
	20	6				X	Centerline of cell, 1.4" from outside of edge plate
	21	27				X	Centerline of cell, 1.4" from outside of edge plate
	22	14				X	Centerline of cell, 1.4" from outside of edge plate
	23	20				X	Centerline of cell, 1.4" from outside of edge plate
	24	--				X	Top edge center of spacer separating cells 1 and 8 from cells 9 and 28
Extras on 1 & 2	25	11			X		Centerline, 0.5" from top of edge plate
	26	11			X		Centerline, 0.5" from bottom of edge plate

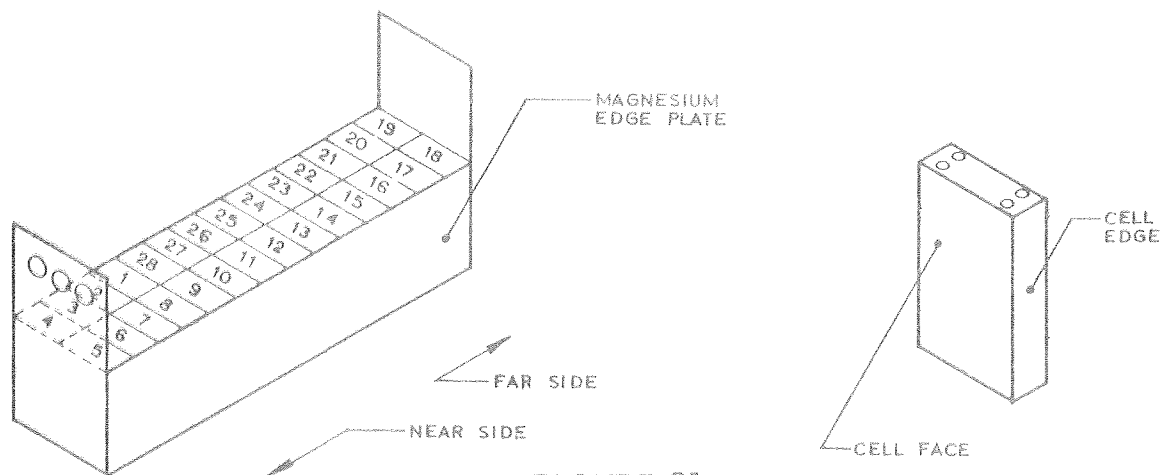


FIGURE 21  
THERMOCOUPLE LOCATIONS

Individual cell voltages can be monitored through a connector on the battery. Total battery voltage is obtained from the appropriate cell-voltage leads. Two additional voltage leads are brought out from the battery for sensing battery voltage at the power supply for charge-control purposes. These leads are shielded.

## 6.0 THERMAL ANALYSIS

### REQUIREMENTS

A contract requirement is a detailed thermal analysis which will predict accurately battery heat generation and temperature over a wide range of operating conditions. A computer program for performing the thermal analysis is to be delivered.

### WORK ACCOMPLISHED

Three methods of predicting heat generation were considered, and the enthalpy voltage method was selected. Experimental correlations of heat generation were obtained using this method, and two computer programs were written for predicting temperature. Good agreement was obtained between predicted and measured temperatures.

Approaches to Heat Generation Correlation. A generalized method of heat generation correlation is necessary for predicting accurately heat generation over a wide range of operating conditions. These three approaches were evaluated for this purpose:

1. Factor analysis method
2. Watt-hour efficiency method
3. Enthalpy voltage method.

Advantages and disadvantages were found for each method as discussed below.

Watt-Hour Efficiency Method. It is sometimes desirable to estimate heat generation even though very little experimental data is available. The power to be delivered is frequently the only well known entity, and a total heat loss prediction is often acceptable. For such applications, watt-hour efficiency is a good basis for estimating the heat generated. The total heat loss for a charge-discharge cycle may then be determined from the efficiency and the energy delivered.

The equations and nomenclature used with this method are as follows.

Repetitive charge-discharge cycling is assumed.

- $Q$  = total heat generated in a charge-discharge cycle (watt-hours)
- $Q_c$  = total heat generated during charge (watt-hours)
- $Q_d$  = total heat generated during discharge (watt-hours)
- $W_d$  = battery energy output during discharge (watt-hours)
- $W_c$  = battery energy input during charge (watt-hours)
- $\eta$  = watt-hour efficiency (discharge/charge)
- $\eta_c$  = watt-hour charge efficiency (stored energy/total energy supplied)
- $\eta_d$  = watt-hour discharge efficiency (recovered energy/stored energy)

The heat generated over a full cycle is then

$$Q = \left( \frac{1-\eta}{\eta} \right) W_d \quad (4)$$

Typical experimental data on watt-hour efficiency are given in Figure 22.

Partition of generated heat between the charge and discharge regimes can be determined experimentally. In tests over a wide range of charge and discharge rates the ratio  $Q_d/Q$  was found to be approximately 2/3. Alternatively, approximations may be obtained by cross-plotting watt-hour efficiency data, and neglecting the small thermal effects due to entropy change. The equation relating charge and discharge efficiencies is

$$\eta = \eta_c \eta_d \quad (5)$$

The heat generated during charge and discharge, respectively, is approximated by

$$Q_c = (1 - \eta_c) W_c = \frac{1 - \eta_c}{\eta} W_d \quad (6)$$

and

$$Q_d = \frac{1 - \eta_d}{\eta_d} W_d \quad (7)$$

BASIS —

- YARDNEY YS-70 CELL
- CHARGE BY CONSTANT CURRENT, LIMITING VOLTAGE
- MAXIMUM CHARGE CURRENT FROM 3 TO 16 AMPERES
- TEMPERATURE FROM 45°F TO 125°F

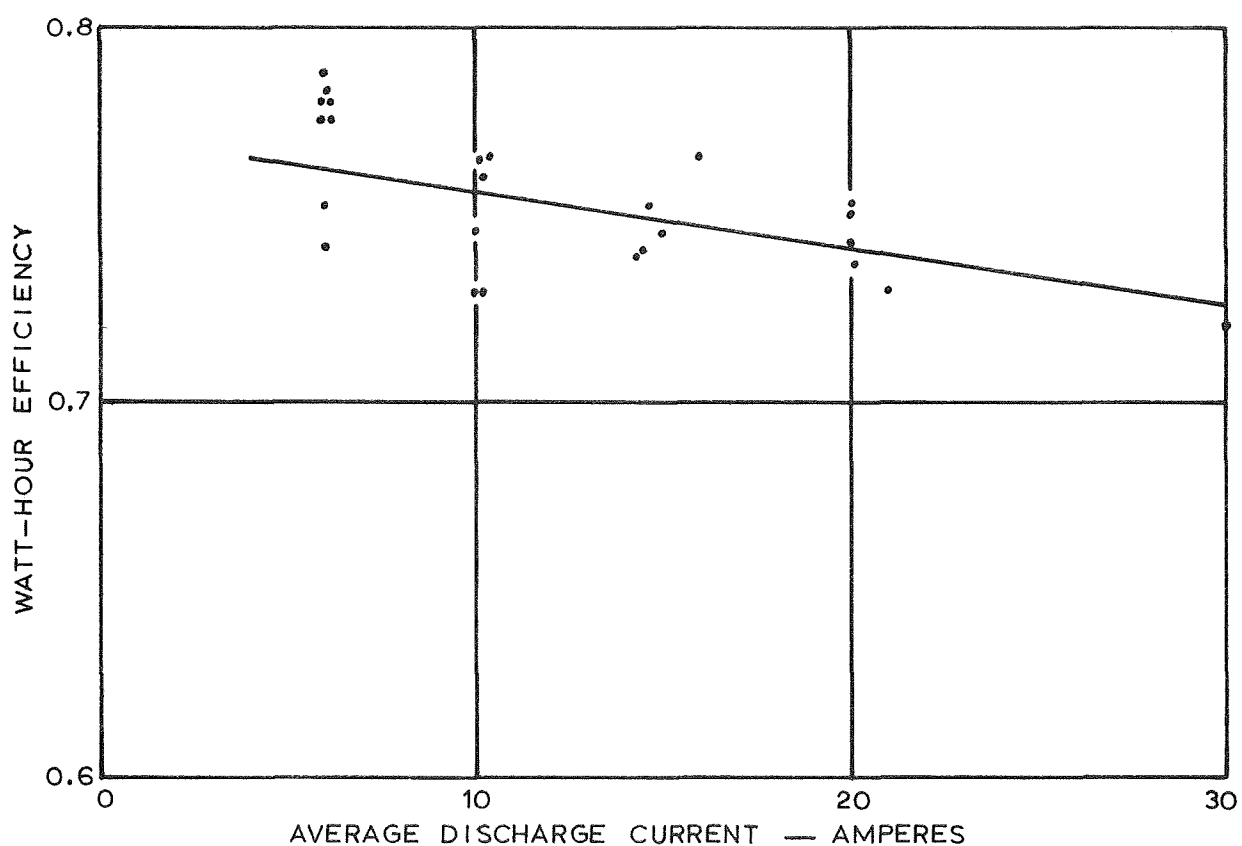


FIGURE 22  
WATT-HOUR EFFICIENCY OF SILVER CADMIUM CELL

The main advantages of this method include:

1. It produces preliminary design data rapidly.
2. It is an easy way to compare different cells and different design conditions. The heat-generation prediction can be provided in parametric form.

The disadvantages of this method are:

1. Total heat generation, rather than the instantaneous heat generation rates is predicted. Analytical procedures could be developed, however, to extend the method to instantaneous rates.
2. Since the calculation is empirical, the experiments may have to be repeated for each cell design of interest.
3. Increased polarization or ohmic losses as the battery ages will alter the results.

Factor Analysis Method. Factor analysis is a statistical approach that can be used to identify the main factors involved in heat generation. A postulated mathematical equation containing functions of candidate factors is tested for its ability to define heat generation. Test data are fitted to this equation by statistical methods, and the main factors involved are then identified. A power series is one of the common equations postulated, and best-fit values for the constants constitute the final results of the analysis. A set of constants so derived can be applied only to one design.

A typical equation used with this method is developed as follows. Define independent variables  $Y_1, Y_2, \dots, Y_m$ . Define dimensional constants  $c_1, c_2, \dots, c_n$ . Let  $q$  equal the instantaneous rate of heat generation. Assume a power series model having up to the fifth power for each independent variable. The resulting equation is

$$q = c_1 + c_2 Y_1 + c_3 Y_1^2 + c_4 Y_1^3 + c_5 Y_1^4 + c_6 Y_1^5 + c_7 Y_2 + c_8 Y_2^2 + \dots + c_n Y_m^5 \quad (8)$$

in which  $n = 1 + 5m$ .



The following variables are considered to be important for a repeating charge-discharge cycle.

1. Charge current
2. Charge duration
3. Limiting voltage during charge
4. Temperature during charge
5. State of charge during charge
6. State of charge during discharge
7. Discharge current
8. Discharge duration
9. Temperature during discharge
10. Number of charge-discharge cycles in the battery's history.

The main advantages of this method include:

1. The important factors influencing heat generation can be identified.
2. This approach can be used to predict voltage as well as heat generation.
3. Chemically generated heat while on inactive stand can be accounted for.
4. The results are empirical, and require a minimum of understanding of the electrochemical processes involved.

The main disadvantages of this method are:

1. The analytical model is an assumed one, and it may not closely represent the actual cell behavior. Interactions between factors can be particularly difficult to evaluate.
2. Many test runs are required before the numerous constants can be evaluated.
3. Since the results are empirical, the experiments may have to be repeated for each cell design of interest.

Enthalpy Voltage Method. The enthalpy voltage method of heat generation prediction is derivable from thermodynamics. It is based on the theory that the heat generation can be determined knowing only cell current, cell voltage, and a term called enthalpy voltage, which may be determined either experimentally or theoretically. The equations used with this method are as follows:

The enthalpy change during a cell reaction is the change in chemical energy content due to the altered chemical composition. The electrical energies withdrawn during discharge and delivered during charge are the time integral products of voltage and current. The difference between them is the energy loss which appears in the form of heat. Thus for one mole

$$Q = \Delta H - \int E i dt \quad \text{for discharge} \quad (9)$$

$$\text{and } Q = \int E i dt - \Delta H \quad \text{for charge} \quad (10)$$

where  $Q$  = total heat generated  
 $\Delta H$  = enthalpy change for the reaction  
 $i$  = current  
 $E$  = voltage at terminals  
 $t$  = time

Charge and discharge are best accounted for by assigning current a positive sign on charge and a negative sign on discharge. The problem of correct units is best handled by expressing the enthalpy change as a voltage. Thus,

$$E_{\Delta H} = \frac{\Delta H}{Z \mathcal{F}} \quad (11)$$

where

$E_{\Delta H}$  = Enthalpy voltage, the voltage corresponding to the heat of reaction of the cell charge-discharge reaction  
 $Z$  = The number of electrons per molecule reacted  
 $\mathcal{F}$  = a Faraday

The heat generation rate for a single electrochemical reaction can therefore be written as

$$q = i (E - E_{\Delta H}) \quad (12)$$

where

$$q = \text{instantaneous heat generation rate}$$

Equation (12) assumes only one chemical reaction, with the term  $E_{\Delta H}$  constant throughout charge and discharge. Under practical operating conditions, the heat generation rate expression must also account for mixed potential reactions and spontaneous reactions. If we assume  $n$  simultaneous electrochemical reactions, then current may be partitioned between the reactions, and the heat generated is as follows.

$$q = ai (E - E_{\Delta H,a}) + bi (E - E_{\Delta H,b}) + \dots + ni (E - E_{\Delta H,n}) + q_{\text{chem}} \quad (13)$$

where

$$a + b + \dots + n = 1.0$$

$$q_{\text{chem}} = \text{the heat generated by spontaneous reactions}$$

An accurate prediction can be obtained by determining the coefficients in equation (13) and using theoretical values for the several enthalpy voltages. If the exact reactions and current distribution in these reactions are not known, then an effective enthalpy voltage may be defined as follows.

$$E_{\Delta H} = aE_{\Delta H,a} + bE_{\Delta H,b} + \dots + nE_{\Delta H,n} + \frac{q_{\text{chem}}}{i} \quad (14)$$

This effective enthalpy voltage, to be used in equation (12), may be determined experimentally. If determined accurately enough, the data can be used to help define the reactions or rates of individual reactions.

The main advantages of this method are:

1. The correlation is directly related to battery chemistry processes, and the results have electrochemical significance.

2. The correlation is simple and encompasses a wide spectrum of operating conditions. Experiments conducted on one cell size or design will often have applicability to other sizes or designs.
3. The increase in polarization or ohmic losses as the battery ages will not alter the validity of the correlation.
4. Improvements in the knowledge of cell reactions can be used to improve heat generation predictions.
5. In a mixed-potential chemical system, the heat generation correlation will provide useful information on the relative rates of the competing reactions.

The main disadvantages of this method are:

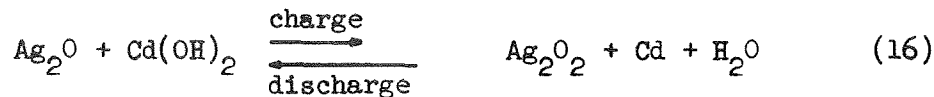
1. At low currents, the calculation requires the difference of two numbers that are nearly equal, and so the percent error may be large, although the absolute error will be small.
2. This method is not suitable when the heat generation due to non-electrochemical reactions is a large fraction of the total heat. For example, a primary silver-zinc cell can generate a small but measurable amount of heat with no current flowing.
3. Data on cell voltage is needed, in addition to the enthalpy voltage, to predict heat generation.

The enthalpy voltage method was selected for this program. Heat generation tests were conducted and the results were correlated by this method. In addition, the theoretical enthalpy voltages shown below were calculated for the dominant reactions in a silver cadmium cell.



$$E_{\Delta H} = 1.250 \text{ volts}$$

Upper Voltage Level



$$E_{\Delta H} = 1.431 \text{ volts}$$

Other reactions of interest in the silver cadmium cell and their calculated enthalpy voltages are as follows.

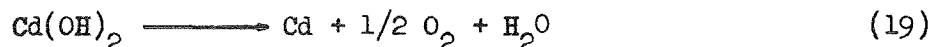


$$E_{\Delta H} = 1.181 \text{ volts}$$



$$E_{\Delta H} = 0.055 \text{ volts}$$

These reactions occur during both charge and discharge. Their reaction rates are not well known.



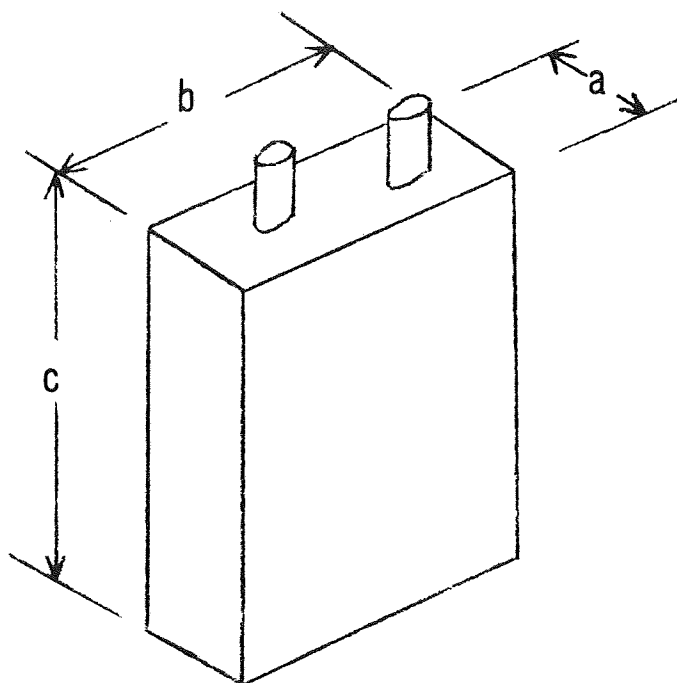
$$E_{\Delta H} = 1.408 \text{ volts}$$

This gas production reaction occurs as the cell approaches full charge, and is of secondary importance in its effect on heat generation.

Heat Generation Test Method. Thermocouples were installed on a Yardney silver-cadmium (YS 70) vented cell. The cell (Figure 23) was then completely encapsulated in waterproofed insulating foam, and the encapsulated assembly was placed in a controlled-temperature water bath. Temperatures, charge and discharge currents, and voltages were continuously monitored as the cell was cycled through charge and discharge.

The instantaneous heat balance of a cell can be expressed as:

$$q = k (T - T_s) + W_c C_c \frac{dT}{dt} \quad (20)$$



		CELL YS 70 - 3
DIMENSIONS	a	1.40 in.
	b	3.63 in.
	c	5.58 in.
AMOUNT OF SILVER		293 grams
AMOUNT OF CdO		395 grams
ELECTRODE AREA		225 in.
WEIGHT		2.51 pounds

FIGURE 23  
SILVER CADMIUM TEST CELL

where

- q = the rate of thermal energy evolved or absorbed by the cell
- k = the equivalent thermal conductance from the cell to the heat sink
- T = the cell temperature
- T<sub>s</sub> = the sink temperature
- W<sub>c</sub> = the weight of the cell
- C<sub>c</sub> = specific heat of the cell
- t = time

Thus, if the thermal conductance and the thermal capacitance are known, then the heat generated by the cell can be determined from the time-temperature plot, obtained as the cell is cycled through charge and discharge.

The average specific heat of the cell for use in equation (20) was measured by observing the temperature rise with time of an electrically-heated insulated cell. Errors due to heat exchange with the environment were minimized by placing the insulated, precooled cell in a constant-temperature water bath, and then determining the temperature-time slope at the point where the cell temperature is equal to the bath temperature. Test results (Figure 24) show that the average specific heat is 0.24 BTU/lb, °F. This value is in good agreement with the specific heat obtained by summing the specific heats of cell components.

The thermal conductance of the insulating encapsulant could not be measured directly or accurately calculated. However, this term was obtained indirectly from test data by using the following reasoning.

If the heat-balance equation is integrated over a complete charge/discharge cycle requiring a time  $t_c$  and if the thermal conductance and capacitance are constant, then the following expression is obtained:

$$\int_0^{t_c} q \, dt = k \int_0^{t_c} (T - T_s) \, dt + (W_c C_c) \int_{T_i}^{T_f} dT \quad (21)$$

where  $T_f$  and  $T_i$  are final and initial cell temperatures for a cycle.

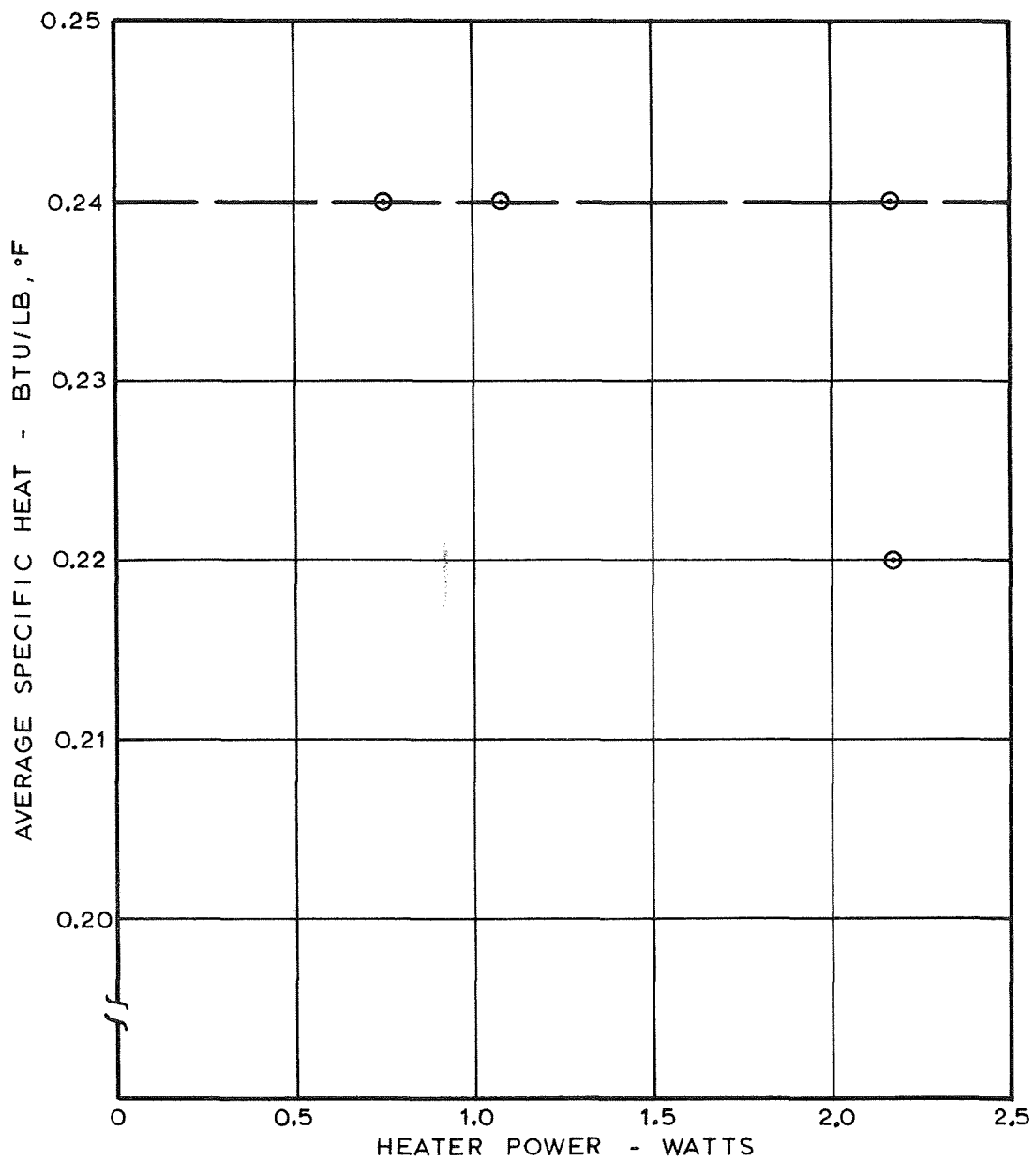


FIGURE 24  
SPECIFIC HEAT TEST OF 70 AH SILVER CADMIUM CELL



The total heat generated within a cycle is equal to the difference between the electrical energy in and the electrical energy out, or:

$$\int_0^{t_c} q \, dt = \int_0^{t_c} E i \, dt \quad (22)$$

Note that the sign of "i" will be positive during charge and negative during discharge.

$$\int_0^{t_c} E i \, dt = k(\bar{T} - \bar{T}_s) t_c + (W_c C_c)(T_f - T_i) \quad (23)$$

where  $\bar{T}_s$  and  $\bar{T}$  are the average temperatures of the sink and of the cell for a cycle, respectively. The temperatures and the thermal capacitance, as well as the quantities in the term on the left side of the equal sign in equation (23) were obtained from test data. The thermal conductance was calculated by solving equation (23) for k.

Experimental Correlation of Heat Generation. Heat generation tests were conducted for a wide variety of conditions, as summarized in Table 11. The tests produced heat generation rates that could be predicted by using equation (12). Although the variables tested had significant effects on the rate of heat generation, the effect on the correlation was only secondary. Typical test results are shown in Figure 25 for charge and discharge.

The greatest difference between predicted and measured heat generation on an instantaneous percentage basis occurred at the end of charge. However, the absolute error in heat generation was small since the end-of-charge current was small.

TABLE 11  
HEAT GENERATION RUNS

RUN	CHARGE		DISCHARGE		CONSTANT CURRENT (CC) OR RESISTIVE LOAD (R)	BATH TEMP. (°F)
	CURRENT (AMPS)	TIME	CURRENT* (AMPS)	TIME		
1	4	20 hrs	3.5	1188 min	cc	65
2	4	20	8	480	cc	65
3	4	19	16	240	cc	65
4	4	19	20	180	cc	65
5	4	19	30	120	cc	65
6	8	10	16	240	cc	65
15-1	12	58 min	15	36	cc	65
-2	12	58	15	36	cc	65
-3	12	58	15	36	cc	65
16-1	12	58	15	36	R	65
-2	12	58	15	36	R	65
-3	12	58	15	36	R	65
17-1	15	58	20	36	cc	65
-2	15	58	20	36	cc	65
-3	15	58	20	36	cc	65
18-1	8	58	10	36	cc	65
-2	8	58	10	36	cc	65
-3	8	58	10	36	cc	65
19-1	8	58	10	36	R	65
-2	8	58	10	36	R	65
-3	8	58	10	36	R	65
20-1	4	58	6	36	cc	65
-2	4	58	6	36	cc	65
-3	4	58	6	36	cc	65
21-1	4	58	6	36	R	65
-2	4	58	6	36	R	65
-3	4	58	6	36	R	65
22-1	4	58	6	36	cc	32
-2	4	58	6	36	cc	32
-3	4	58	6	36	cc	32
23-1	15	58	20	36	cc	32
-2	15	58	20	36	cc	32
-3	15	58	20	36	cc	32
24-1	5	10 hrs	15	2 hrs	cc	32
-2	5	10	15	2	cc	32
-3	5	10	15	2	cc	32
25-1	5	10	15	2	R	32
-2	5	10	15	2	R	32
-3	5	10	15	2	R	32
26-1	5	10	15	2	cc	65
-2	5	10	15	2	cc	65
-3	5	10	15	2	cc	65
27-1	5	10	15	2	R	65
-2	5	10	15	2	R	65
-3	5	10	15	2	R	65

\* TO LIMITING VOLTAGE

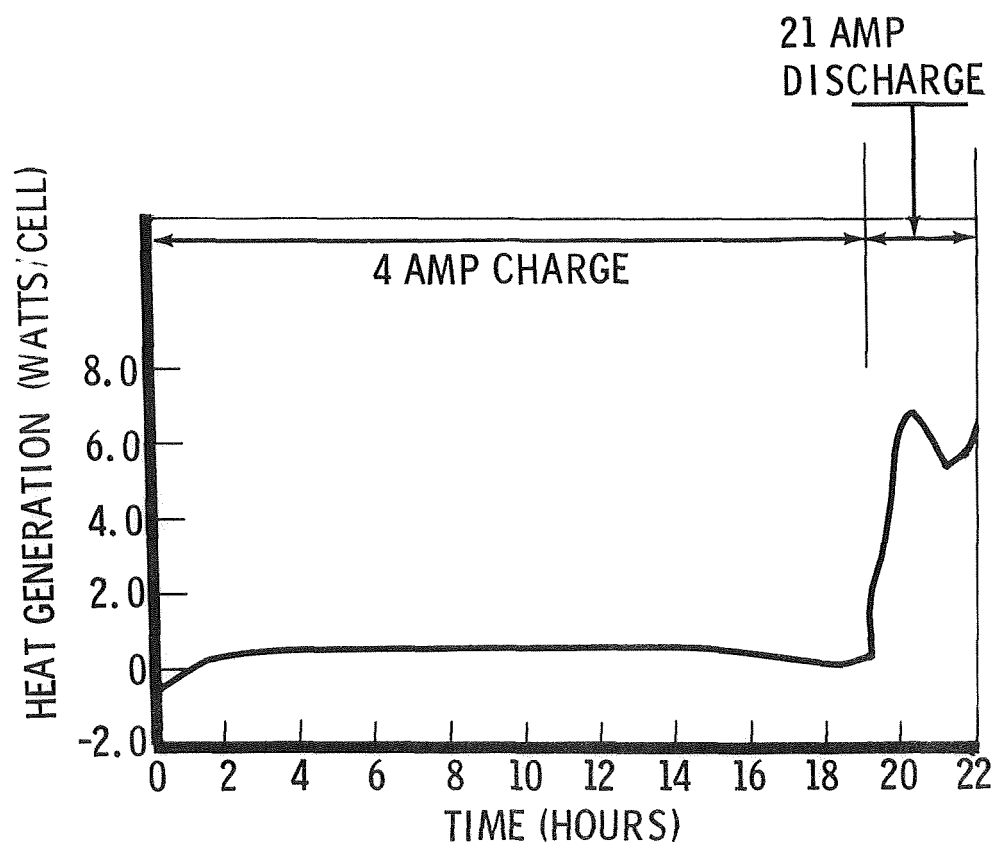


FIGURE 25

TYPICAL HEAT GENERATION TEST RESULTS

The correlation of the enthalpy voltage during charge is summarized in Figure 26. The best fit of the experimental data is shown by the solid line, and the theoretical values are also shown for comparison. The major difference between theory and experiment is that the experimental results show a gradual increase of the enthalpy voltage with time when on the upper plateau.

For discharge, the correlation results in an enthalpy voltage of 1.43 volts for the upper plateau, 1.30 volts for the lower plateau, and an empirical function between these values to bridge the transition between upper and lower plateaus. Typical enthalpy voltage data is given in Figure 27. The best fit of the experimental data shown for the transition region is recommended for use in making analytical predictions. In using Figure 27, correlation time zero must be matched with the onset of the lower voltage-plateau.

Temperature Prediction. The temperature of the battery is predicted by means of an analytical network model of the real battery, solved with a digital computer. The model consists of lumped-mass nodes, heat sources at the nodes, and radiation and solid conductors between nodes. The equation which is solved by the computer is

$$T_1^+ = T_1 + \frac{\Delta t}{C_1} \left[ \sum_j K_{j1} (T_j - T_1) + S_1 \right] \quad (24)$$

where  $T_1^+$  is the future temperature of a typical node  $i$  with heat transfer to  $j$  other nodes. The present temperature is  $T_1$ , thermal capacitance is  $C_1$ , heat sources are designated  $S_1$ , conductors are  $K_{j1}$ , and time is  $t_1$ . Knowing the present temperatures, this equation is applied to each node to yield new temperatures for the complete network.

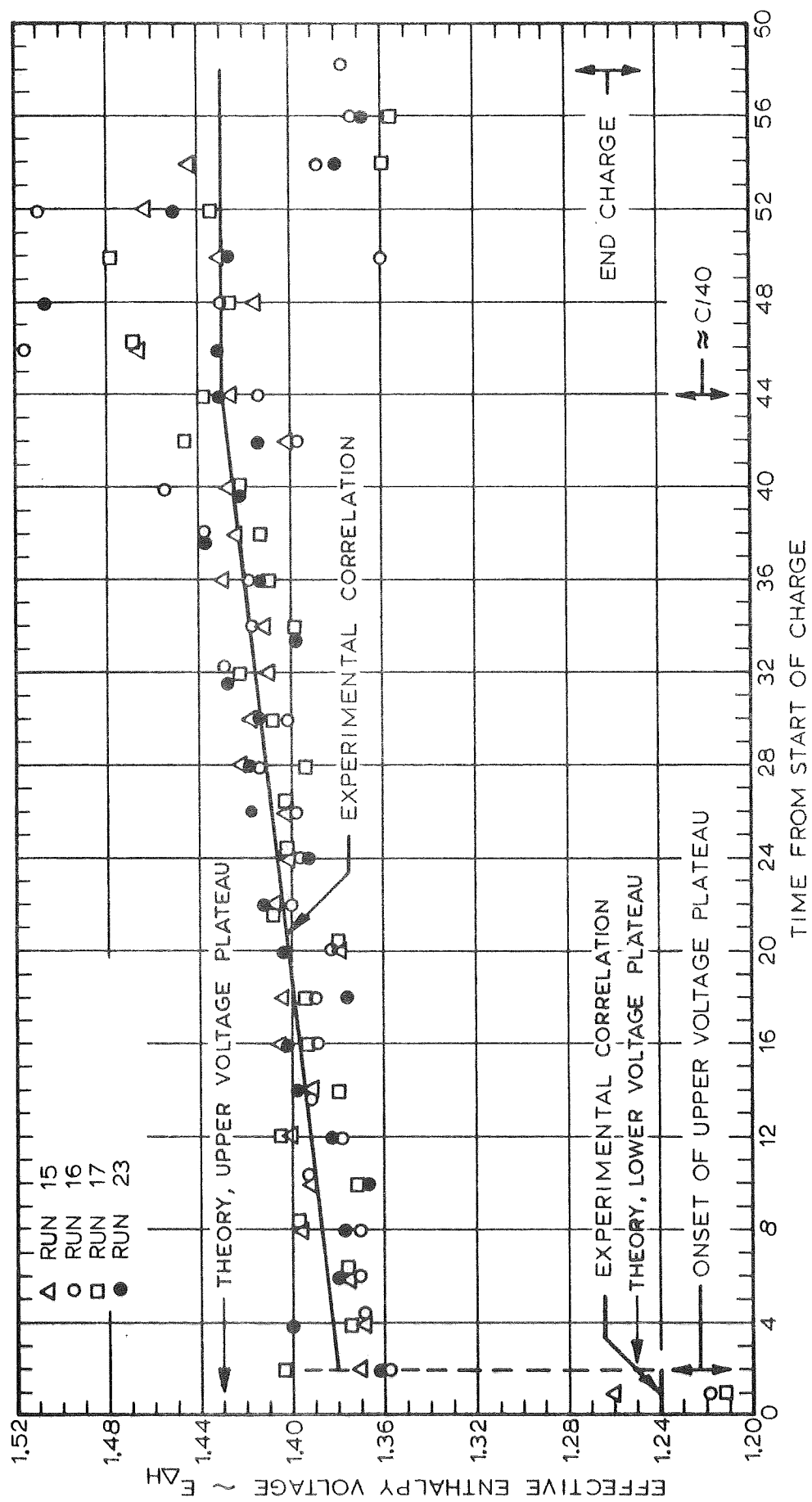


FIGURE 26  
CORRELATION OF HEAT GENERATION ENTHALPY VOLTAGE  
DURING CHARGE

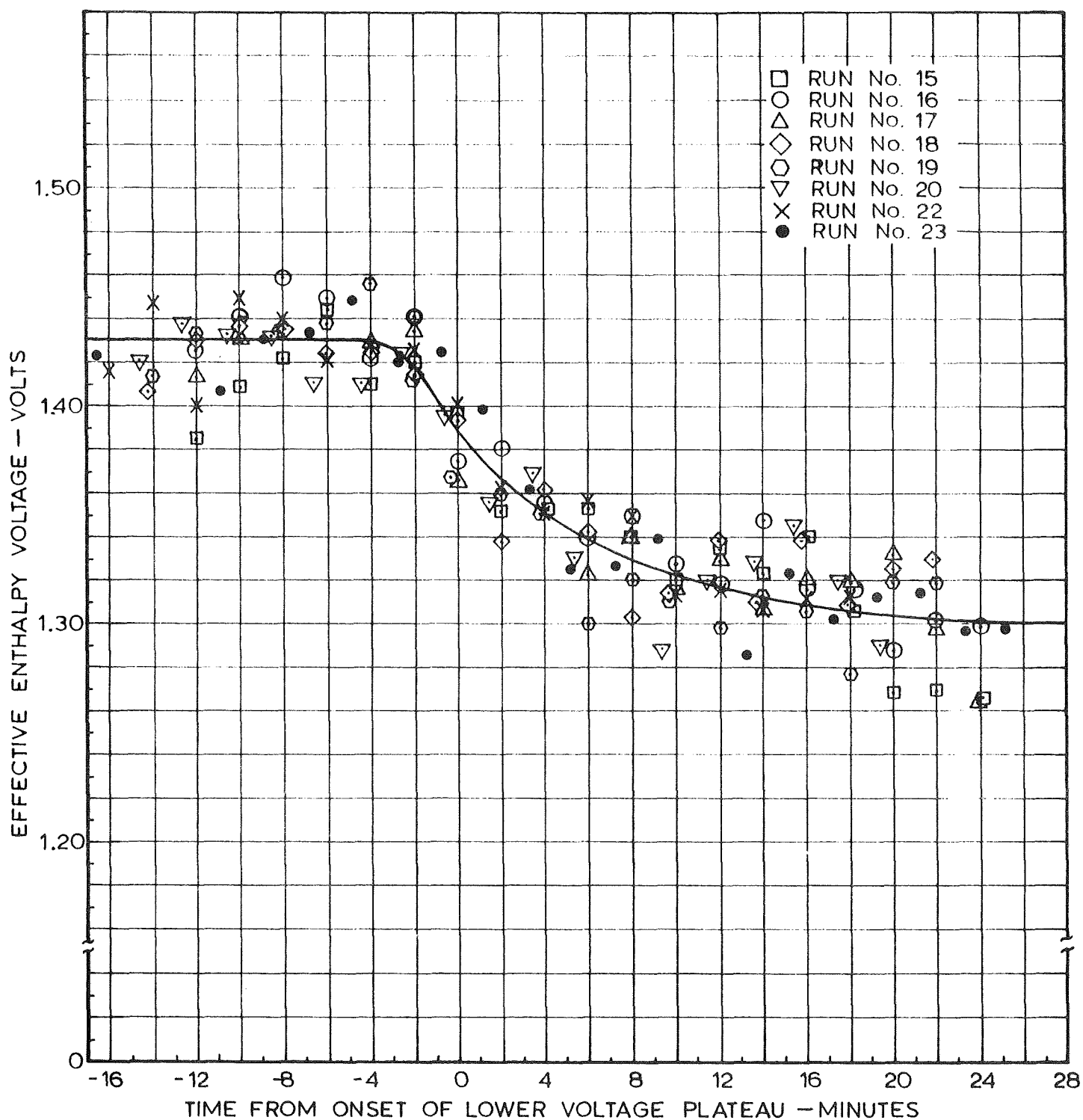


FIGURE 27

CORRELATION OF HEAT GENERATION ENTHALPY VOLTAGE DURING DISCHARGE

In order to obtain thermal conductance data, tests were performed on a 70 ampere-hour silver cadmium cell. The cell was placed in series with a material of known thermal conductivity, and the temperature gradients were compared. Figure 28 shows the test arrangement. Plexiglas Type 2 was chosen as the comparison material because its thermal conductivity is in the proper range and is known accurately.

Test results show that the apparent thermal conductivity parallel to the plates is  $0.42 \text{ BTU/Hr, ft}^2, ^\circ\text{F/ft}$ ; perpendicular to the plates the conductivity is  $0.27 \text{ BTU/Hr, ft}^2, ^\circ\text{F/ft}$ . Results were found to be the same for both a charged cell and a discharged cell, within the experimental error. Also, the experimental results showed fair agreement with theoretical predictions, which gives confidence in the method being used.

The temperature prediction analysis has been used to provide design criteria for battery packaging, as previously discussed. For that analysis, a preliminary model of a single cell was postulated. The analysis produced the data shown in Figures 14 and 15. A refinement of that thermal model was used in the final temperature prediction program.

Thermal Analysis Computer Programs. Two computer programs have been created for thermal analysis of silver-cadmium batteries. The programs have been checked out, verified by comparison with laboratory tests, and are fully described in References 4 and 5. One program analyzes a single cell, and is identified as AS 2747. The other program (AS 2748) analyzes an entire battery. Both programs are coded in Fortran IV for the SNU 1108 computer.

Both programs have flexibility which will permit in-depth thermal studies of batteries. Physical dimensions and material properties can be changed, and heat generation can be varied if desired. The primary cooling method is a cold plate attached to the bottom of the battery case, but radiation and convection heat transfer between the battery case and the environment can also be handled.

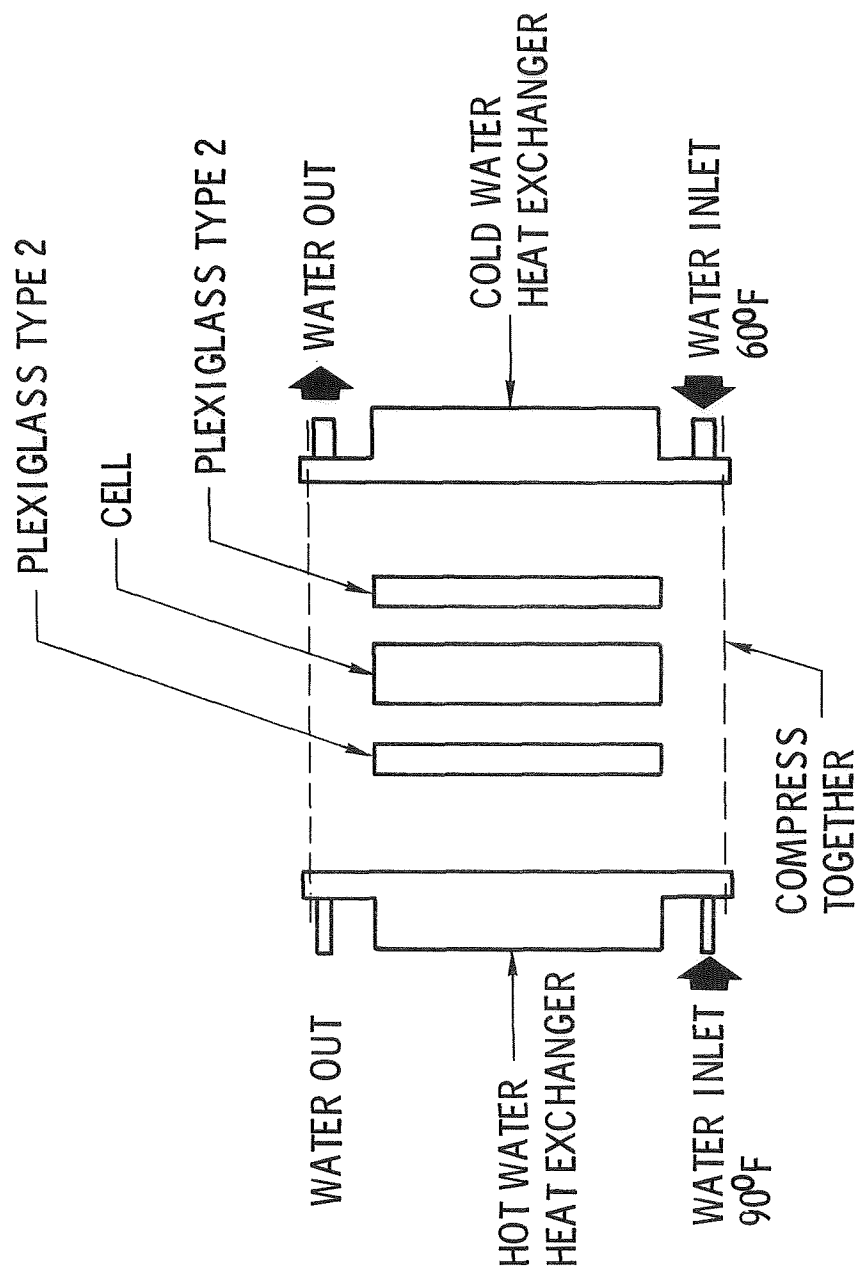


FIGURE 28  
CELL THERMAL CONDUCTIVITY TEST



Summary of Battery Thermal Analysis Computer Program (AS 2748) The battery program is a macroscopic analytical model. Its function is to determine temperature gradients that can occur in the entire battery package. The computation will show the effects of cell imbalance, non-symmetrical packaging, and cold plate asymmetry. Cold plate temperature can be varied as a function of time, with linear temperature gradients permitted in both the length and width direction. Heat generation can be varied from cell to cell, and physical dimensions and material properties can be changed if desired.

Input data for this program are as follows.

A. Mission-time varying functions. This input is composed of tables.

1. Environmental temperature - a single time varying environmental temperature is used for both radiation and convection heat transfer between the battery case and environment.
2. Cold-plate inlet temperature - a node corresponding to inlet of the cold plate can be time varying.
3. Cold-plate temperature gradient - a linear temperature gradient is provided in both the "length" and "width" directions of the cold plate. Both gradients may be time-varying functions.
4. Heat generated - time varying functions required for this calculation are current, cell average voltage, and effective enthalpy voltage.

B. Constant-value input functions. Normally these would not be changed, but they are in "battery language" and can be changed if desired.

1. Geometry and thermal properties of spacers between cells.
2. Geometry and thermal properties of battery-case sides and ends.
3. Thermal contact resistance between spacers and case bottom. This resistance can be made zero for welded or cast cases without causing problems with the computing-time step.

4. Thickness and thermal properties of the insulation around the battery, if used.
5. Cell thermal conductivity in the X, Y and Z directions.
6. Heat generated within each cell. This heat generation may be uniform or may vary among the cells. Uniform heat generation will result automatically unless distribution between cells is specified. Nonuniform heat generation is obtained by specifying for each cell its percentage above or below the average heat generation for the battery.
7. Convection heat transfer between battery case and environment. This input is based on atmospheric pressure. A zero-gravity or zero-pressure input is obtained through the FUNCT subroutine.

The computer printout for this program includes, in addition to the input data, the following:

A. Temperatures

1. Eight nodes for each cell
2. Two nodes for cold plate under each cell
3. One node for each terminal (2 per cell)
4. Cold plate inlet temperature
5. Cold plate temperature gradient in "length" and "width" directions ( $^{\circ}\text{F}$  for each cell)

B. Heat transfer rates

1. Cell bottom to battery case bottom (each cell)
2. Spacer to battery case bottom (each spacer)
3. Battery case side to battery case bottom at each cell
4. Total heat from battery to cold plate.

C. Heat generation rates

1. Each cell
2. Total battery

Summary of Single Cell Thermal Analysis Computer Program (AS 2747). The single cell program is a microscopic analytical model. Its function is to give fine resolution of temperature gradients within a cell, calculating data of a type that cannot be measured easily. This program will be useful in predicting the effects of cell design changes, and in analyzing effects of non-uniform design or non-uniform heat generation. Physical dimensions and material properties can be changed as required, and heat generation can be varied within the plates and from plate to plate.

Input data for this program are as follows:

- A. Mission-time varying functions. This input is made with tables.
  - 1. Environmental temperature. A single time-varying environmental temperature is used for both radiation and convection heat transfer between the cell and environment.
  - 2. Cold-plate temperature. This temperature is assumed to be isothermal but time-varying.
  - 3. Heat generated. Time varying functions required for this parameter are current, cell average voltage, and effective enthalpy voltage.
- B. Constant-value input functions. Normally these inputs would not be changed, but they are in "battery language" and can be changed if desired.
  - 1. Anode plate dimensions and thermal properties
  - 2. Cathode plate dimensions and thermal properties
  - 3. Physical and thermal properties of electrolyte and separators in X, Y and Z directions
  - 4. Cell-case dimensions and thermal properties
  - 5. Geometry and thermal properties of spacers between cells
  - 6. Geometry and thermal properties of adhesive on cell.
  - 7. Heat generation. This is normally uniform within the cell, but it may be made non-uniform through the FUNCT subroutine.
  - 8. Convection heat transfer with the environment. This heat transfer is based on atmospheric pressure. A zero-gravity or zero-pressure condition may be specified through FUNCT subroutine.

The printout for this program includes the input data and the following;

A. Temperatures.

1. Temperatures on plates, in groups of five plates
2. Temperatures on spacers
3. Temperature of battery case side

B. Heat transfer rates

1. Cell bottom to battery case bottom
2. Spacer to battery case bottom
3. Cell to spacer
4. Battery case side to battery case bottom
5. Total heat from cell to cold plate

C. Heat generation rates

1. Each group of five plates
2. Total for the cell

Comparison with Experiments. Two laboratory tests were conducted on completed batteries to compare temperatures with computed predictions. "Worst case" test conditions were chosen. The first test was designed so that the heat storage in the battery would be a major factor, and the second test was designed so that the external heat exchange would have its greatest effect.

In the first test an isothermal battery attached to a cold plate was discharged at about 30 amperes for 0.6 hours, then left inactive for a long period. In the second test a battery was cycled to simulate the design 94-minute orbit (about 18 amperes charge, 29 amperes discharge). Temperatures, voltage and current were recorded. The current and voltage values were used as inputs for the analytical predictions. Analytical and experimental temperatures are compared in Figures 29 and 30. The largest difference is 2°F, which is considered acceptable. Both experimental error and analytical inaccuracy contribute to this difference.

It is interesting to observe the difference in temperature slope between analytical and experimental results for the first test after power was stopped. Part of this difference is attributed to spontaneous chemical reactions.

BASIS:

- EXPERIMENTAL BATTERY RUN C-1
- DISCHARGE 0.6 HOURS, THEN OPEN CIRCUIT

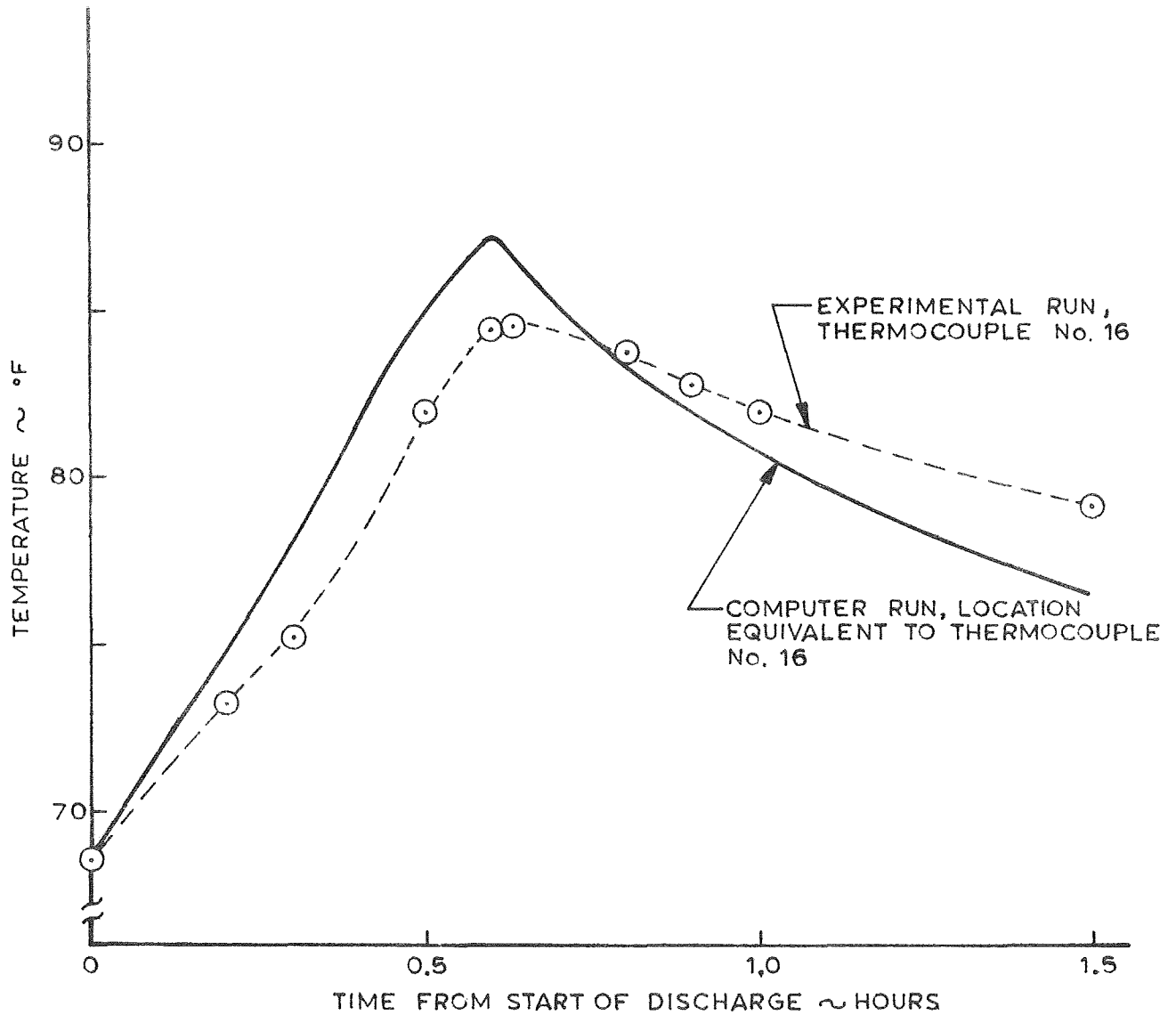


FIGURE 29  
COMPARISON OF ANALYTICAL AND EXPERIMENTAL BATTERY  
TEMPERATURES, CASE 1

BASIS

- EXPERIMENTAL BATTERY RUN C-4
- 96 MINUTES CYCLE, 36 MINUTES DISCHARGE AT 29.6 AMPERES, THEN 58 MINUTES CHARGE AT 15 TO 18.5 AMPERES.
- COLD PLATE AT 68.5°F

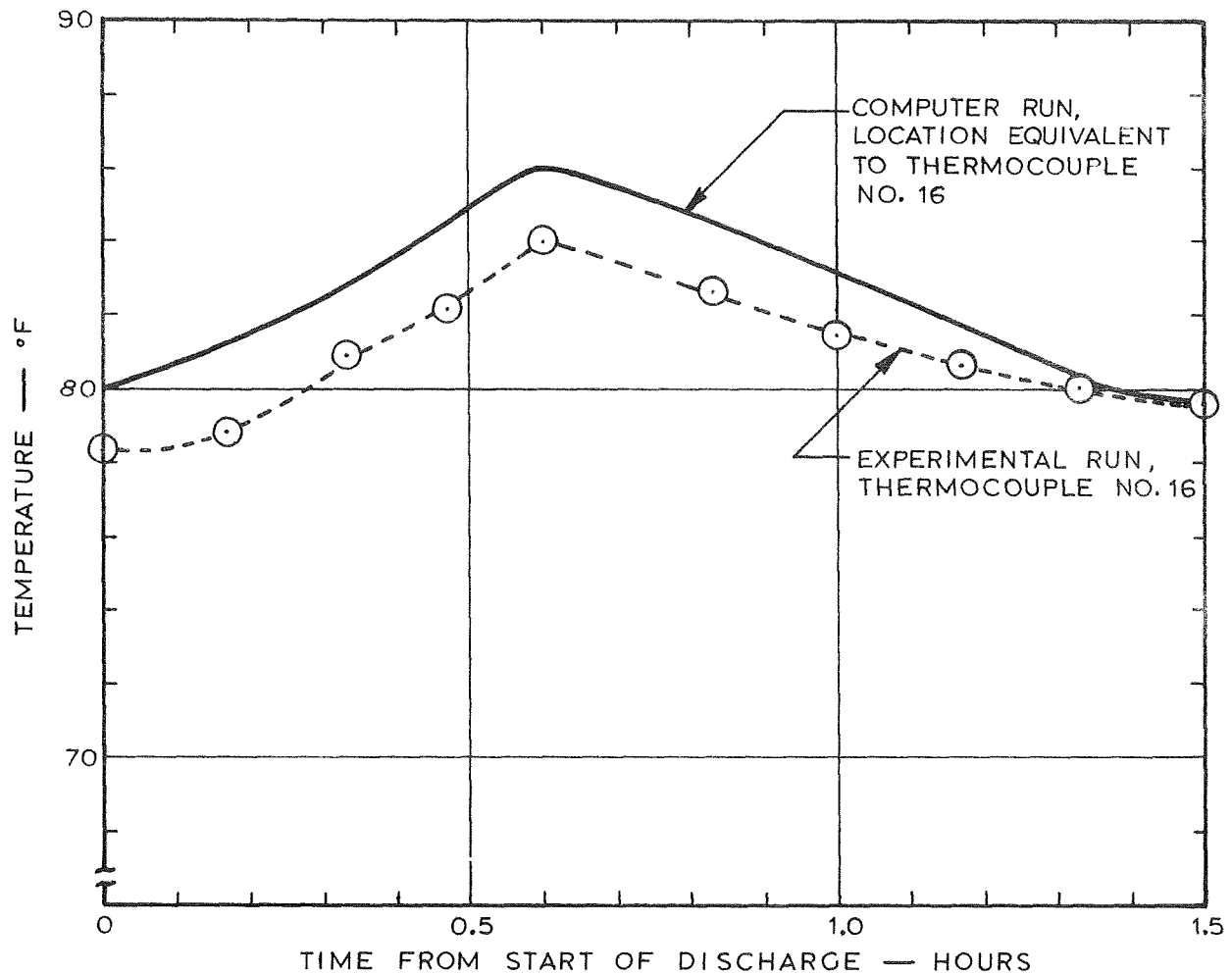


FIGURE 30  
COMPARISON OF ANALYTICAL AND EXPERIMENTAL BATTERY  
TEMPERATURES, CASE 2

## 7. CALORIMETER DESIGN

### REQUIREMENTS

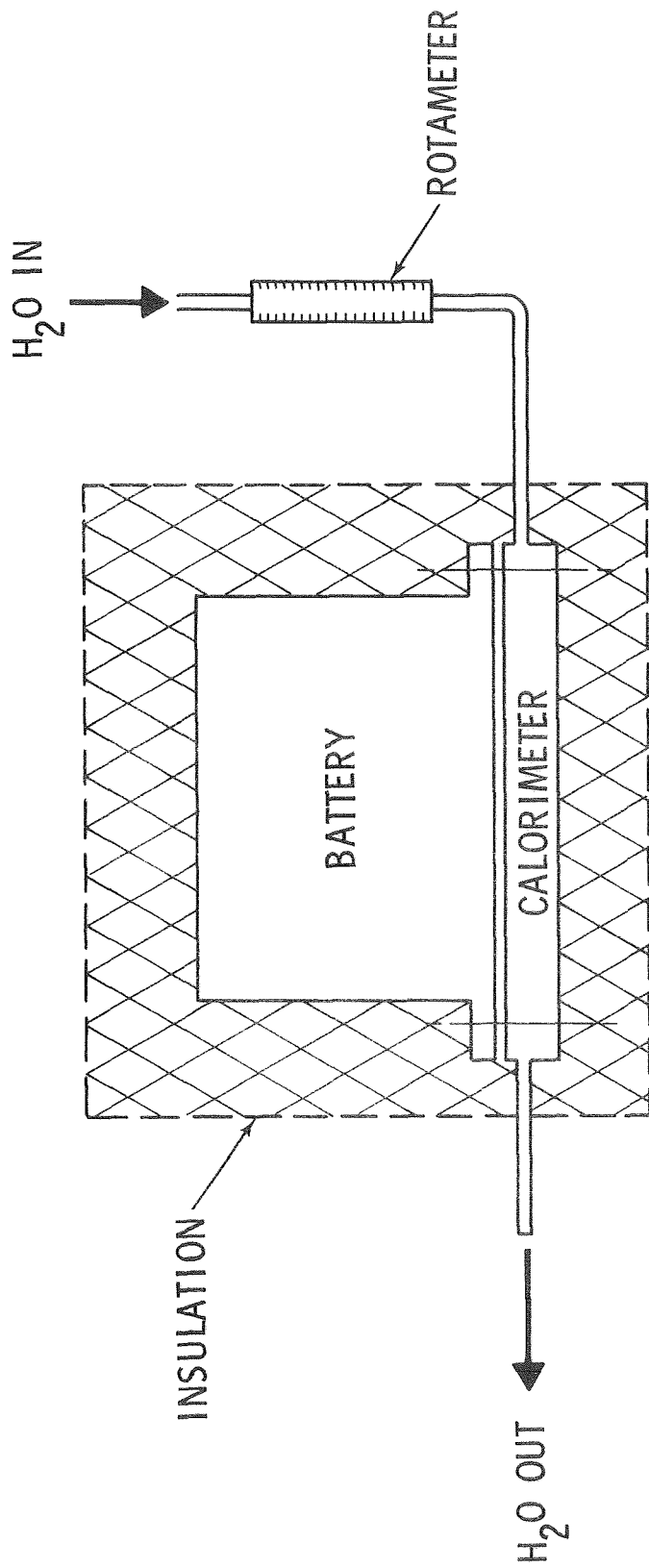
A contract requirement is the design and fabrication of two calorimeters for detailed measurement of internal heat generation in the batteries. In addition, it is required that two batteries be specially instrumented for calorimeter tests.

### WORK ACCOMPLISHED

Concept. The calorimeter concept adopted is shown in Figure 31. The NASA-furnished coldplate normally used in tests is replaced by a heat exchanger designed for thermal measurements, and the battery-calorimeter assembly is insulated to minimize heat exchange with the environment. Heat input to the fluid is determined by measurement of fluid flow rate, and inlet and outlet temperatures. Heat stored is measured by recording battery temperature change with time. The heat generated is then the sum of heat flow to the fluid plus heat stored in the battery and calorimeter.

This approach to calorimetry was chosen for these reasons:

1. This method will determine heat generation rates effectively.
2. Temperature distribution in the battery during heat generation testing will be the same as during other tests. Therefore, battery chemistry should be the same.
3. Heat generation rates are separated into realistic proportions between heat stored and heat rejected, which is a necessary breakdown for designing thermal control.
4. The calorimeter can serve as a cold plate prior to and following heat generation testing. Thus, heat generation tests can be conducted without disrupting life tests.



$$\boxed{\text{HEAT GENERATED}} = \boxed{\text{HEAT TO FLUID}} + \boxed{\text{HEAT STORED}}$$

#### MEASUREMENTS

1. BATTERY TEMP \_\_\_\_\_ THERMOCOUPLES
2. FLOW RATE \_\_\_\_\_ ROTAMETER
3. FLOW  $\Delta T$  \_\_\_\_\_ THERMOPILE OR THERMISTERS

FIGURE 31

CALORIMETER CONCEPT



Calorimeter Heat Exchanger. Battery heat is transported to the fluid flowing in the heat exchanger. This heat flow is sensed as a temperature rise in the fluid. Design objectives for the heat exchanger were

1. The temperature difference between the battery and heat exchanger should be as small as possible,
2. The heat exchanger should be nearly isothermal, and
3. The heat exchanger should have low mass for fast response.

The design of the heat exchanger is necessarily a compromise between isothermal operation and minimum transfer of heat between inlet and outlet fluids. Isothermal operation exposes the battery to a uniform-temperature cold plate, a realistic simulation of space-flight conditions. This requires a heat exchanger with high conductance. However, high conductance also results in unwanted heat transfer between inlet and outlet fluids. Such heat transfer results in regenerative heating of the battery. The adopted heat exchanger design produces a temperature difference of 1.3°F on the heat exchanger when the heating load is the highest (94 minute orbit).

A photograph of the heat exchanger appears in Figure 32 , and a drawing of the design is given in Figure 33 . Hole alignment of screws was assured by drilling heat exchanger holes using the same template that was used in drilling the bottom of the battery case. A flat mating surface was obtained by resurfacing the heat exchanger after soldering the tubing to the plate.

A thin film of silicon grease is used between the heat exchanger and mating battery surface to aid heat transfer. It is recommended that this grease film be left on the heat exchanger when it is not in use to prevent corrosion.

Temperature Difference Sensor. The critical measurement in the calorimeter is the temperature difference between the cooling fluid at the inlet and outlet of the heat exchangers. Two temperature difference sensors were tested and evaluated. The first was a copper-constant thermopile connected to sense temperature difference directly. The advantages of this thermopile are that it is simple and its output voltage will vary only 4-1/2 percent over the required 60°F to 90°F range. The disadvantages are fragility and low voltage output.

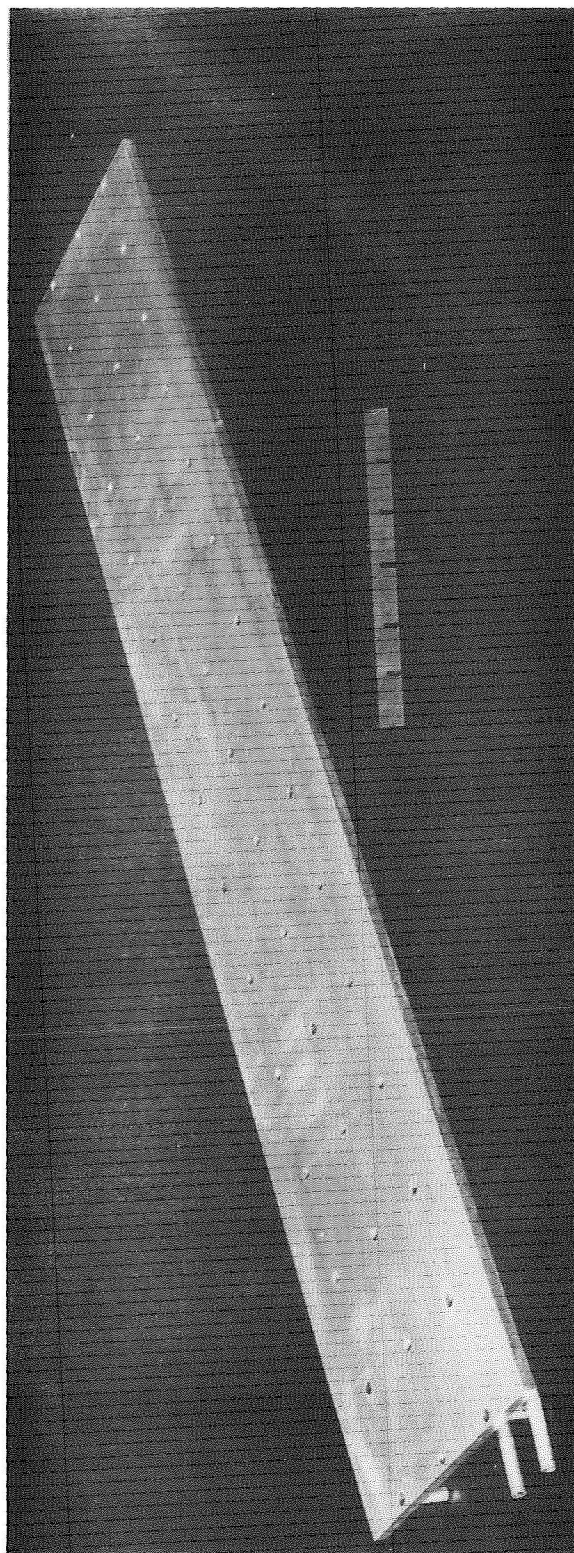


FIGURE 32  
CALORIMETER HEAT EXCHANGER



The second method of measuring temperature difference is to use thermistors and a balanced bridge to linearize the output. The advantages of this method are its high sensitivity and its high voltage output. The disadvantages are greater cost and complexity.

Both temperature difference sensors were tested in the laboratory. The thermistor approach was selected, primarily because it will be easier to use.

The thermistor pairs should be well balanced so that the calorimeter can be operated at different temperatures with minimum error. Oceanographic Iso-Curve thermistors were selected. Good balance is achieved by combining two thermistor elements to form each thermistor assembly. The thermistors are physically located in 1/4-inch nylon plumbing tees for connection to 1/4-inch copper tubing on the calorimeter heat exchangers.

A schematic of the sensing components is shown in Figure 34. The balanced bridge circuit uses the two sensing thermistors ("A" and "B") plus a temperature mismatch compensating thermistor and the necessary padding resistors. This circuit is installed in the charge-discharge controller cabinet on a removable circuit card.

Figure 35 shows the test setup for calibration of temperature difference sensors. A constant pressure was maintained by a standpipe with an overflow. A circulating pump drew water from a 5-gallon reservoir to keep the standpipe overflowing. The water from the standpipe ran through the compensating thermistor - "C" tee, the "A"-leg thermistor tee, the immersion-heater, the "B"-leg thermistor tee, and back to the reservoir. Water flow was measured by catching the stream in a beaker mounted on a torsion balance, and timing the accumulation of 2 Kg of water with a stop watch. Power to the heater was controlled with a Variac and measured with a wattmeter. The thermistor-bridge output was measured with a Fluke model 801 digital voltmeter.

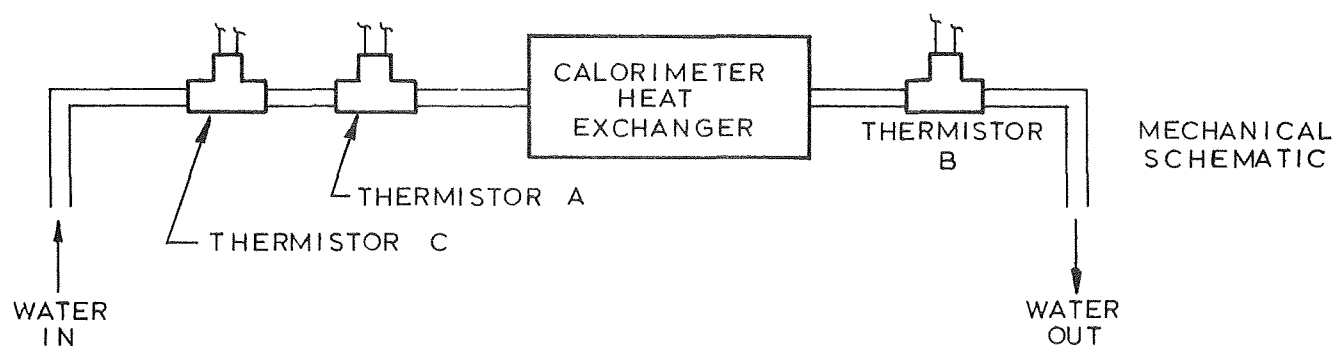
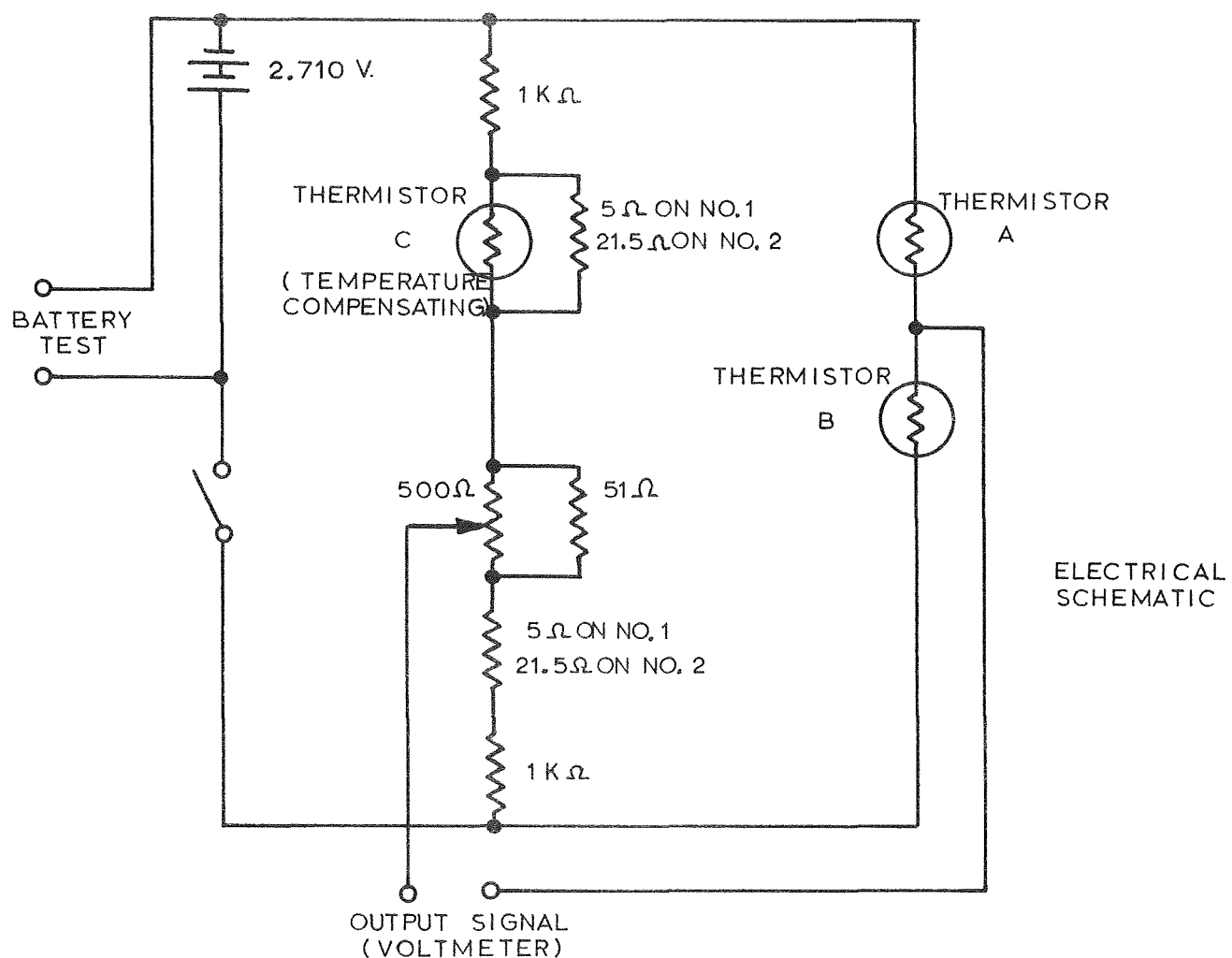


FIGURE 34  
SCHEMATIC OF CALORIMETER TEMPERATURE DIFFERENCE SENSOR

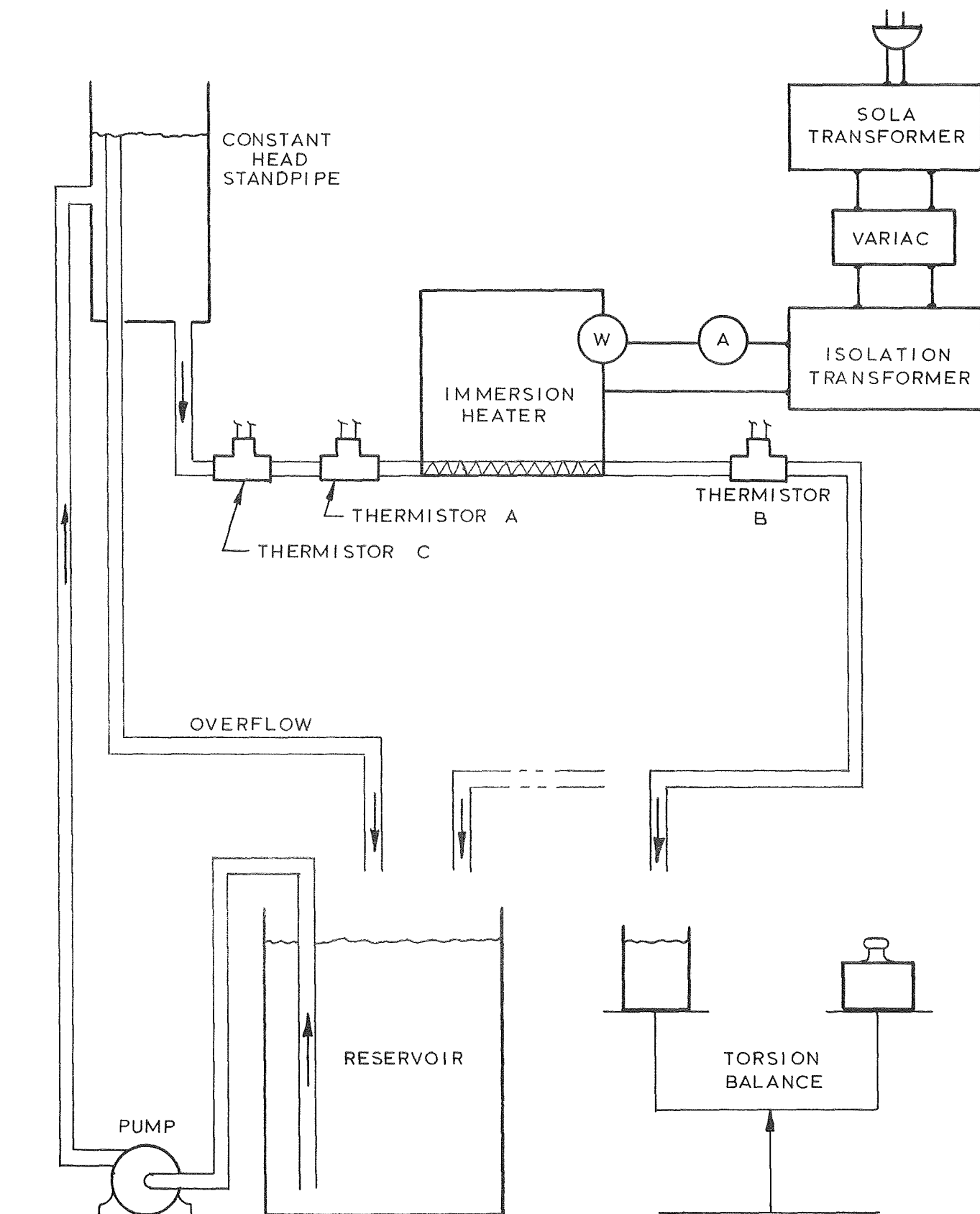


FIGURE 35  
TEST SET-UP FOR CALIBRATION OF CALORIMETER  
TEMPERATURE DIFFERENCE SENSORS

The padding resistors were adjusted by trial and error to minimize the zero shift over the working temperature range, with no power to the heater. Calibration was accomplished by applying power to the heater in 10-watt steps from 0 to 100 watts, recording the bridge output for each power setting. Such runs were made with water inlet temperatures of about 60°, 70°, 80°, and 90°F. Water flow was measured before and after each run, with the maximum flow deviation being 0.6 percent.

Figure 36 gives typical calibration test data, and shows that the bridge output varies linearly with power input. Bridge output slopes were combined with flow rates to produce the sensitivity curves given in Figure 37. The maximum variation of the curves from any test point is  $\pm 1$  percent.

Calorimeter Insulated Box. Insulation around the battery and heat exchanger limits heat exchange with the environment to a minimum but predictable amount. This insulation forms a rigid box which supports the battery (Figure 38). The box is made in two halves with a sponge gasket between halves.

Open-cell urethane foam was selected for the insulation on the basis of compatibility with room ambient and vacuum conditions. Fiberglass laminate forms the inner and outer shells of the box. Flexible foam insulation is used around cable connections. A drawing of the insulated box is shown in Figure 39.

The rate of heat loss from the battery through the insulated box to the ambient air was measured during a calibration test with a dummy battery. The dummy battery was identical in size to the test batteries, being a test battery metal case containing simulated cells of wood and aluminum. Nine resistance heaters distributed within the dummy battery simulated internally generated heat. Power and instrumentation cables penetrated the insulated box to simulate the operating conditions. The heat exchanger was attached to the dummy battery, but it was not connected to water lines.

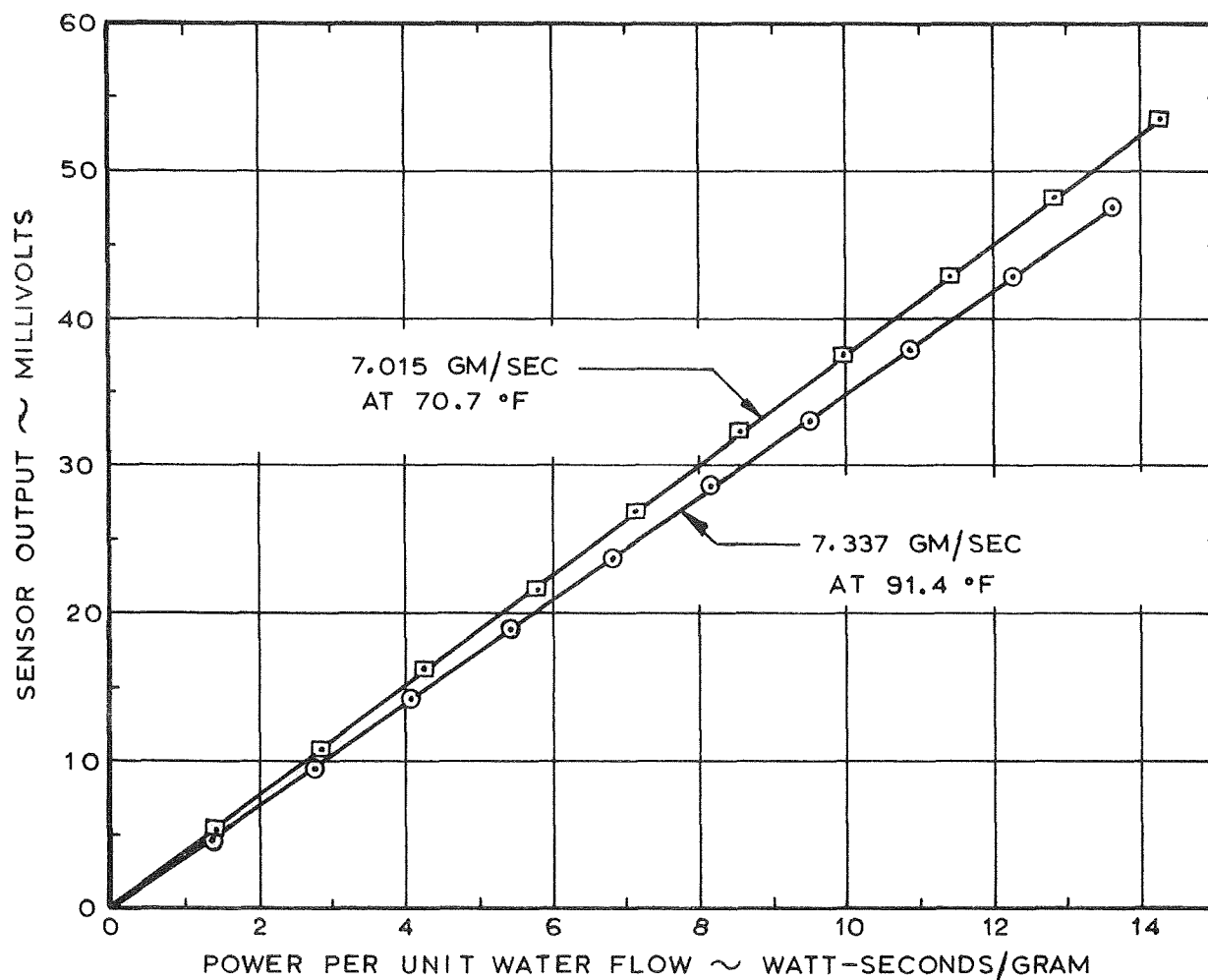


FIGURE 36

TYPICAL CALIBRATION DATA FOR  
TEMPERATURE DIFFERENCE SENSOR NO. 2



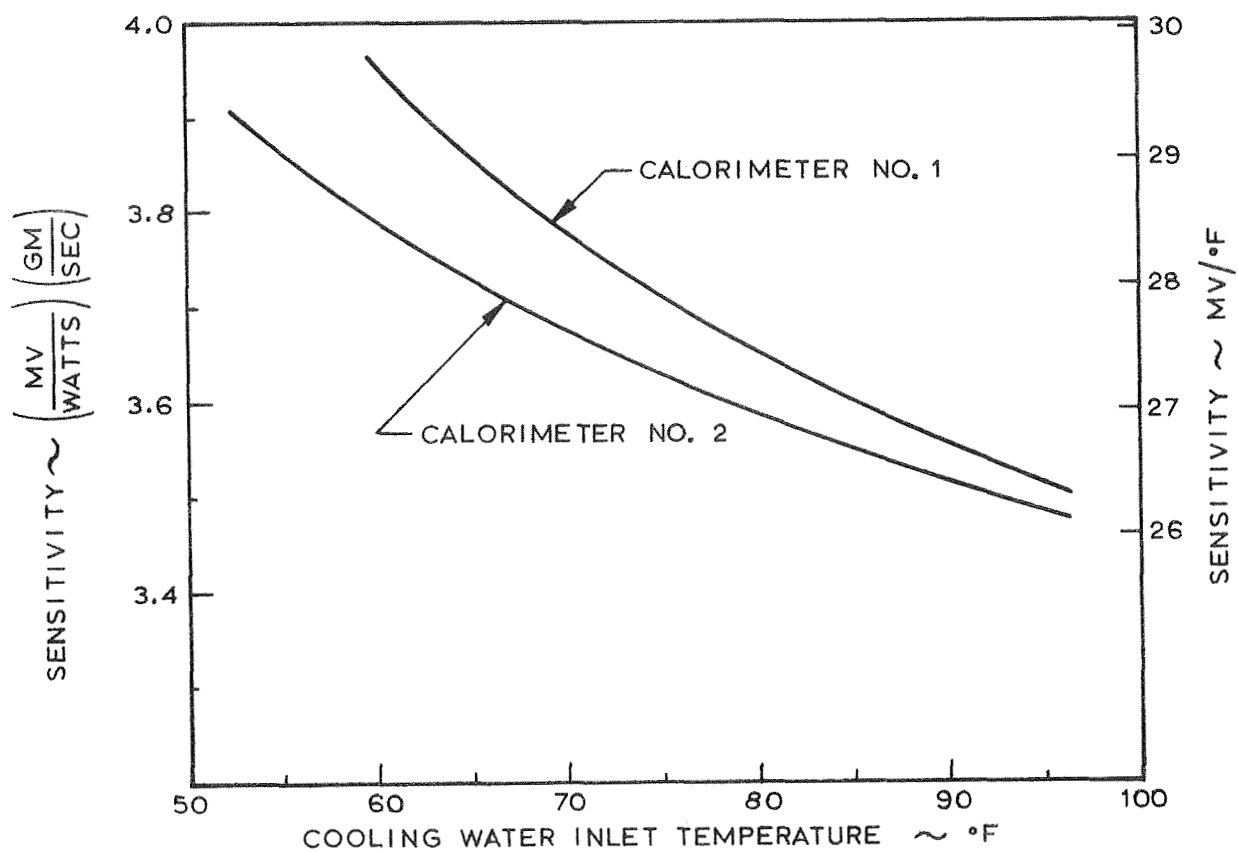
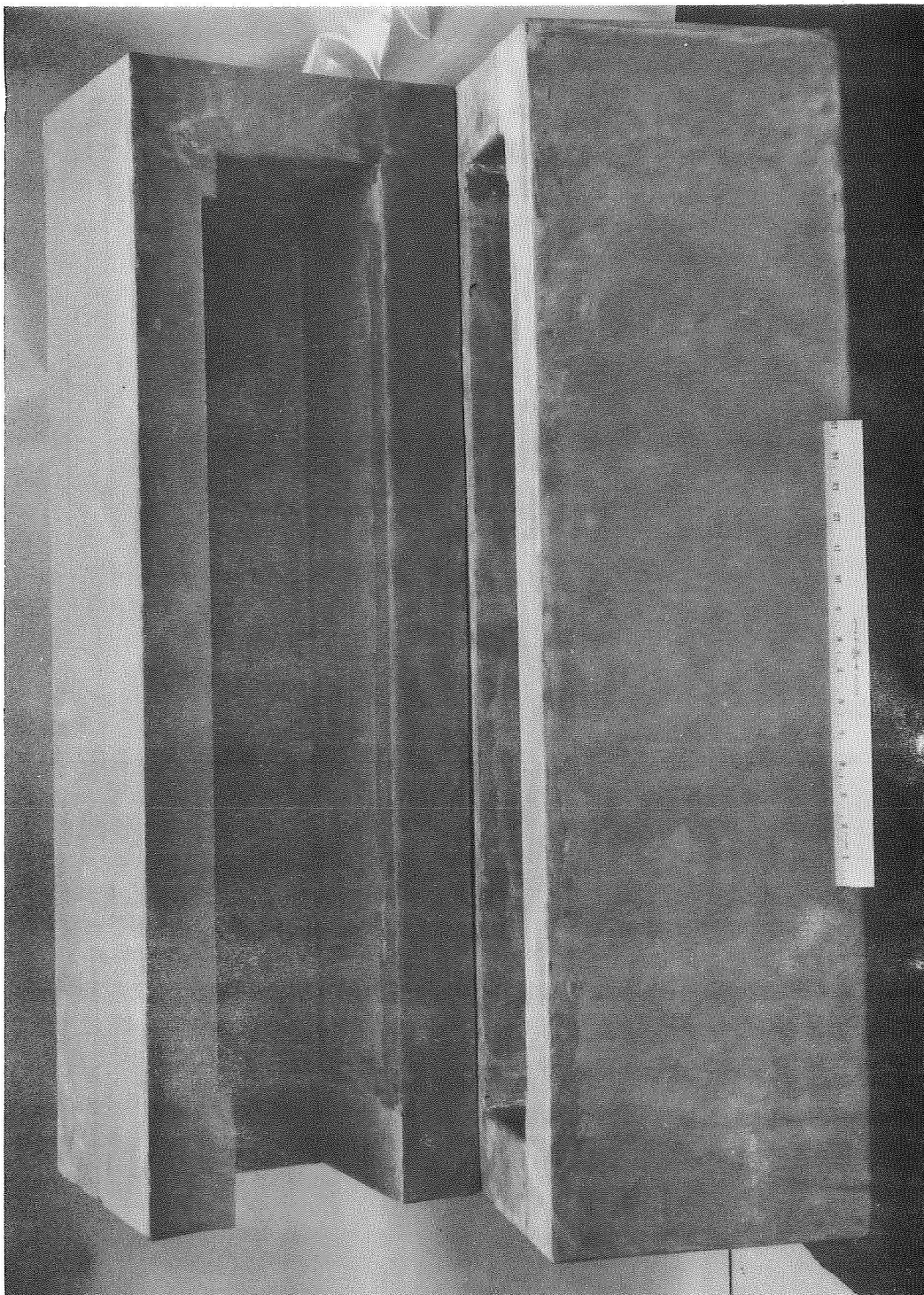
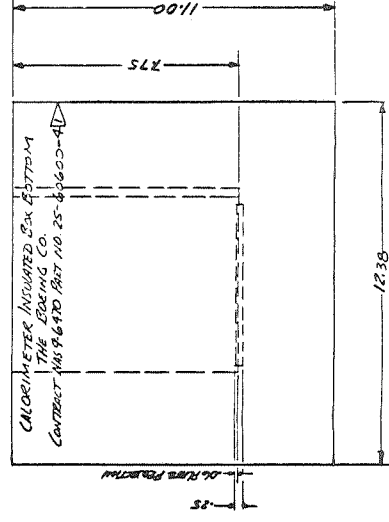
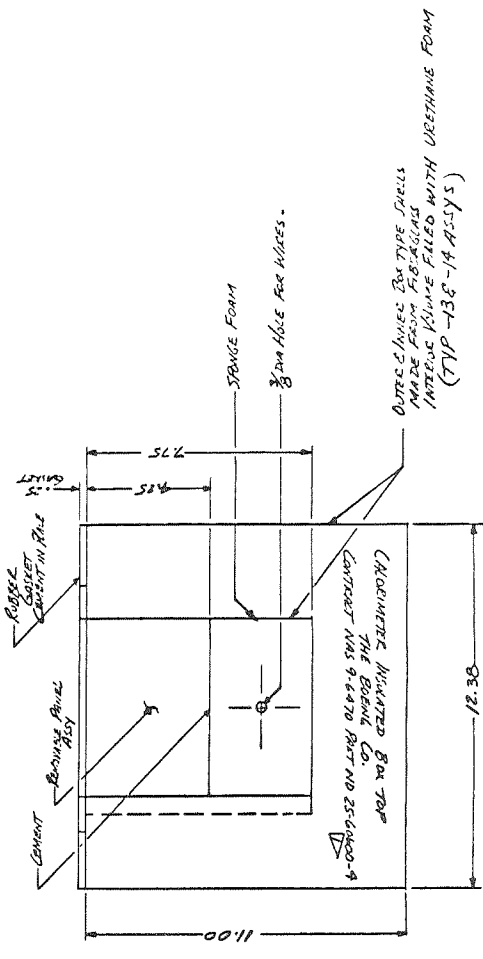
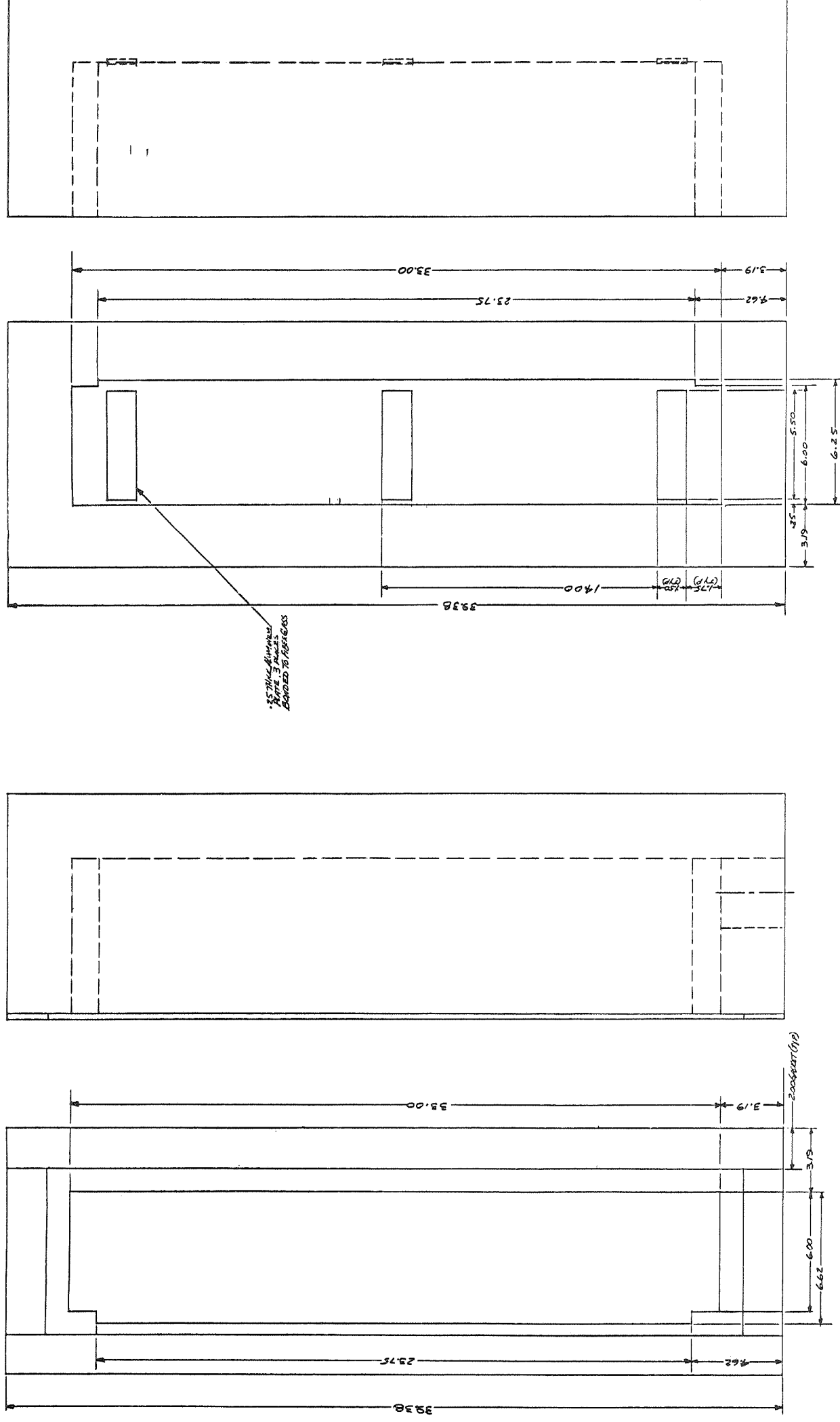


FIGURE 37


SENSITIVITY CURVE - CALORIMETER  
TEMPERATURE DIFFERENCE SENSOR



**FIGURE 38**  
**CALORIMETER INSULATED BOX**



-13 ASSY  
BOX TOP

-14 ASSY   
BOX BOTTOM

▷ 25-60600-4 CALORIMETER INSULATED BOX ASSEMBLY IS -13 ASSEMBLY  
PLANT ON -14 ASSEMBLY

PAGE 94

[illegible]

FIGURE 39

Twenty-four hours were allowed for temperatures to reach equilibrium. The overall thermal conductance was then calculated, and the results are shown in Figure 40. The approximate components of the thermal conductance are shown in Table 12.

Calorimeter Computer Program. A computer program was developed and checked out for processing calorimeter test data. This program is coded in FORTRAN IV for use on the SRU 1108 computer, and it is identified within The Boeing Company by the number AS 2602. A users manual (Reference 2) and test cases which fully describe the program have been supplied to NASA.

Major computer inputs are temperatures, flow rate, a voltage which is proportional to fluid temperature difference, insulation correction factors, and a fluid friction correction. This input format is made identical with laboratory data-taking format so that input cards may be punched without transcription of the data. The output of the program is heat generation versus time, separated into heat stored and heat transferred to the cooling fluid.

BASIS —

- 80°F AMBIENT AIR
- BATTERY AND HEAT EXCHANGER INSTALLED
- ALL THREE CABLES ATTACHED

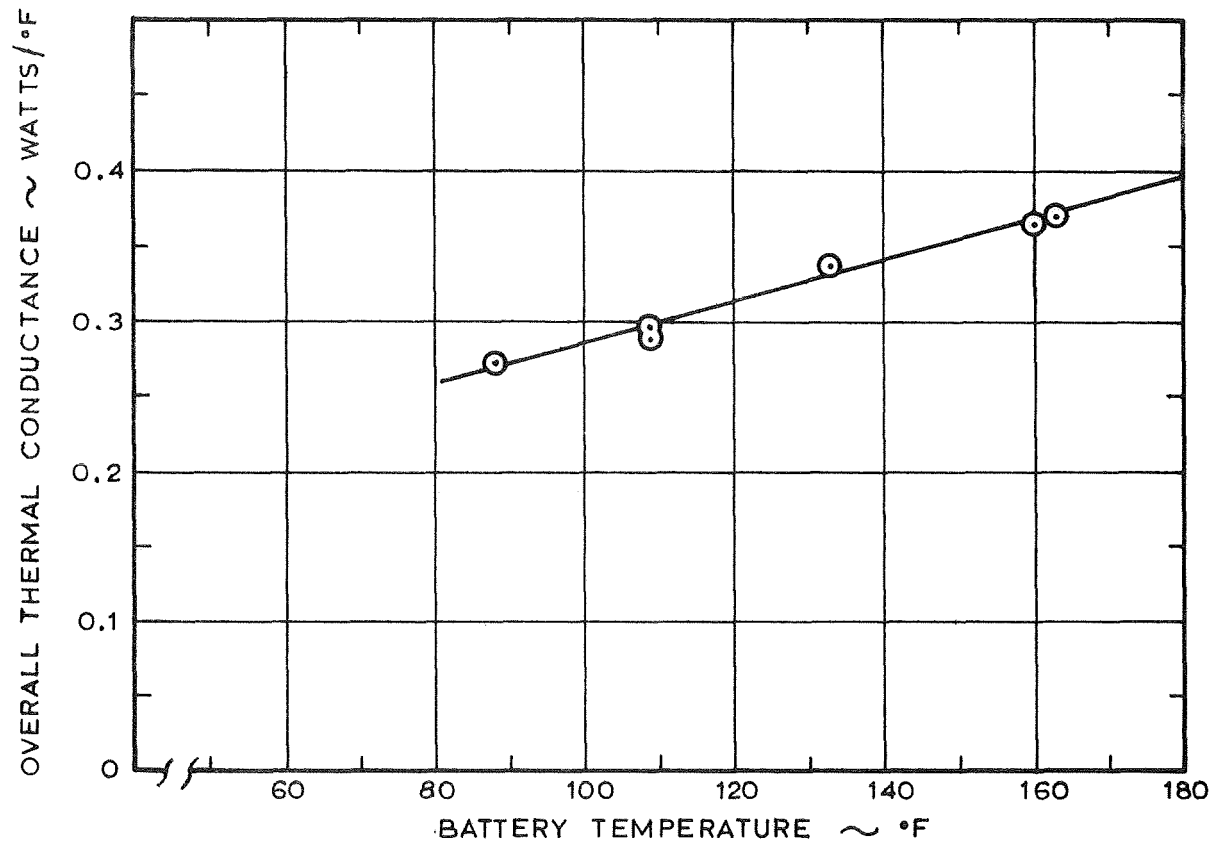


FIGURE 40

THERMAL CONDUCTANCE OF  
BATTERY CALORIMETER INSULATION BOX

TABLE 12  
CALCULATED PARTITION OF CALORIMETER THERMAL CONDUCTANCE

SURFACE	CONTRIBUTING FRACTION
Two vertical sides	0.54
Bottom	0.15
Top	0.15
Near End*	0.10
Far End	0.06
	<hr/>
Total	1.00

\* The three cables are located at the near end.

## 8. BATTERY CHARGE-DISCHARGE CONTROLLER

### REQUIREMENTS

The Boeing Company is required to develop and provide four charge-discharge controllers for cycling the batteries. Two identical cabinets are to be provided, with two controllers in each cabinet. The controllers are identical, except that one in each cabinet has a manually-adjustable load, whereas the other has a programmable load. The manually-adjustable load must be variable up to at least 70 amperes. The programmable load must provide a minimum of 10 load levels on a single discharge cycle over a current range of 0.7 to 210 amperes, with individual "on time" adjustable from one second to two hours.

A variety of direct reading and analog readout instruments are required. Instruments requiring development are:

1. An ampere-hour meter with analog readout, reading up to 100 ampere-hours;
2. A watt-hour meter with analog readout and reading up to 2500 watt-hours.

### WORK ACCOMPLISHED

Two charge-discharge controller cabinets were designed, built and tested. All components and functions performed satisfactorily, meeting or exceeding all the requirements. Two controller instruction manuals were also prepared and delivered to NASA (References 3 and 6). These manuals contain detailed information on components, calibration and adjustments, operating procedures, trouble shooting, and wiring.

General Description. Each 19-inch by 7-foot controller cabinet contains two independent charge-discharge controllers, one for battery A and the other for battery B. The controllers are identical, except that one has a manually-adjustable resistance load, whereas the other has a programmed resistance load. A simplified functional diagram of the controller is shown in Figure 41. Photographs of the cabinet appear in Figures 42 and 43, and the front cabinet layout is shown in Figure 44. A block diagram and schematic appear in Figures 45 and 46, respectively.

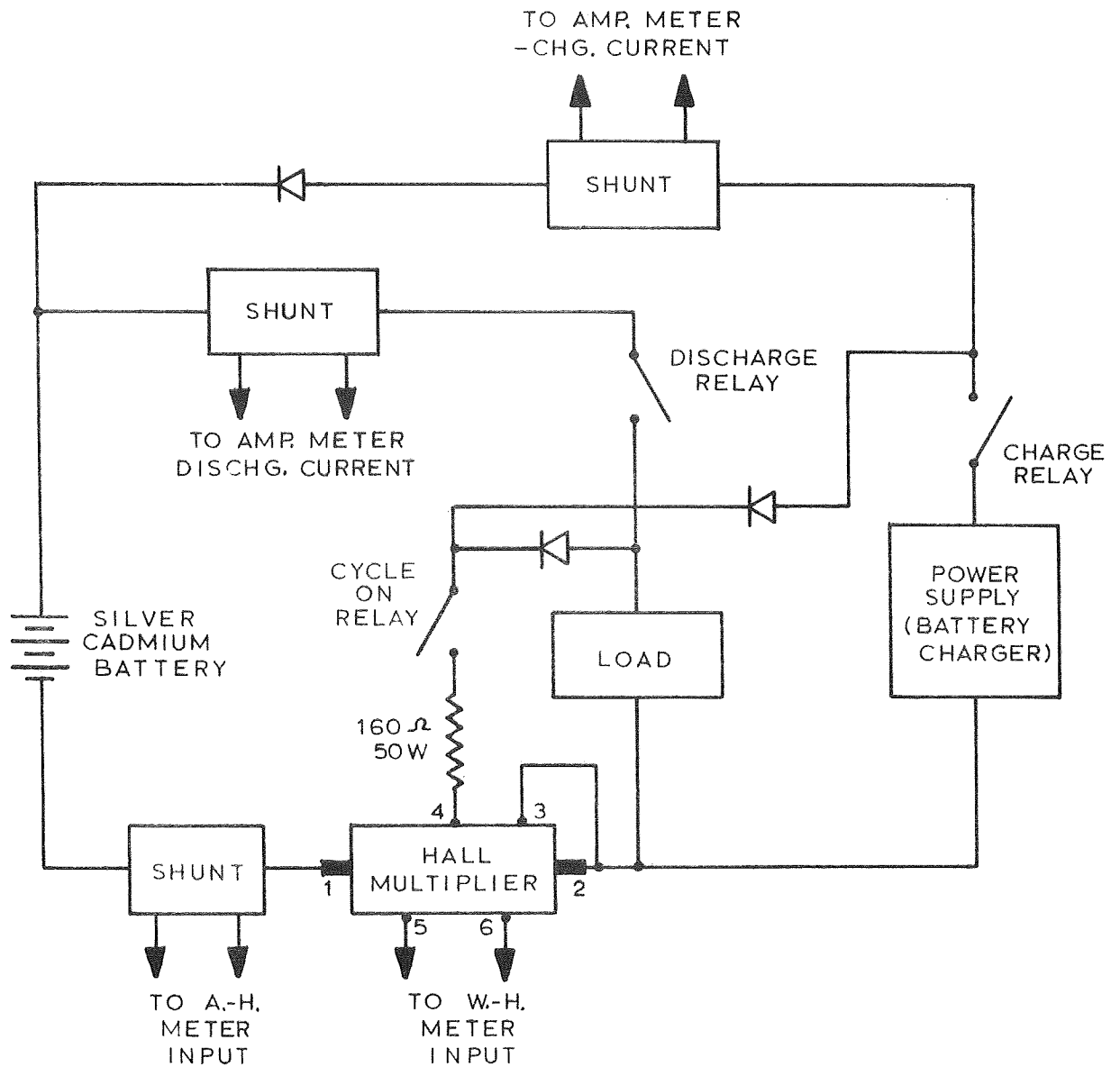


FIGURE 41

## SIMPLIFIED CHARGE-DISCHARGE CONTROLLER



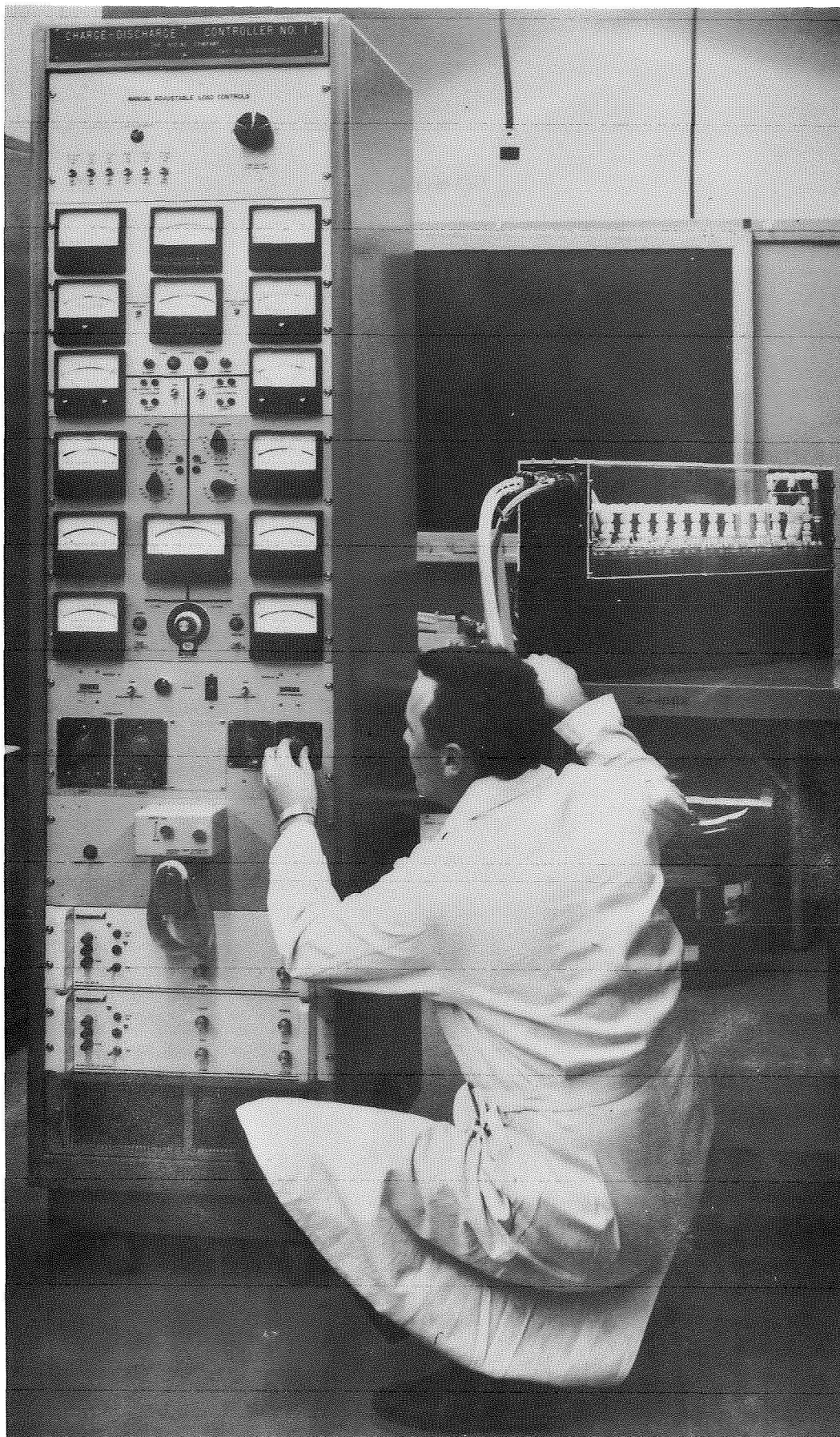


FIGURE 42  
CHARGE-DISCHARGE CONTROLLER FRONT VIEW  
100

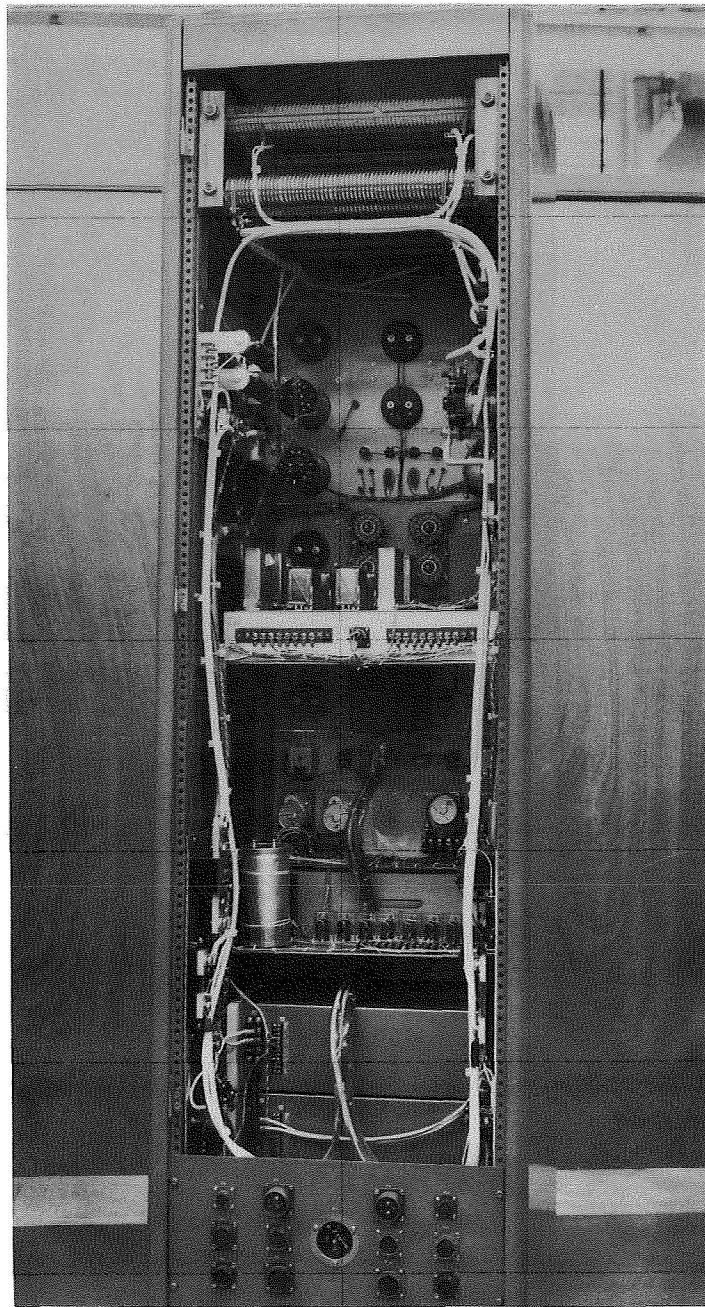


FIGURE 43  
CHARGE-DISCHARGE CONTROLLER REAR VIEW

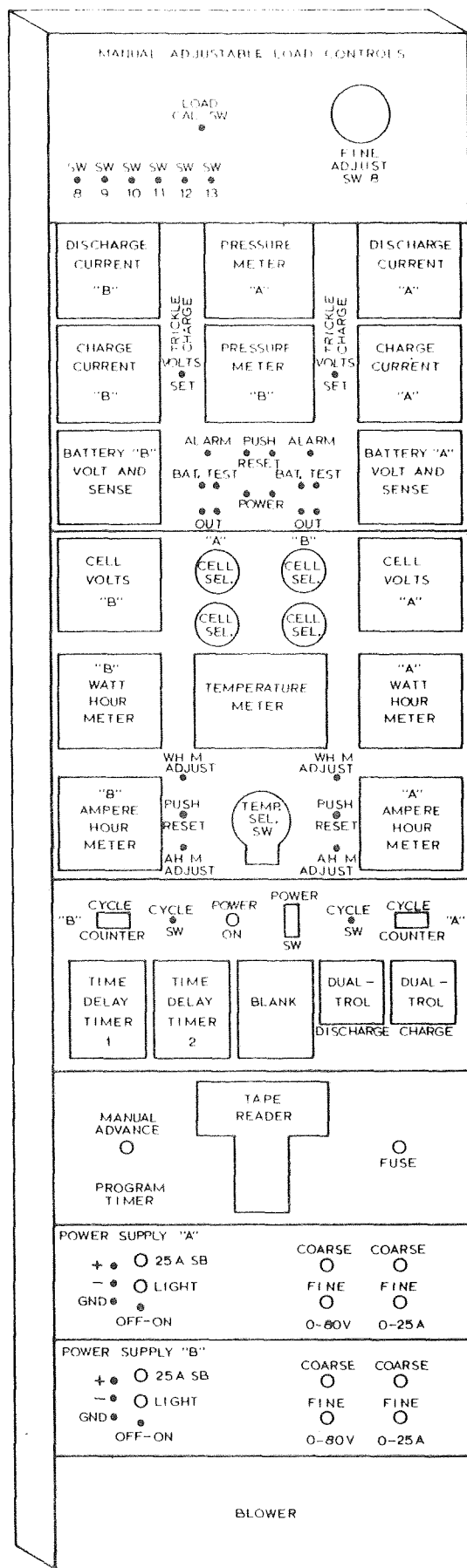


FIGURE 44

FRONT CABINET LAYOUT



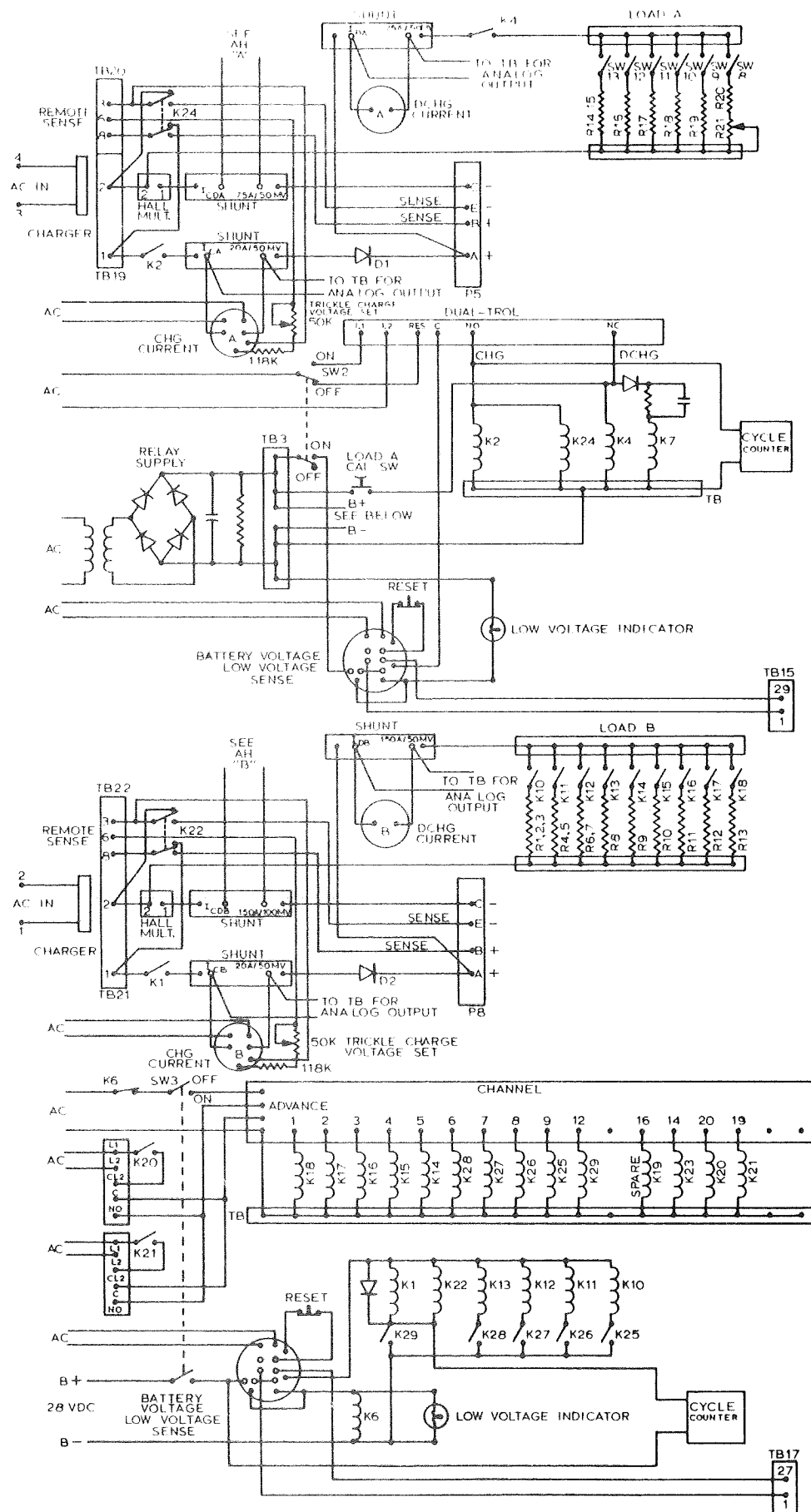


FIGURE 46

# BATTERY CHARGE-DISCHARGE CONTROLLER SCHEMATIC

The front of the cabinet contains meters for monitoring battery operation, timers for controlling the charge/discharge cycle, power supply controls for setting the battery charge voltage and current, air filters, switches and adjustments. The meters display battery charge and discharge current, battery and cell voltages, battery pressure and temperature, ampere-hours, and watt-hours. In addition to instrument displays, the cabinet provides analog signals for recording the above data.

The battery voltmeter has a low-voltage contact which is used to protect the battery against reversal during discharge; it also has a high voltage contact which lights a warning during inadvertent overcharge. The battery charge current ammeter has a low-current contact which can be used to provide a two-step charge control.

A Dual-Trol timer controls the charge-discharge cycle for the manually adjustable load, and a punched tape programmer controls the charge-discharge cycle and load profile for the programmed load. Time delays are used to control the stepping sequence of the punched tape programmer.

Ampere-hour and watt-hour meters are provided for each controller. The ampere-hour meter measures and integrates a voltage that is proportional to current. The watt-hour meter uses a Hall multiplier to obtain a signal that is proportional to the product of voltage and current, and this signal is then integrated to obtain watt-hours.

Three shunts are used in each controller, one to measure charge current, the second to measure discharge current, and the third to provide a signal for the ampere-hour meter. The interconnection of the shunts is shown in Figure 41. The three separate shunts are necessary for measurement accuracy, since there is a large difference between the maximum charge current (20 amperes) and the maximum discharge current (210 amperes).

The controller requires 110-volt, 60-Hz a.c. power, 3-phase, 20 amperes per phase. Phase "A" supplies power to one power supply, phase "B" supplies power to the other power supply, and Phase "C" supplies power for the remaining equipment including instrumentation and timers.



The controller is designed for two-step charge control in which the battery is charged initially at a constant current until a predetermined limiting terminal voltage is reached. The battery charging current will then decrease as a consequence of the inherent characteristic of the battery. When the current decreases to a predetermined value the charging voltage is caused to drop from its limiting value to some lower voltage that corresponds to a trickle charge. The trickle charge continues until discharge is commenced.

The experimenter is not constrained to use the two-step charge procedure with the charge-discharge controller. Simple dial settings will make the two-step feature inoperative, allowing charging by other procedures. Typical controller settings are given in Table 13.

Manually Adjustable Load. The manually adjustable load can be varied from 0.56 to 70.0 amperes, based on a 28-volt battery voltage. A schematic of this load is shown in Figure 47. Closing appropriate switches in the 9 through 13 group will provide a load current within 2.2 amperes of the desired value. Closing switch 8 connects in a rheostat having a range of 0.56 to 2.8 amperes for fine adjustment of current. Table 14 shows the combinations of switch positions that provide the various current values based on a 28-volt d.c. source. Also shown are resistances for computing discharge currents at other voltages.

Currents higher than 70 amperes can be obtained by changing the wire attachment points on the spiral resistors. However, this will result in gaps in the spectrum of attainable currents.

A load calibration switch is provided to permit checking the load resistance prior to cycling a battery. This switch energizes the discharge relay to permit testing the load with an external power supply or an ohmmeter.

Dual-Trol Recycling Timer. A recycling Dual-Trol timer controls the charge-discharge cycle for the battery connected to the manual adjustable load (Battery "A"). This timer consists of two individual timing mechanisms which sequentially pulse a latching relay. One timing mechanism controls the charge duration, and the other controls the discharge duration.

TABLE 13  
TYPICAL CHARGE-DISCHARGE CONTROLLER SETTINGS

	94 Minute Orbit	12 Hour Orbit	24 Hour Orbit
Charge Duration	58 minutes	10 hours	22 hours
Discharge Duration	36 minutes	2 hours	2 hours
Depth of Discharge	25 percent	75 percent	75 percent
Discharge Current	29.2 amperes	26.2 amperes	26.2 amperes
Charge Current, Max.	18.8 amperes	6.5 amperes	3.0 amperes
Charge Voltage, Max.	43.40 volts (1.55 v/cell)	42.84 volts (1.53 V/cell)	42.84 volts (1.53 V/cell)
2-Step Charge Current Trip	6.0 amperes	0.75 amperes	0.75 amperes
2-Step Trickle Charge Voltage	39.76 volts (1.42 V/cell)	39.62 volts (1.415 V/cell)	39.63 volts (1.415 V/cell)
Low Discharge Voltage Set	29.0 volts	27.0 volts	22.0 volts *
High Charge Voltage Alarm	47.0 volts	47.0 volts	47.0 volts

\* May be increased to 27.0 volts if large current pulses are absent.



NOTE: INDICATED CURRENT BASED ON 28 VOLTS

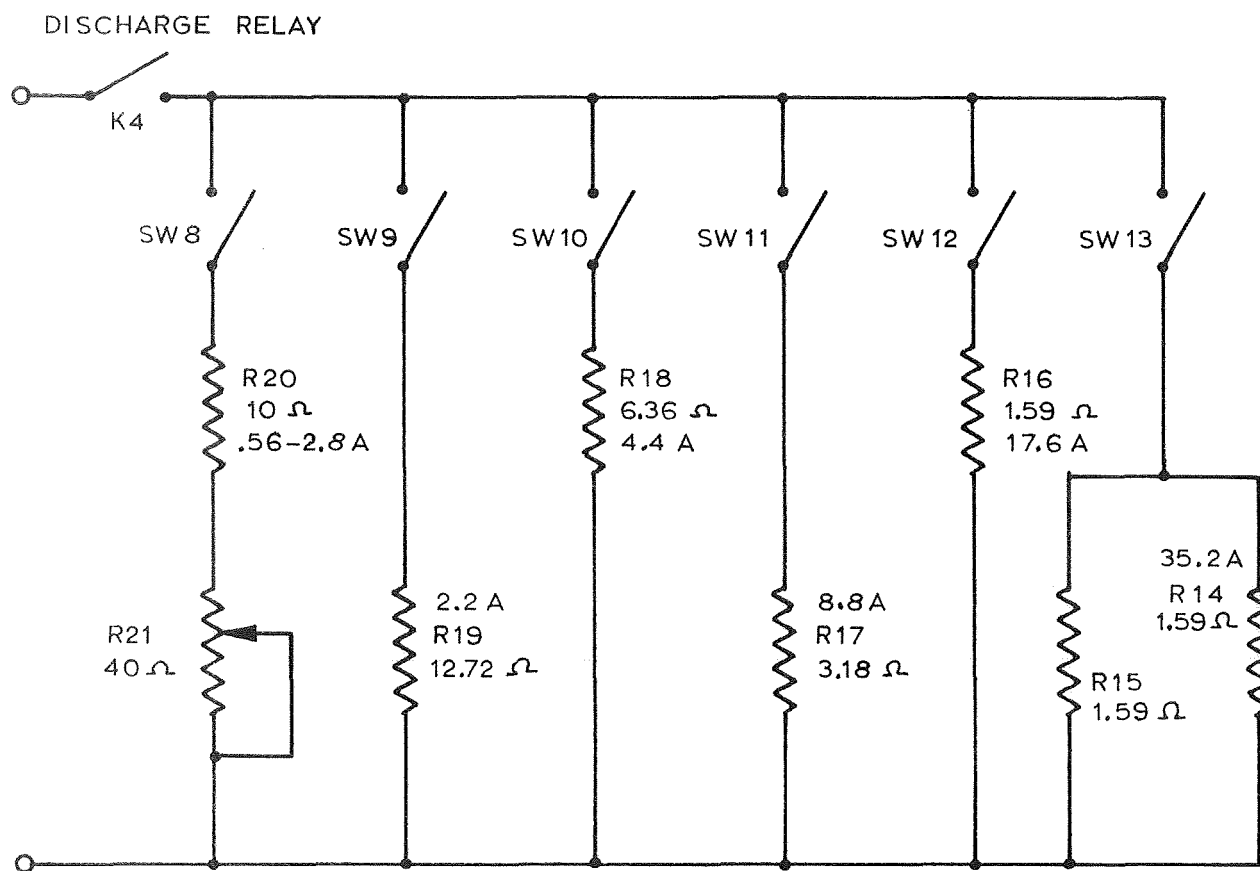


FIGURE 47

MANUALLY ADJUSTABLE LOAD

TABLE 14  
SWITCH COMBINATIONS FOR MANUALLY ADJUSTABLE LOAD

<u>SWITCHES CLOSED</u>	<u>CURRENT RANGE - AMPERES*</u>	<u>RESISTANCE RANGE - OHMS</u>
8	0.56 - 2.8	50.000 - 10.000
8-9	2.71 - 5.0	10.332 - 5.600
8-10	4.96 - 7.2	5.645 - 3.889
8-9-10	7.16 - 9.4	3.911 - 2.979
8-11	9.36 - 11.6	2.991 - 2.414
8-9-11	11.56 - 13.8	2.422 - 2.029
8-10-11	13.76 - 16.0	2.035 - 1.750
8-9-10-11	15.96 - 18.2	1.754 - 1.538
8-12	18.16 - 20.4	1.542 - 1.373
8-9-12	20.36 - 22.6	1.375 - 1.239
8-10-12	22.56 - 24.8	1.241 - 1.129
8-9-10-12	24.76 - 27.0	1.131 - 1.037
8-11-12	26.96 - 29.2	1.039 - 0.959
8-9-11-12	29.16 - 31.4	0.960 - 0.892
8-10-11-12	31.36 - 33.6	0.893 - 0.833
8-9-10-11-12	33.56 - 35.8	0.834 - 0.782
8-13	35.76 - 38.0	0.783 - 0.737
8-9-13	37.96 - 40.2	0.738 - 0.697
8-10-13	40.16 - 42.4	0.697 - 0.660
8-9-10-13	42.36 - 44.6	0.661 - 0.628
8-11-13	44.56 - 46.8	0.628 - 0.598
8-9-11-13	46.76 - 49.0	0.599 - 0.571
8-10-11-13	48.96 - 51.2	0.572 - 0.547
8-9-10-11-13	51.16 - 53.4	0.547 - 0.524
8-12-13	53.36 - 55.6	0.523 - 0.504
8-9-12-13	55.56 - 57.8	0.504 - 0.484
8-10-12-13	57.76 - 60.0	0.485 - 0.467
8-9-10-12-13	59.96 - 62.2	0.467 - 0.450
8-11-12-13	62.16 - 64.4	0.450 - 0.435
8-9-11-12-13	64.36 - 66.6	0.435 - 0.420
8-10-11-12-13	66.56 - 68.8	0.421 - 0.407
8-8-10-11-12-13	68.76 - 71.0	0.407 - 0.394

\* Based on 28 V d.c. power source

The timer operation consists of closing a pair of contacts after a pre-set delay. The cycle will always start with the operation of the discharge timer. When the DISCHARGE START switch is turned on, this timer will start its cycle. When its red pointer reaches zero, the timer closes a normally open switch, which pulses one of the coils on the latching relay, simultaneously switching the load contacts and starting the charge timer. When the charger timer completes its time cycle, it pulses the other coil on the latching relay, and the timer returns back to its start position. This sequence continues until the discharge-start switch is turned off. The Dual-Trol timer is used only with the manual adjustable load.

The timer modules installed in the controller provide from three minutes to 3 hours discharge duration and from 30 minutes to 30 hours charge duration. A spare one-hour timer which is interchangeable with the other timers provides additional testing flexibility.

Programmed Load. The programmed load provides any desired battery discharge current between 0.7 and 210 amperes in 0.7 ampere increments based on a 28 volt battery. A schematic of this load is shown in Figure 48. The load values are achieved by closing load relays. A separate channel in the punched tape programmer is assigned to each load relay. Table 15 shows the hole punches that provide the 305 possible load values. Channels 1 through 9 of the punched tape programmer control relays which connect appropriate load resistors to the load bus. Relays K15 through K18 in the punched tape programmer control load resistors directly, and relays K25 through K29 indirectly control load resistors by means of relays K10 through K14, respectively.

The resistance values used in the programmed load were selected to produce a binomial series expansion of attainable current. However, resistors R1 through R7 can be readjusted for higher current if so desired by changing the lead attachment points on the resistors.

NOTE: INDICATED CURRENT BASED ON 28 VOLTS

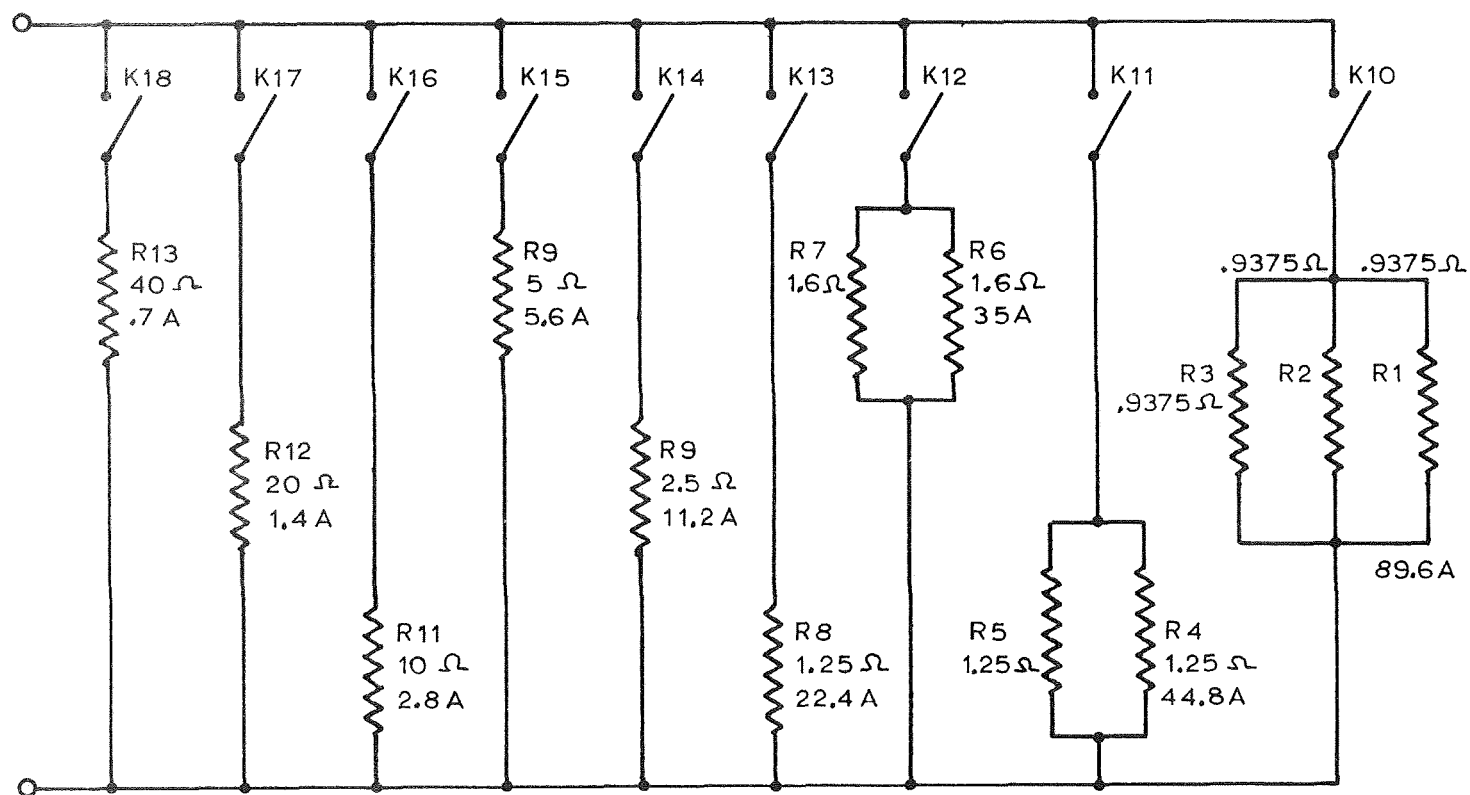


FIGURE 48

PROGRAMMED LOAD

# TABLE 15

## PUNCHED TAPE COMBINATIONS FOR PROGRAMMABLE LOADS

I*	R	Punch Channel									I*	R	Punch Channel									I*	R	Punch Channel									I*	R	Punch Channel												
(AMPS)	(OHMS)	1	2	3	4	5	6	7	8	9	(AMPS)	(OHMS)	1	2	3	4	5	6	7	8	9	(AMPS)	(OHMS)	1	2	3	4	5	6	7	8	9	(AMPS)	(OHMS)	1	2	3	4	5	6	7	8	9				
.7	40.0	X									57.4	.492							X	X			114.1	.2468	X	X				X			170.8	.164	X					X	X	X					
1.4	20.0		X								58.1	.483	X						X	X			114.8	.246		X				X			171.5	.1632	X	X				X	X	X					
2.1	13.333	X	X								58.8	.476		X					X	X			115.5	.2432	X	X				X			172.2	.1626		X				X	X	X					
2.8	10.0			X							59.5	.471	X	X					X	X			116.2	.2415		X	X			X			172.9	.1621	X	X				X	X	X					
3.5	8.0	X	X								60.2	.465			X				X	X			116.9	.2397	X	X	X			X			173.6	.1615	X	X				X	X	X					
4.2	6.666		X	X							60.9	.460	X	X					X	X			117.6	.238			X	X		X			174.3	.1607	X	X	X				X	X	X				
4.9	5.72	X	X	X							61.6	.455	X	X					X	X			118.3	.237	X		X	X		X			175.0	.1600				X			X	X	X				
5.6	5.0				X						62.3	.449	X	X	X				X	X			119.0	.2355		X	X	X		X			175.7	.1594	X				X			X	X	X			
6.3	4.45	X			X						63.0	.4447				X			X	X			119.7	.2342	X	X	X		X	X			176.4	.1587		X	X			X			X	X	X		
7.0	4.0		X		X						63.7	.440	X		X	X	X					120.4	.2325			X	X	X		X			177.1	.1583	X	X			X			X	X	X			
7.7	3.638	X	X		X						64.4	.435		X	X	X	X					121.1	.2312	X	X	X	X		X			177.8	.1574			X	X				X	X	X				
8.4	3.333		X	X							65.1	.430	X	X		X	X	X				121.8	.230		X	X	X	X		X			178.5	.1568	X	X	X				X	X	X				
9.1	3.078	X	X	X							65.8	.426			X	X	X	X				122.5	.2287	X	X	X	X		X			179.2	.1562		X	X	X				X	X	X				
9.8	2.857	X	X	X							66.5	.4218	X	X	X	X	X					123.2	.2275					X	X		X		179.9	.1558	X	X	X	X				X	X	X			
10.5	2.666	X	X	X	X						67.2	.417	X	X	X	X	X					123.9	.2261	X				X	X		X		180.6	.155				X			X	X	X				
11.2	2.500				X						67.9	.4125	X	X	X		X	X				124.6	.2245					X	X		X		181.3	.1547	X			X			X	X	X				
11.9	2.353	X			X						68.6	.408					X	X	X			125.3	.2233	X				X	X		X		182.0	.154	X			X			X	X	X				
12.6	2.221		X		X						69.3	.404	X				X	X	X			126.0	.2223		X			X	X		X		182.7	.1533	X	X				X			X	X	X		
13.3	2.105	X	X		X						70.0	.400			X				X			126.7	.2216	X	X			X	X		X		183.4	.1526			X			X			X	X	X		
14.0	2.0			X	X						70.7	.3965	X	X			X	X				127.4	.220			X			X		X		184.1	.1521	X	X			X			X	X	X			
14.7	1.905	X	X		X						71.4	.3922		X	X			X	X			128.1	.2185	X	X			X	X		X		184.8	.1518		X	X			X			X	X	X		
15.4	1.84	X	X	X	X						72.1	.388	X	X	X			X	X			128.8	.2175		X	X			X	X		X		185.5	.1510	X	X	X				X			X	X	X
16.1	1.74	X	X	X	X						72.8	.3847				X	X	X				129.5	.2163	X	X	X			X	X		X		186.2	.1504			X	X			X			X	X	X
16.8	1.666				X	X					73.5	.381	X			X	X	X				130.2	.215					X		X		X		186.9	.1499	X			X	X			X	X	X	X	
17.5	1.60	X			X	X					74.2	.3777		X		X	X	X				130.9	.214	X		X			X	X		X		187.6	.1495	X	X	X			X			X	X	X	
18.2	1.538		X	X	X						74.9	.374	X	X		X	X	X				131.6	.213		X	X			X	X		X		188.3	.1487	X	X			X	X			X	X	X	
18.9	1.472	X	X	X	X						75.6	.3702			X	X	X	X				132.3	.2117	X	X	X			X	X		X		189.0	.1482		X	X	X			X			X	X	X
19.6	1.428		X	X	X						76.3	.367	X	X	X	X	X					133.0	.2109			X	X		X	X		X		189.7	.1478	X	X	X			X			X	X	X	
20.3	1.38	X	X	X	X						77.0	.3642		X	X	X	X	X				133.7	.2097	X	X	X			X	X		X		190.4	.1470	X	X	X			X			X	X	X	
21.0	1.332	X	X	X	X						77.7	.3608	X	X	X	X	X					134.4	.2085					X	X		X		191.1	.1466	X	X	X	X			X			X	X	X	
21.7	1.29	X	X	X	X						78.4	.3575					X	X	X			135.1	.2076	X				X	X		X		191.8	.1460						X			X	X	X	X	
22.4	1.25				X						79.1	.354	X				X	X				135.8	.2062		X			X	X		X		192.5	.1454	X					X			X	X	X	X	
23.1	1.213	X			X						79.8	.3515						X	X			136.5	.2053	X	X			X	X		X		193.2	.1450		X				X			X	X	X	X	
23.8	1.175	X			X						80.5	.348	X					X	X			137.2	.204			X			X		X		193.9	.1446	X	X				X			X	X	X	X	
24.5	1.142	X	X		X						81.2	.345		X				X	X			137.9	.2032	X	X	X			X	X		X		194.6	.144		X			X			X	X	X	X	
25.2	1.112		X		X						81.9	.342	X	X				X	X			138.6	.202		X	X			X	X		X		195.3	.1434	X	X			X			X	X	X	X	
25.9	1.081	X	X		X						82.6	.339			X			X	X			139.3	.2012	X	X	X			X	X		X		196.0	.143		X	X			X			X	X	X	
26.6	1.051	X	X	X	X						83.3	.336	X	X				X	X			140.0	.200					X		X	X		X		196.7	.1424	X	X	X			X			X	X	X
27.3	1.027	X	X	X							84.0	.333		X	X			X	X			140.7	.1992	X		X			X	X		X		197.4	.1418				X			X			X	X	X
28.0	1.0			X	X						84.7	.331	X	X	X			X	X			141.4	.1982		X	X			X	X		X		198.1	.1414	X											

Punched Tape Programmer. The punched tape programmer is used with the programmed loads for battery "B". It performs five functions:

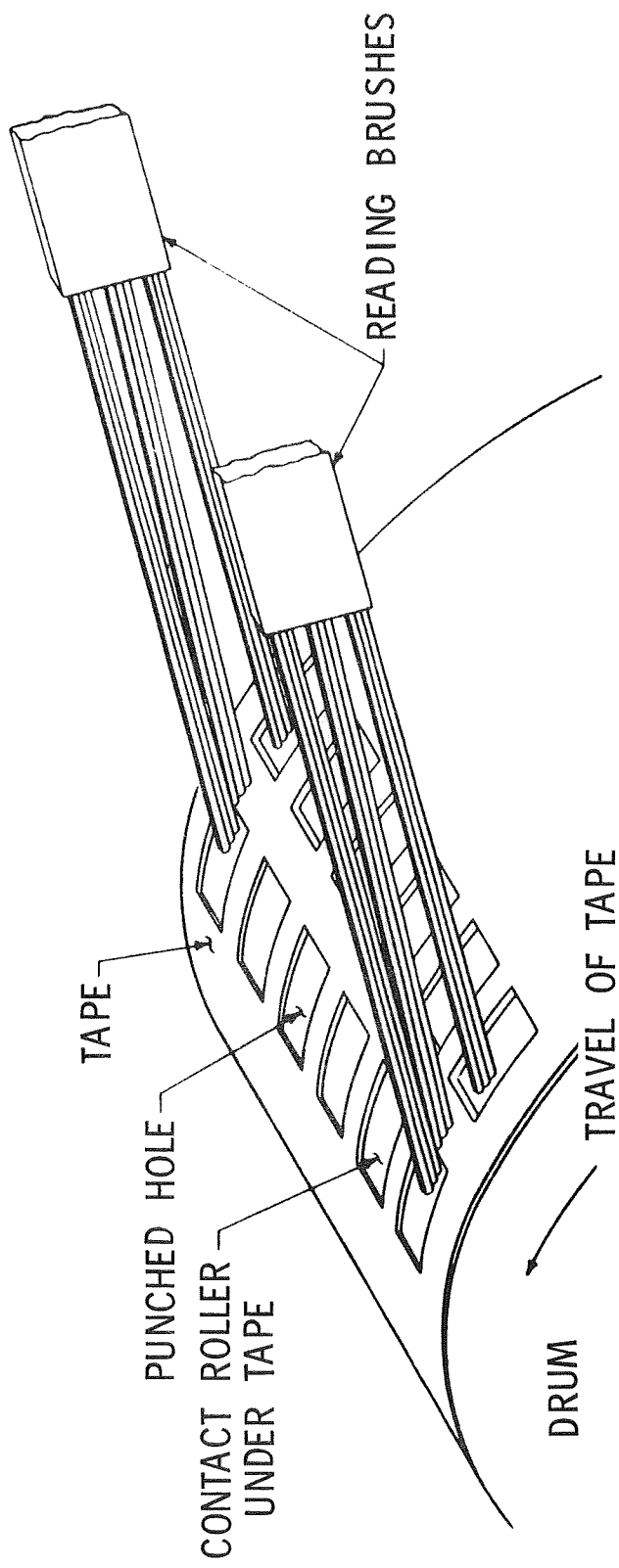
1. Selects resistor loads for battery discharge.
2. Selects timers for the loads.
3. Provides one-second time intervals.
4. Switches the battery from discharge to charge and visa versa.
5. Resets the ampere-hour and watt-hour meters.

The punched tape programmer has 22 channels. Each channel has a brush which completes a circuit through a hole in the tape (Figure 49 ). These brushes achieve a "make before break" switch closure even though there is a small strip of paper in the tape between successive holes for a given channel. A switch closure is thus sustained for as long as the tape is punched in its channel.

The punched tape is advanced by a stepping drive which can also provide fast-advance. The fast-advance rate is one line per second, and it is inhibited by channel 22. When channel 22 is not punched the tape will advance at the rate of one line per second until the channel-22 brush falls on a punched hole. Load durations of longer than one second are obtained by using channels 19 and 20, which activate delay timer 1 and delay timer 2, respectively.

Seven of the 22 channels are not assigned charge-discharge control functions. These may be used by NASA for controlling other events, such as start of recording instruments prior to scheduled load changes, and subsequent stopping of such recorders.

Delay Timer. The delay timers are used in conjunction with the punched tape programmer to establish the longer time duration intervals for both discharge and charge. These timers feature an external clutch with automatic reset, which allows the complete timing/switching movement of the timer to reset in less than 0.2 second. Delay timer 1 can be set anywhere between 15 seconds and 15 minutes, and delay timer 2 can be set from 30 seconds to 30 minutes.



#### DESCRIPTION

- THE STEPPING DRIVE ADVANCES THE TAPE THROUGH THE READER LINE
- MOVEMENT OF THE TAPE OCCURS UPON RECEIPT OF PULSE
- PROVIDES A FAST ADVANCE WHICH TRANSPORTS THE TAPE AT ONE LINE PER SECOND

FIGURE 49

PUNCHED TAPE PROGRAMMER

Charging Power Supply. The charging power supply provides constant-current or constant-voltage regulations with automatic crossover. The constant-current and constant-voltage levels can be independently adjusted from zero to 20 amperes and 50 volts. Some of the operating characteristics of this unit are:

Regulation	$\pm 0.01\% + 2 \text{ mV line}; \pm 0.03\% + 6 \text{ mV load}$
Ripple	500 microvolts RMS or 0.002%, whichever is greater
Stability	0.01% + 1 mV for 8 hours after warmup

The output voltage regulation of the power supply was measured with line voltage and putput current being varied. Results, presented in Table 16 show that output voltage changed only 75 millivolts over the full output current range, whereas line voltage variation had a negligible effect on output voltage. Output ripple was also checked, and found to be 1.80 millivolts ~~RMS~~ at an output of 45 volts.

Relay Power Supply. The relay power supply provides unregulated d.c. to the instrumentation and control components of the two controllers in one cabinet. Unregulated 24-28 V.d.c. is provided to relays, counters, panel lights, voltage regulators for the pressure transducers, and to voltage regulators for the ampere-hour/watt-hour meter reset circuits.

Voltage Instrumentation. Individual cell voltages are displayed on a 0 to 2 volt meter, utilizing two 2-deck wafer switches for selective monitoring of the 28 cells in a battery. Voltage jacks are provided on the cabinet to permit precise voltage monitoring with an external digital voltmeter. The analog output in the back of the cabinet permits simultaneous monitoring of all 28 cells of each battery.

The battery low and high voltage cutoff is obtained with a contactless meter-relay having five elements: (1) a d'Arsonval  $\pm 1\%$  accuracy meter, (2) a light source that provides a uniform light field, (3) a photoconductive cell, (4) a mechanism for positioning the cell with respect to the indicating pointer, and (5) a vane, attached to the moving element, which moves between the light and the cell to change the amount of light reaching the cell.



TABLE 16

VOLTAGE REGULATION OF CHARGE-DISCHARGE CONTROLLER POWER SUPPLY

AC LINE VOLTAGE INPUT	OUTPUT VOLTAGE AT CONSTANT CURRENT						
	0.0 AMPS	1.5 AMPS	3.0 AMPS	5.0 AMPS	9.0 AMPS	14.0 AMPS	22.0 AMPS
105	45.004	44.986	44.981	44.978	44.965	44.950	44.930
110	45.004	44.987	44.981	44.978	44.965	44.950	44.930
115	45.004	44.987	44.981	44.978	44.965	44.950	44.930
120	45.004	44.987	44.981	44.978	44.965	44.950	44.930
125	45.004	44.988	44.981	44.978	44.965	44.950	44.930

In operation, the light from a small lamp enters a V-shaped prism mounted to a bracket on the meter mechanism. As the indicating pointer approaches the set point, the vane swings between the prism and the photo-conducting cell, cutting off the light and causing the resistance of the cell to increase sharply. The cell is one arm of an a.c. bridge in the optical meter relay. The connections are such that as the resistance of the cell increases, the bridge output reverses phase and an SCR is turned off. When the SCR stops conducting, a load relay in series with the SCR drops out and control action is initiated.

Current Measurements. Discharge current for the manual adjustable load ("A" side) is measured with a 75A/50mV shunt, and the discharge current for the programmed load ("B" side) is measured with a 150A/50MV shunt. The charge current in each case is measured with a 20A/50 mV shunt.

The charge-current instrument is a contactless meter-relay of the same type as the battery voltage meter. The relay feature of the meter is used in two-step charge control.

Temperature Measurement. Battery temperature is measured by copper-constantan thermocouples. Thermocouple locations are shown in Figure 21 . Temperatures for individual thermocouples are displayed on a Fahrenheit-Centigrade meter, using a 2-deck wafer switch for selection. The meter draws a slight current, which is compensated for in the meter design. An analog output is provided so that every thermocouple can be read simultaneously with auxiliary instruments.

Pressure Measurement. Figure 90 is a schematic of the pressure measurement circuit. The input for the pressure transducer circuit is 7 volts regulated d.c. This voltage is obtained from a 7-volt regulator in the operational amplifier chassis. Each transducer has its own 7-volt regulator for isolation.

The output of the transducer is displayed on a millivoltmeter with a 20-microampere full-scale movement, but calibrated to record 0 to 25 psia. The meter sensitivity is 2 mv/psia. The calibration data for pressure measurement is given in Reference 6 .

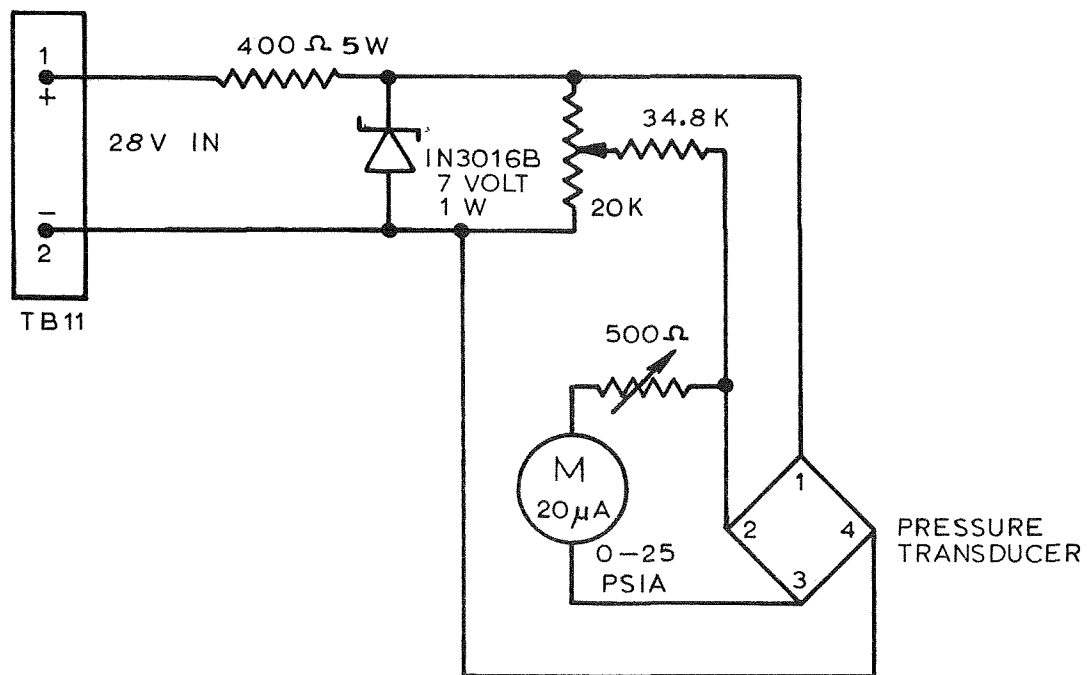


FIGURE 50

## PRESSURE MEASUREMENT SCHEMATIC

Ampere-Hour Meter. The ampere-hour meter consists of an operational amplifier, capacitor, resistor, voltmeter and current shunt. The operational amplifier integrates a voltage proportional to current, using the voltage developed across the current shunt. The theoretical output of the amplifier is

$$E_{out} = \frac{1}{RC} E_{in} t \quad (25)$$

where R is in ohms, C is in farads, and t is the time in seconds. The design value of R is 2.4 megohms and of C is 10 microfarads. A trim pot in series with R provides a fine adjustment because the value of C will not be exactly the design value of 10 microfarads.

In order to minimize the error the capacitor must have a high insulation resistance, and the amplifier must have low offset current and voltage. The amplifier has a built-in balance adjustment which reduces the error caused by offset current and voltage.

Battery cycling will normally start with a discharge. The ampere-hour meter will initially read 70 A-H. As the battery is discharged the ampere-hour indication will decrease until the charge cycle begins, at which time the ampere-hour reading will start to increase. It will continue to increase until the start of the next discharge cycle, whereupon the ampere-hour meter will reset to 70 A-H. The reset voltage, which is 7 volts, is supplied by the relay power supply.

The input power for the operational amplifier is supplied by a +15, -15-volt regulated power supply. Each amplifier has a separate power supply to achieve isolation. The output of the amplifier is 1 volt per 10 ampere hours, with a range of 0 to +10 Vdc. An analog 0-to-10 volt signal is provided in addition to the meter display. A schematic of the ampere-hour meter is shown in Figure 51.

Figure 52 shows results of calibration tests on the ampere-hour meter. The maximum error is seen to be well within one percent.

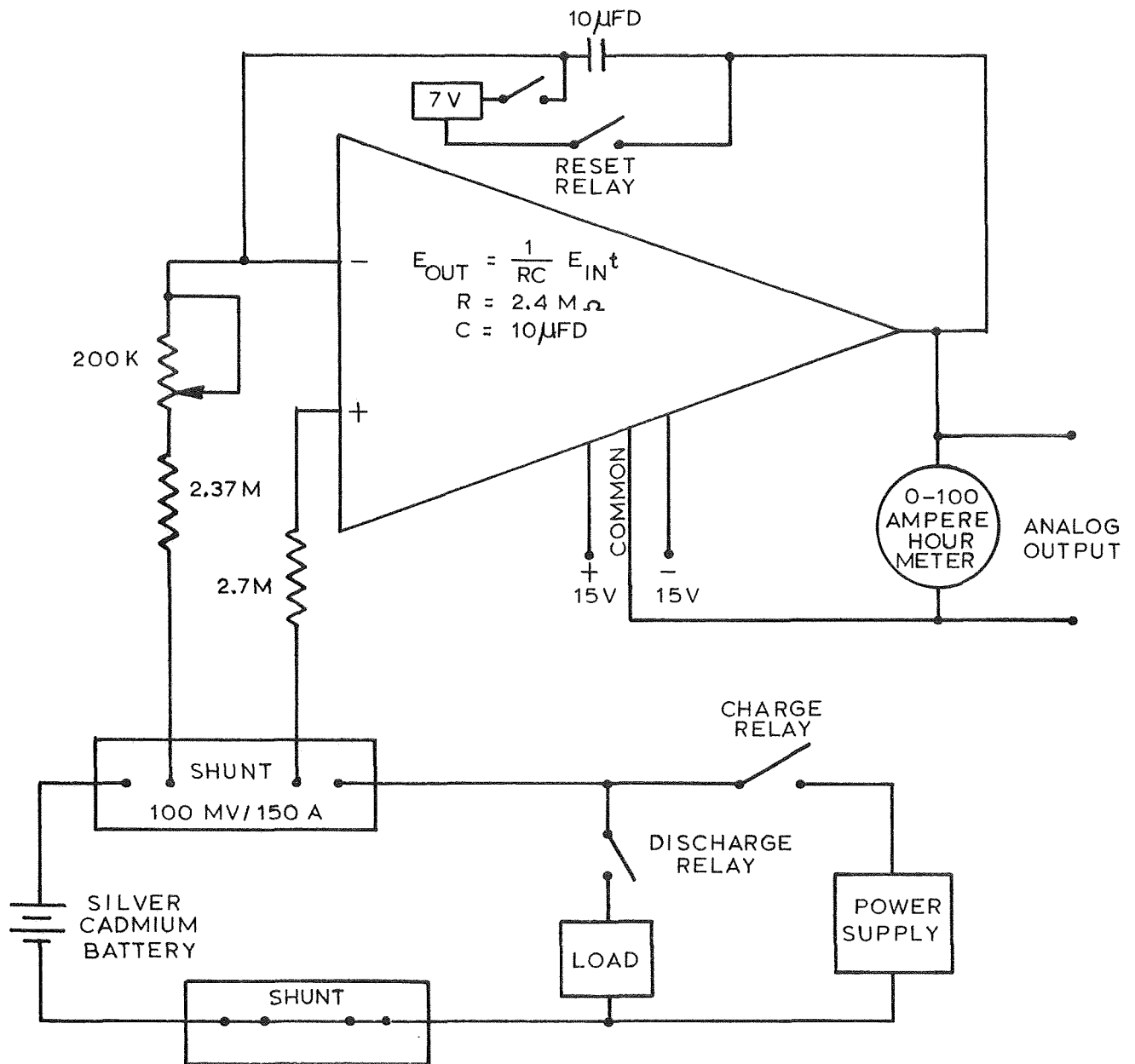


FIGURE 51  
AMPERE-HOUR METER SCHEMATIC

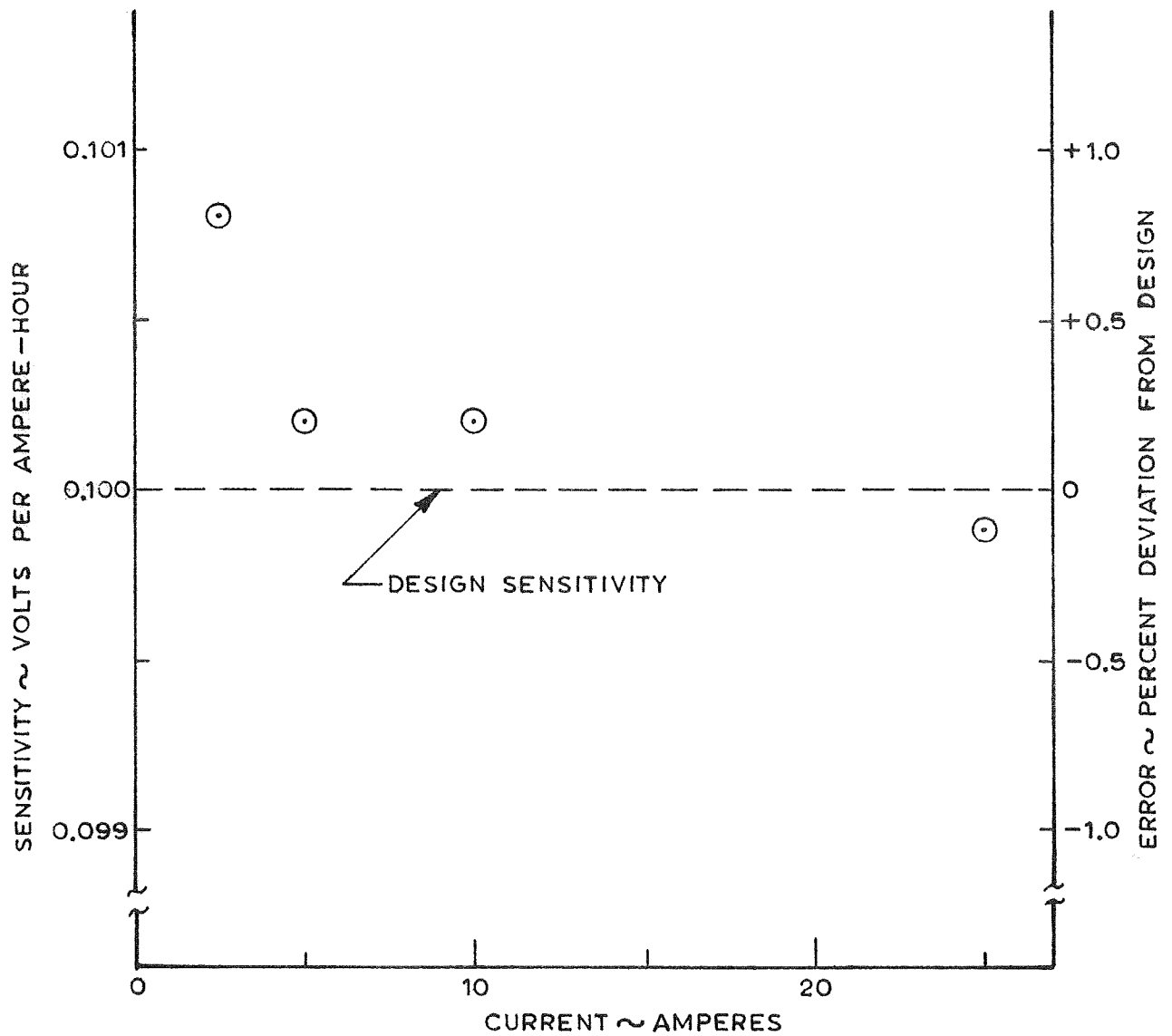


FIGURE 52  
CALIBRATION OF AMPERE-HOUR METER

Watt-Hour Meter. The watt-hour meter consists of a Hall-effect multiplier, operational amplifier, capacitor, resistors, and voltmeter. The Hall-effect multiplier produces an output proportional to the product of battery voltage and current.

The battery voltage input to the Hall-effect multiplier has a 180-ohm resistor which limits input current to 250 milliamperes at maximum battery voltage of 50 volts. The current input comes directly from a shunt.

The output of the Hall-effect multiplier is approximately 27 mV per watt. This voltage is fed to the operational amplifier where it is integrated with time to produce a signal proportional to watt-hours. The output of the operational amplifier is displayed on a voltmeter which is calibrated to read 250 watt-hours per volt. An analog output is also provided in addition to the meter display.

A schematic of the watt-hour meter is shown in Figure 53. The results of calibration tests (Figure 54 ) show that the maximum error is well within one percent.

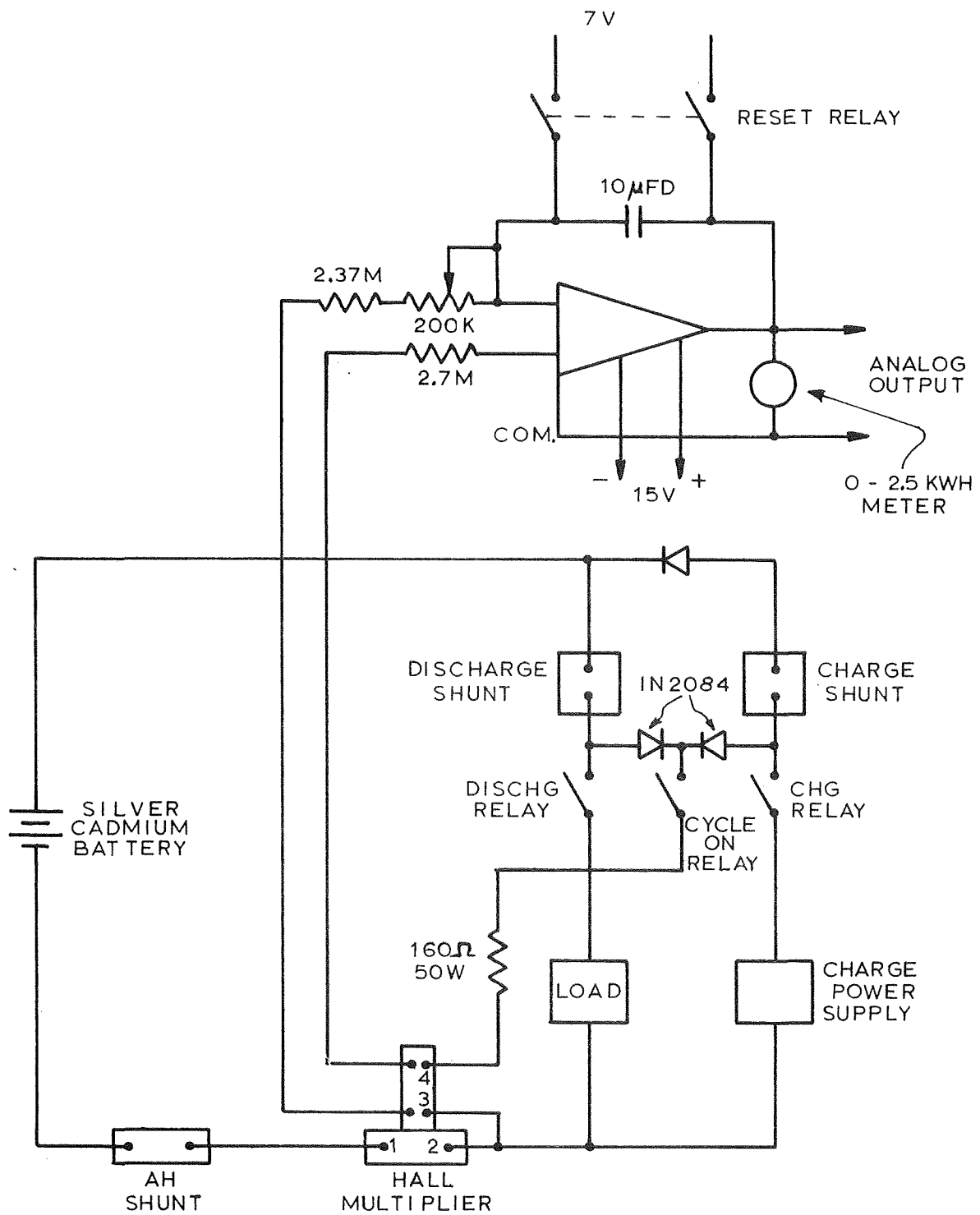


FIGURE 53

## WATT-HOUR METER SCHEMATIC



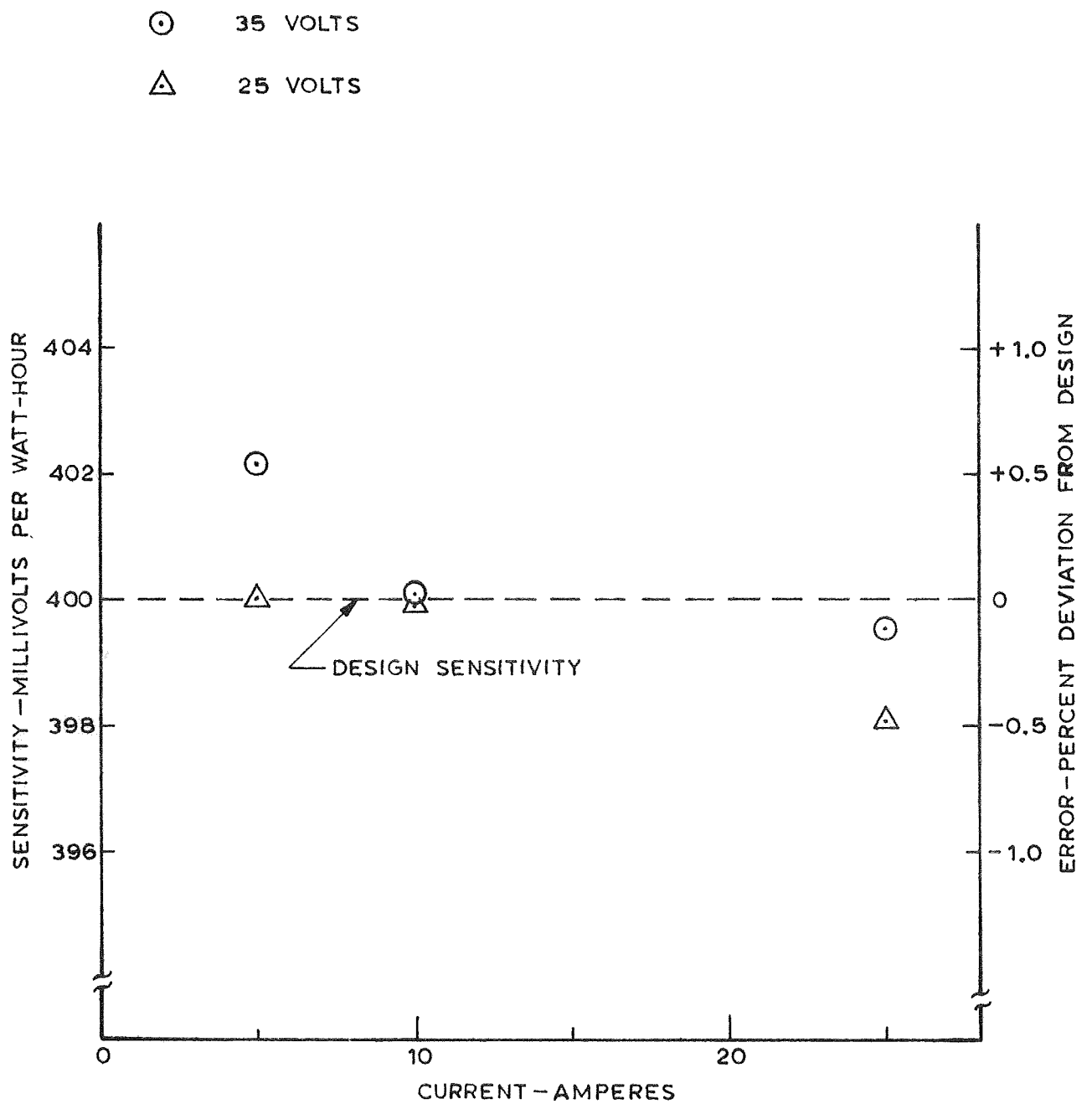


FIGURE 54

CALIBRATION OF WATT-HOUR METER

## 9.0 CONCLUSIONS

Batteries, charge-discharge controllers, calorimeters, and required accessories were designed, built, calibrated and delivered in accordance with contract requirements. All critical components were tested to verify that they met performance requirements.

It is appropriate to note development concepts which have been suggested during this program, but which were outside the scope of the contracted work. The most practical of these concepts are:

1. Ampere-hour and watt-hour meters. No suitable integrating meters could be found when this program was started. The integrating principle developed in the course of this program worked so well that it would seem appropriate for an instrument-making organization to use this principle in producing a useful line of integrating instruments. Such instruments could use new economical integrated-circuit operational amplifiers that could possibly be made to function without auxiliary sources of power.
2. Coulometer charge control. The integrating principle could be developed into a precise charge control for spacecraft batteries. Compensation for temperature effects within the control as well as within the battery require careful development.
3. Calorimetry. The use of compensated thermistors produced a calorimeter of unprecedented accuracy. This work must certainly have application to other calorimetry problems.
4. Load programming. The flexibility of a punched-tape programmer supplemented by delay timers does not appear to be generally recognized. Further design exploration of the punched-tape programmer concept could produce a battery tester with unusual flexibility and self-adapting features.

## 10. REFERENCES

1. Quality Assurance Requirements and Inspection Plan for Silver-Cadmium Cell, May 10, 1967.
2. Instruction Manual, Battery Calorimeter Computer Program, AS 2602, June 30, 1967.
3. Components Information Manual, Battery Charge-Discharge Controller, August 7, 1967.
4. Instruction Manual, Cell Thermal Analysis Computer Program, AS 2747, October 25, 1967.
5. Instruction Manual, Battery Thermal Analysis Computer Program, AS 2748, October 25, 1967.
6. Instruction Manual, Battery Charge-Discharge Controller Cabinet, October 25, 1967.

## 11 APPENDIX

### ADVANCED BATTERY ENERGY STORAGE SYSTEM

#### STATEMENT OF WORK

##### 1.0 INTRODUCTION

This program is to develop a silver-cadmium secondary battery energy storage system to meet power requirements of manned earth orbital missions of up to one year duration.

##### 2.0 DESCRIPTION OF TASKS

2.1 The contractor shall provide a total of eight (8) silver-cadmium batteries of more than 70 ampere-hours capacity each.

2.2 The contractor shall develop and provide a battery charge/discharge controller capable of independently cycling batteries over the range of test conditions in Section 3.1.3. The controller is not to be flight hardware, but the basic design and approach should be applicable to a flight system. The method of charge/discharge control of the battery shall be proposed by the contractor according to the requirements imposed by the proposed battery design. The method selected shall meet the functional specifications set forth in the statement of work.

2.3 The contractor shall perform a detailed thermal analysis of the battery to include both analytical and experimental considerations to accurately predict heat generation under a wide range of operating modes.

2.4 The contractor shall also provide calorimeter(s) to use in conjunction with two of the above batteries (sec. 2.1) which have been especially instrumented, to perform detailed measurements of internal heat generation.

### 3.0 BATTERY SPECIFICATIONS

#### 3.1 Electrical

- 3.1.1 Cell size at C/2 rate of discharge to an end voltage of 0.6 volts shall be greater than 70 ampere-hours (with battery operating temperature between 60-90°F).
- 3.1.2 Battery voltage at the end of 75% depth of discharge of C/2 rate shall be greater than 28.0 volts with battery operating temperature between 60-90°F. This constitutes the definition of battery failure point.
- 3.1.3 The battery shall be capable of operation under the following range of test conditions with programmed and fixed loads:
  - (a) The battery shall have a design life goal of 5500 charge/discharge cycles at 25 percent depth of discharge with a 58 minute charge, 36 minute discharge cycle.
  - (b) The battery shall have a design life goal of 200 charge/discharge cycles at 75 percent depth of discharge with a 10 hour charge, 2 hour discharge.
  - (c) The battery shall have a design life goal of at least 100 charge/discharge cycles at up to 75 percent depth of discharge on a 24 hour cycle (22 hour charge, 2 hour discharge) with a widely varying load to include maximum duration peaks of 10 seconds at the 3C rate.At no time during the above testing should the steady state (< 1 sec. peak) battery voltage fall below 25 volts..

#### 3.2 Physical

- 3.2.1 Battery shall operate in the pressure range of  $10^{-6}$  mm Hg to 760 mm hg, and ambient temperature range of 0-160°F when mounted on coldplating with temperature range of 60-90°F.

- 3.2.2 Two of the eight batteries shall be instrumented for temperature as outlined in the Section 3.3.6. The remaining 6 batteries shall each have internal temperature sensors as follows: Internal temperatures shall be measured by copper constantan thermocouples at not less than six points in each battery. At least two cells shall have thermocouples mounted top and bottom. The primary aim of this requirement is to accurately determine thermal gradients in the battery during operation.
- 3.2.3 Internal battery pressure shall be measured in all eight batteries by a strain gage or reluctance pressure transducer. D.C. or 400 c.p.s. excitation and readout for this transducer will be supplied by the contractor in the charge/discharge controllers.
- 3.2.4 Battery shall have individual cell voltage monitoring capability.
- 3.2.5 Power leads shall be brought out through a connector. A mating connector shall also be provided by the contractor.
- 3.2.6 All voltage, temperature, and pressure measurement leads shall be brought out through a connector(s). Mating connector(s) shall also be provided by the contractor. Weight of sensors and leads shall not be considered in section 3.2.7.
- 3.2.7 Battery design weight goal shall be less than 85 pounds. However, battery weight should be minimized consistent with meeting the performance specifications.
- 3.2.8 Battery is not to be a flight prototype, but battery design must consider flight conditions.

### 3.3 Thermal

- 3.3.1 An analysis of thermal characteristics of the battery shall be made by the contractor. The primary purposes of this analysis are (1) to determine the heat generated within the battery, both total amount and rate with respect to position in duty cycle; and (2) to establish, with the aid of an existing computer thermal analyzer program, the capability for predicting the heat generated over a range of operating conditions.

### 3.3 Thermal (contd)

Battery internal heat generation measurements are needed to determine the thermal loading imposed on the spacecraft's thermal control system over an entire mission duration. The ability to predict the amount of heat evolved by the battery will be especially useful in consideration of various mission applications of Ag-Cd secondary batteries.

- 3.3.2 The contractor must evolve an analytical method of determining transient and steady state internal heat generation in conjunction with experimental measurements obtained on a prototype of the proposed battery. The derivation of a quantitative relationship for heat evolved by the battery as a function of current density and other necessary parameters must be made giving due regard to the silver electrode potential at various stages of charge and discharge. This method will produce input data for the thermal analyzer computer program in section 3.3.1.
- 3.3.3 The contractor shall also generate a thermal model, or network, of the batteries to be used in the thermal analyzer computer program. This model is to be evolved with the aid of measurements made on the prototype battery by the contractor. The data shall include detailed battery materials properties and their variation with temperature, temperature gradients, electrical characteristics, and other information necessary to generate the thermal model.
- 3.3.4 In conjunction with the information generated in Section 3.3.2 and 3.3.3, the contractor shall perform necessary modifications on an existing thermal analyzer computer program. The result of these modifications will be a computer program which will accurately predict temperatures and heat evolution of the battery. The contractor shall make use of NASA MSC computer facilities.

- 3.3.5 Before delivery of the batteries the contractor shall substantiate experimentally the prediction capability of the overall computer program for battery thermal characteristics and heat generation. This shall be done for two or more test cases such that the program is checked out over the range of its capability.
- 3.3.6 Of the eight batteries to be delivered, two batteries shall be instrumented such that detailed calorimetric measurements may be made at MSC.
- 3.3.7 The contractor shall provide the means - calorimeter(s) - by which the heat generation rates of the above two batteries are measured.
- 3.3.8 A detailed computer program user's manual will be provided by the contractor. The program(s) developed under this contract shall be programmed using Fortran IV language, with complete absence of assembly-language routines other than those available on the MSC system. The program(s) should not have on-line card read, on-line printout, or senswitch options. They shall be accompanied by all source decks and listings, a set of test cases (data decks), a set of printout from test cases, complete explanation of input options, and flow charts and equations used. The program(s) shall be compiled and executed on the MSC computer configurations, with test cases supplied or approved by the cognizant MSC engineers.

#### 4.0 BATTERY CHARGE/DISCHARGE CONTROLLER (BCDC) FUNCTIONAL SPECIFICATIONS

##### 4.1 Electrical

- 4.1.1 The contractor shall provide suitable, well-filtered DC power supplies for all system DC power. Each supply shall be mounted at the bottom of the equipment cabinet. All interconnection wiring shall be done by the contractor.



- 4.1.2 The electrical input to the power supplies and other electrical power requirements for the controllers shall be, if practical, 115 VAC, 60 cycle, single phase.
- 4.1.3 The discharge capability of the controller loads is specified in Sections 4.4.2 and 4.4.3.
- 4.1.4 The following instrumentation will be provided by the contractor:
- (a) Built in ampere-hour and watt-hour meters. The amp-hour meter shall have a capacity of 100 amp-hours. The watt-hour meter shall have the capacity of 2500 watt-hours. Both meters shall have an accuracy of  $\pm 1\%$ . These meters shall automatically reset at the end of each cycle, or charge and discharge mode.
  - (b) Current meter.
  - (c) Battery voltage meter with an adjustable photo-sensitive low voltage cut-off for shutting off the controller if the battery voltage drops below an acceptable level.
  - (d) Voltage sensing for each cell.
  - (e) Pressure readout.
  - (f) Temperature meter calibrated in  $^{\circ}\text{F}$  with a multi-position switch to measure the temperature at all points specified in Section 3.2.2. If desired, the contractor may supply only one meter for each controller cabinet.
- 4.1.5 Analog readout signals from each of the items in Section 4.1.4 shall be provided to a suitable terminal strip for each controller.
- 4.1.6 The contractor shall provide necessary pressure measurement capabilities as outlined in Section 3.2.3.
- 4.1.7 The Battery Charge/Discharge Controller design shall have current sensing logic circuitry which monitors the value of the decreasing charging current and at some low preset value, switches the previously set charge voltage to a lower value near the open circuit voltage of the battery, thus preventing overcharge.

## 4.2 Controller Physical Specifications

- 4.2.1 The contractor shall provide four controllers capable of independently testing four batteries. Two controllers each shall be placed in two cabinets.
- 4.2.2 Separate, independent loads shall be provided for each controller. The loads shall be provided for each cabinet as follows: a single adjustable load and a programmed load.
- 4.2.3 BCDC shall operate in ambient conditions of 5 to 15 psia pressure and 60 to 90°F temperature.
- 4.2.4 BCDC shall be a high efficiency device utilizing bread-board type construction (not flight hardware) and flight type components.
- 4.2.5 BCDC is to be capable of being mounted in a standard 19 inch electrical equipment rack.
- 4.2.6 A suitable terminal strip shall be provided for connection of input power, battery, control signal, and load resistance.
- 4.2.7 Meters, indicators, and controls shall be mounted on a front panel. The meters shall be  $\pm 1$  percent ammeter for charge and discharge current,  $\pm 1$  percent voltmeter for battery voltage, and a  $\pm 1\%$  for the temperature and pressure meters.
- 4.2.8 The contractor shall provide a resettable cycle counter for total charge/discharge cycles.

## 4.3 Charge/discharge Timer Specifications

- 4.3.1 One timer and one punched-tape programmer shall be provided for each controller cabinet.
- 4.3.2 For compatibility with available equipment, "Dual-Trol" model timers shall be used for the adjustable loads. These timers are made by the Industrial Timer Corporation. These timers are of the recycle type and have two settable dials.

- 4.3.3 Each cabinet shall be provided with a timer that shall have one dial with a range of zero to 30 hours labeled "Charge" and one dial with a range of zero to 3 hours labeled "discharge".
- 4.3.4 The punched tape programmer shall control the programmable load.
- 4.4 Discharge Load Specifications
  - 4.4.1 Two independent loads shall be provided for each controller cabinet as specified in Section 4.2.2.
  - 4.4.2 The single, adjustable load shall have a minimum current capability of C; i.e., at least 70 amps.
  - 4.4.3 The programmed load shall have current capabilities variable from C/100 to 3C with a minimum of 10 load levels over a single discharge cycle. Individual load level "on time" shall be adjustable from a one-second minimum to a 2-hour maximum.
  - 4.4.4 Necessary blowers, etc. for cooling the loads and controllers shall be provided by the contractor.
- 4.5 Equipment Cabinet Specifications
  - 4.5.1 A standard electrical equipment cabinet with 19 inch wide panel mounting provision shall be used.
  - 4.5.2 The cabinet shall have removable side panels and a removable rear door.
  - 4.5.3 The cabinet shall be on swivel composition wheels of no less than 3 inches in diameter.